Swiss Needle Cast Cooperative

Annual Report 2025

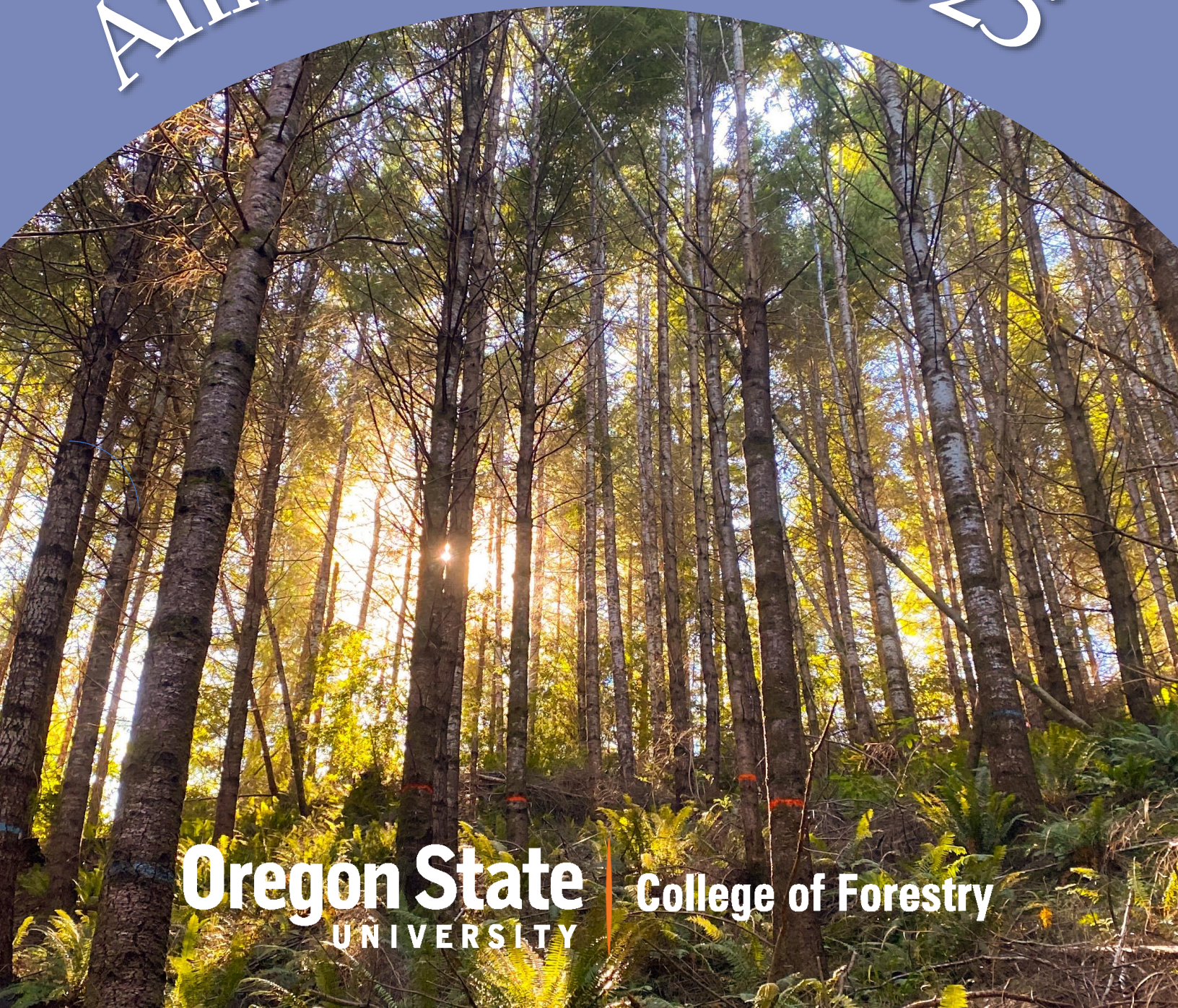

Oregon State University | College of Forestry

Members of the Swiss Needle Cast Cooperative

Cascade Timber Consulting

Nuveen Natural Capital

Oregon Department of Forestry

Starker Forests

Rayonier

USDA Forest Service

Weyerhaeuser Corporation

Swiss Needle Cast Cooperative Staff

Jared LeBoldus – Director and Associate Professor of Forest Pathology

Adam Carson – Associate Director and Faculty Research Assistant

Cristian González – Research Associate

Contents

SNCC Income Sources and Expenditures: 2025

Income	
Membership dues	*84,000*
Oregon State Legislature	*95,000*
Carry-over	*279,910*
Total 2024 Income	**$458,910**
Expenditures	
Salaries and wages	*185,401*
Travel	*20,458*
Operating expenses	*10,698*
Materials and Supplies	*8,380*
Indirect Costs (@17.5%)	*15,826*
Total 2024 Expenditures	**$240,763**
Balance	**$218,147**

SNCC Background and Organization

A major challenge to intensive management of Douglas fir in Oregon and Washington is the current Swiss needle cast (SNC) epidemic. Efforts to understand the epidemiology, symptoms, and growth losses from SNC have highlighted gaps in our knowledge of basic Douglas-fir physiology, growth, and silviculture. The original mission of the Swiss Needle Cast Cooperative (SNCC), formed in 1997, was broadened in 2004 to include research aiming to ensure that Douglas-fir remains a productive component of the Coast Range forests. The SNCC is located in the Department of Forest Engineering, Resources and Management within the College of Forestry at Oregon State University. The Membership is comprised of private, state, and federal organizations. Private membership dues are set at a fixed rate. An annual report, project reports, and newsletters are distributed to members each year. Our objective is to carry out projects in cooperation with members on their land holdings.

SNCC Mission

To conduct research on enhancing Douglas-fir productivity and forest health in the presence of Swiss needle cast and other diseases in coastal forests of Oregon and Washington.

SNCC Objectives

(1) Understand the epidemiology of Swiss needle cast and the basic biology of the causal fungus, *Nothophaeocryptopus gaeumannii*.

(2) Design silvicultural treatments and regimes to maximize Douglas-fir productivity and ameliorate disease problems in the Coast Range of Oregon and Washington.

(3) Understand the growth, structure, and morphology of Douglas-fir trees and stands as a foundation for enhancing productivity and detecting and combating various diseases of Douglas-fir in the Coast Range of Oregon and Washington.

Oregon State University
Department of Forest Engineering Resources and Management
Oregon State University, 216 Peavy Forest Science Complex
Corvallis, Oregon 97331 || P 541-737-4952 F 541-737-4316
ferm.forestry.oregonstate.edu

3/17/2026

To: Swiss Needle Cast Cooperative Members
From: Jared LeBoldus, Director, SNCC

Dear SNCC Membership,

The 2025 field season marked another productive and scientifically rich year for the Swiss Needle Cast Cooperative. As the SNC epidemic continues to shape Douglas-fir management across western Oregon and Washington, the work of the Cooperative has never been more important. This year's accomplishments reflect the strength of our collaborations, the dedication of SNCC staff, and the continued support of our membership.

Major Research Accomplishments in 2025

Our research portfolio expanded substantially this year. We completed foliage retention analyses for the first two-thirds of the research and monitoring plot network, revealing continued relationships between elevation, coastal proximity, and disease severity—patterns that appear consistent across sampling periods. We also advanced our work in the Cascade foothills, documenting improvements in foliage retention and reductions in disease severity for many stands between 2024 and 2025. These datasets are laying the groundwork for a deeper understanding of long-term SNC dynamics across diverse environments.

This year also saw significant progress in our seedling screening program. Under the leadership of Dr. Cristian González, we developed and tested a host-derived liquid culture medium and multiple inoculation approaches that provide a more reliable framework for screening Douglas-fir families for SNC tolerance under controlled greenhouse conditions. These advances represent foundational steps toward efficient early-stage identification of tolerant families.

Dr. González has also started scouting for the pre-commercial thinning trial and has completed 37/42 site visits. The PCT experiement will hopefully be established this fall.

Progress on the Ten-Year Remeasurement

The ten-year remeasurement effort reached a major milestone in 2025. Adam Carson completed foliage sampling of the second third of the network (plots established in 2014). The final set of plots (established in 2015) were remeasured in fall 2025, and foliage sampling for these remaining stands will be completed in spring 2026, concluding the decade remeasurement cycle. The Cooperative now has an unprecedented dataset spanning installation through ten years of disease development, offering insights into foliage retention dynamics, growth impacts, and landscape-scale disease patterns. Comprehensive analyses synthesizing all three cohorts will be a major focus for 2026.

Expansion of Cascade Foothills Monitoring

The second full assessment of the Cascade Foothills transects was completed in spring 2025. These monitoring data continue to highlight persistent but variable disease pressure across the foothills and have already provided valuable comparisons with the coastal SNC zone. Improved foliage retention and reduced disease severity in many foothills stands between 2024 and 2025 are encouraging indicators of stability in these environments. Continued long-term monitoring will allow us to assess whether these trends persist under shifting climate and stand conditions.

Thank you to the SNCC membership for your continued support of this Cooperative. Your involvement enables the long-term research, monitoring, and scientific leadership necessary to promote resilient Douglas-fir forests. We look forward to building on the momentum of 2025 and advancing critical work to better understand and manage Swiss needle cast in the years ahead.

Sincerely,

Jared M. LeBoldus, Associate Professor – Forest Pathology,
Botany and Plant Pathology & The Forest Engineering, Resources and Management Department
Director of the Swiss Needle Cast Cooperative: https://sncc.forestry.oregonstate.edu/
Oregon State University | Ph: 541-737-1907 | Fax: 541-737-3575

Ten-Year Remeasurement of the Swiss Needle Cast Cooperative Research and Monitoring Plots, and the Second Full Assessment of the New Network of Monitoring Transects in the Cascade Foothills

2025 Research Activities of the Swiss Needle Cast Cooperative

Adam Carson[1], Gabriela Ritóková[2], Dave Shaw[1], Jared LeBoldus[1,3]

[1] SNCC, Forest Engineering, Resources, and Management, Oregon State University, [2]Oregon Department of Forestry, [3]Department of Botany and Plant Pathology, Oregon State University

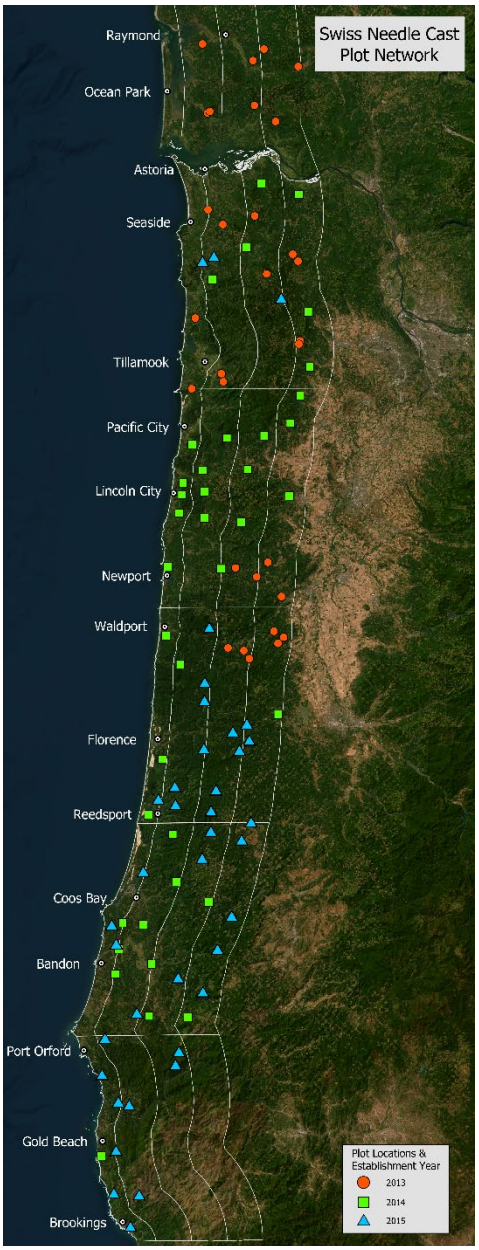

Figure 1. Distribution map of the SNCC research plot network.

Remeasuring the Research and Monitoring Plot Network

The research and monitoring plot network (RPN), established by the Swiss Needle Cast Cooperative (SNCC), consists of 106 plots installed in Douglas-fir plantations distributed across the Coast Range in Oregon and southwest Washington (Fig. 1). Installation of the network began in 2013 and took three years to complete. Nine of the research plots have since been lost due to precommercial thinning, windthrow and wildfire. This network provides information on the geographic distribution and disease severity of Swiss needle cast (SNC) across the landscape, as well as growth and yield impacts to Douglas-fir. The first five-year remeasurement of the remaining plots was completed in 2020. From this first re-measurement, cubic volume growth loss of 30-35% was estimated in heavily infected SNC stands with low needle retention (Mainwaring et al. 2020). This is a reduced estimate from the previous 50% growth loss calculated in 2011 (Maguire et al. 2011). Furthermore, initial assessments of foliage retention within the RPN found that disease severity increased and foliage retention decreased with latitude (Ritóková et al. 2021). Analyses from the initial and first remeasurement of the RPN can be found in the 2020 SNCC Annual Report.

The second five-year remeasurement (ten-years post establishment) of the RPN is currently underway and will conclude in 2026. The measurements of the first third of plots (those established in 2013) were completed in the fall of 2023, and foliage samples were collected from these plots to assess needle retention and disease severity in the spring of 2024. Measurements of the second third of plots (those installed in 2014) were completed in the fall of 2024 and were sampled in the spring of 2025. Growth measurements from the final third of plots in the network were taken during the fall of 2025, and foliage samples will be collected from those plots during the

spring of 2026, concluding the third five-year measurement of the network. Analysis of the data from the first third of plots, and their implications for cubic volume growth loss, are discussed in the 2023 SNCC annual report (Mainwaring et al. 2024) and a growth impact assessment from the second third of plots can be found in the 2024 annual report (Mainwaring et al. 2025). Comprehensive growth impact and foliage retention analyses from all network plots will be included in the 2026 annual report. Here, we outline preliminary foliage retention results from the first two thirds of plots included in the study.

Foliage Retention Results from Two Thirds of the Plot Network

Although the first two thirds of plots in the network exclude many plots within the southernmost latitudinal zones (Fig. 1), differences in foliage retention were observed. Across all plots sampled in 2024 and 2025, the mean plot-level foliage retention was 2.51 years and ranged from 1.14-3.94 years. This represents a reduction in the overall mean foliage retention on the same plots compared to the five-year assessment but matches the mean retention found during the first collection period (Fig. 2). The elevation of the plots ranged from 157-2311 ft (48-704 m), and a positive relationship was observed between foliage retention and elevation ($R^2 = 0.24$, Fig. 2). Additionally, foliage retention decreased with distance from the coast ($R^2 = 0.55$), but no relationship was observed between foliage retention and latitude ($R^2 = 0.002$).

Compared to samples collected during the first and second assessments, foliage retention decreased in the southwest Washington, and Coos Bay latitudinal sampling zones and increased in the Florence sampling zone (Fig. 3). Overall, the Newport zone had the greatest median foliage retention and a wide distribution of ratings for each sampling period. Furthermore, median foliage retention for all three sampling years was reduced in plots located within longitudinal zones closest to the coast compared to plots located a distance of 15 miles or greater from the coast (Fig. 4, Fig 5). However, a reduction in median foliage retention was observed during the 3rd sampling period within the 15-25-mile zone (Fig. 4). These preliminary results suggest that the correlations found by Ritóková et al. (2021) between foliage retention and elevation, and coastal proximity may remain temporally consistent across sampling periods overall. Subsequent analyses of the remaining plots in the network will include a wider geographic range of the SNC zone and should aid in further elucidating foliage retention and disease dynamics.

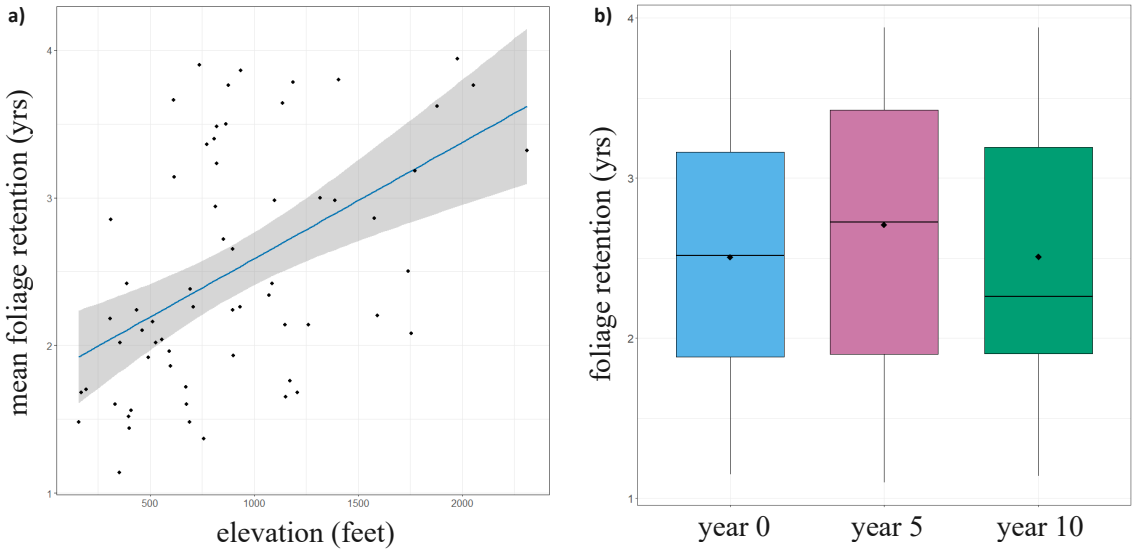

Figure 2. (a)Scatter plot showing the relationship between mean foliage retention and elevation from plots sampled in 2024 and 2025 $R^2 = 0.24$; (b) box plots showing the distribution of foliage retention across the three sampling periods. Note: ◆ indicates mean foliage retention

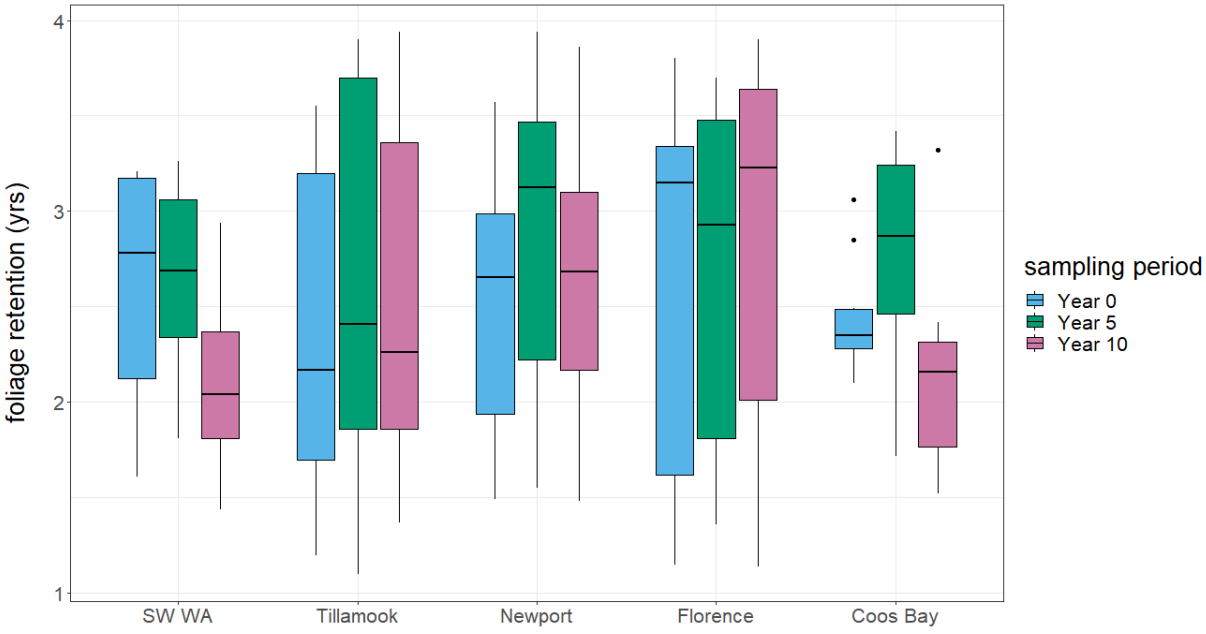

Figure 3. Box plots showing foliage retention within latitudinal zones by sampling period. Note: results from the Florence and Coos Bay sampling zones are preliminary and are based on a partial data within each zone.

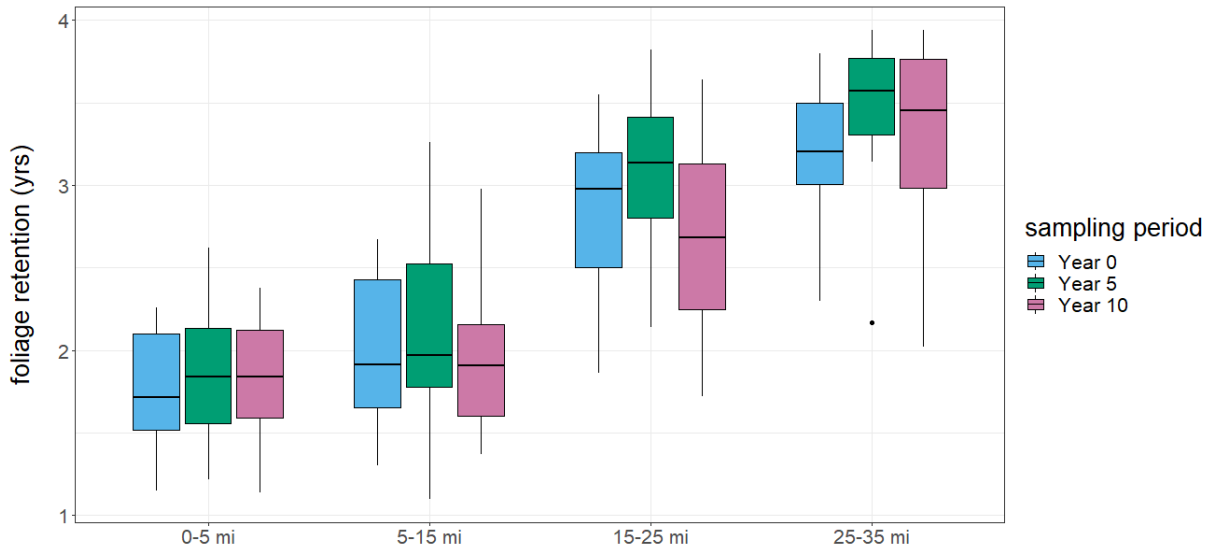

Figure 4. Box plots showing foliage retention within longitudinal sampling zones by sampling period. Note: results are preliminary and are based on an incomplete number of plots in each sampling zone.

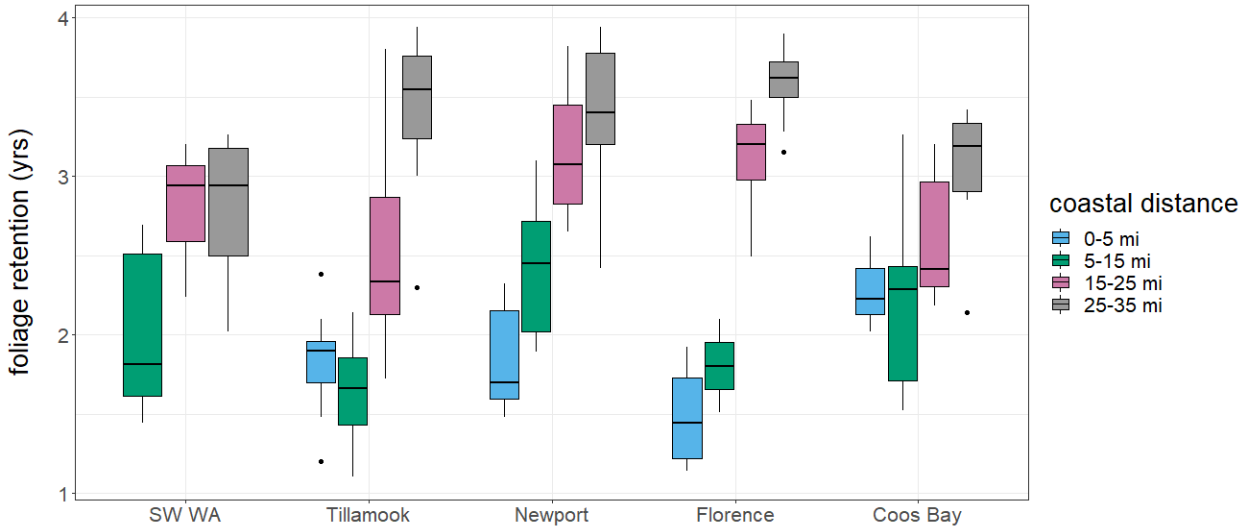

Figure 5. Box plots showing foliage retention within longitudinal sampling zones by sampling period. Note: results are preliminary and are based on an incomplete number of plots in each sampling zone.

Swiss Needle Cast Transects in the Oregon Cascade Foothills

Background

In addition to the RPN, the SNCC monitors SNC disease conditions within the foothills of the Cascade mountains using a network of monitoring transects. Thirty-five transects were installed in 10-to-15-year-old Douglas-fir stands in the spring and summer of 2023 (Fig. 6). Each selected stand contains a single 100-meter transect with five sample points located at 20-meter intervals. At each sample point, the nearest co-dominant or dominant Douglas-fir on each side of the transect are selected for a total of 10 trees per stand. Diameter at breast height, foliage retention, and disease severity is collected for each sampled tree. Each transect is representative of the stand in which it was established.

The transects are surveyed annually with the aim of evaluating SNC conditions using an index rating system for disease severity (Fig. 7) and foliage retention (Fig. 8). The second full assesment of the new transect network occurred in the spring of 2025.

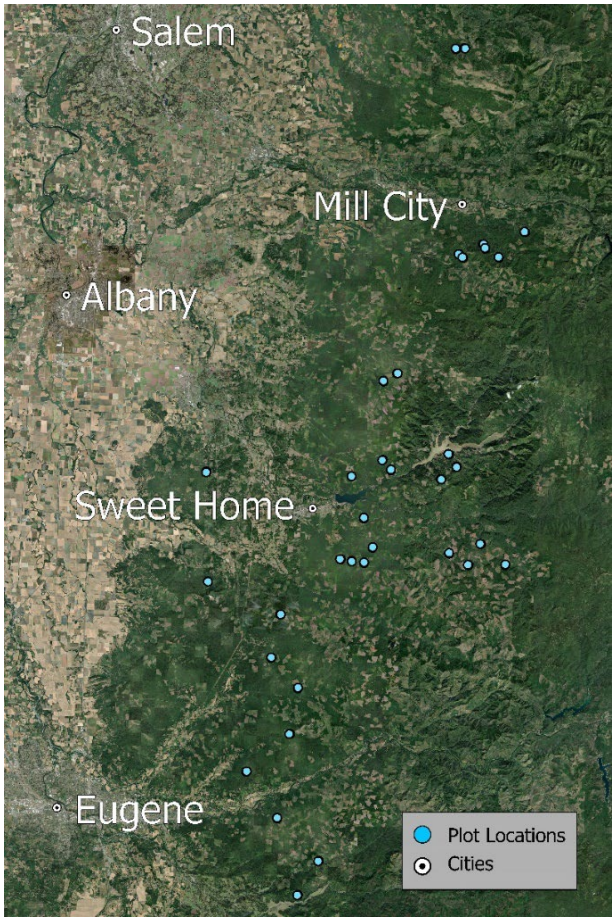

Figure 6. Distribution map of the Cascade foothills SNC monitoring transects.

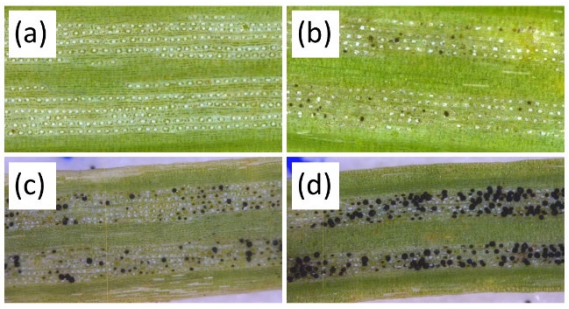

Figure 7. Disease severity index rating for cascade monitoring transects. (a) No pseudothecia present = 0; (b) light stomatal occlusion, up to 20% = 1; (c) moderate occlusion, between 20-50% = 2; (d) heavy occlusion, above 50% = 3.

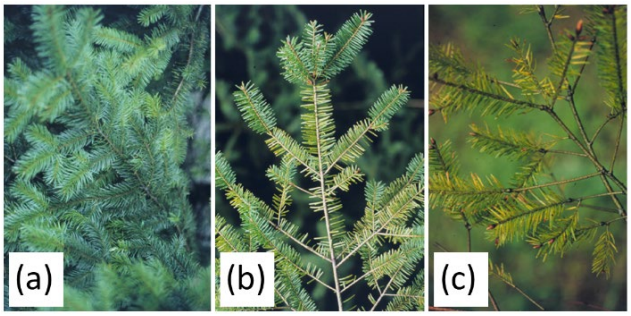

Figure 8. Examples of foliage retention ratings on 4-year lateral branches. (a) Full needle retention across all 4 cohorts = 4.0; (b) near full retention on 1st & 2nd cohorts, partial retention on 3rd & 4th cohorts = 2.4; (c) partial retention on 1st cohort only = 0.9.

Results

Overall, the results were similar to what has been observed in previous assessments, indicating that the disease is present over time despite observed improvements in foliage retention and reduced disease severity. The elevation of transects within the plot network ranged from 478-3273 ft (146-998 m). The mean foliage retention of each plot varied from 2.1-3.9 years, and the mean index rating for disease severity ranged from 0.6-2.4 (light to moderate). Across all stands surveyed, the median foliage retention was 3.6 years (Fig. 9), and the median disease severity was 1.5 (Fig. 9). No relationship was observed between foliage retention and latitude ($R^2 = 0.048$) or foliage retention and longitude ($R^2 = 0.074$). Additionally, no relationship was observed between disease severity and latitude ($R^2 = 0.099$), but there was a weak relation between disease severity and longitude ($R^2 = 0.17$).

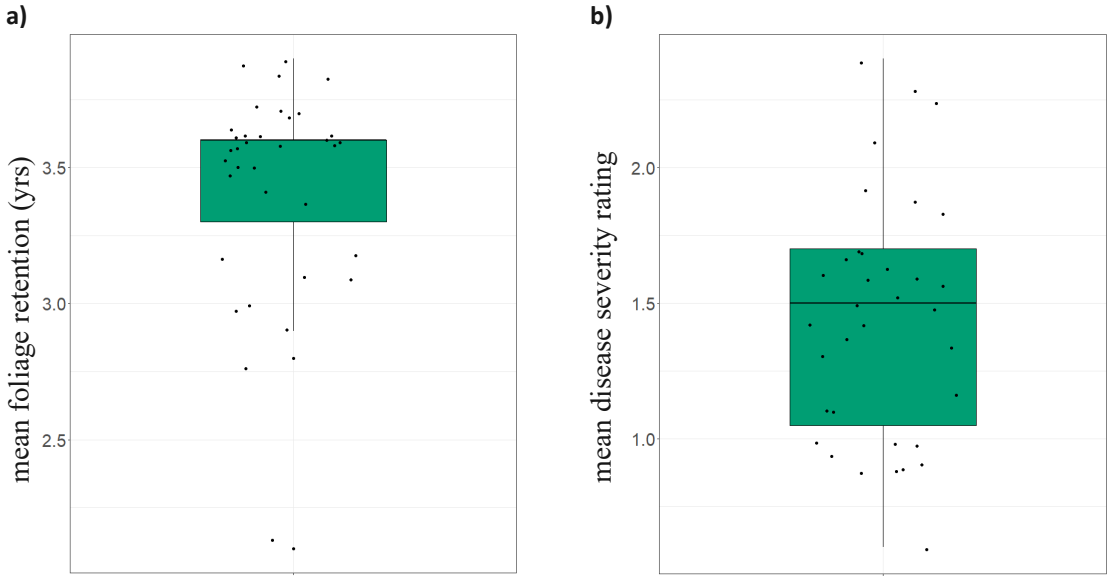

Figure 9. Box and dot plots showing the 2025 results for mean foliage retention (a) and mean disease severity (b)

A negative association was observed between disease severity and foliage retention (R^2= 0.21, Fig. 10). Additionally, elevation was found to be negatively associated with disease severity (R^2= 0.31, Fig. 11) and positively associated with foliage retention (R^2= 0.11, Fig 11).

Comparisons of the 2024 and 2025 results, found that foliage retention slightly improved in those stands overall (Fig. 12, Fig. 13). The mean 1-year change in foliage retention (0.1 years) was positive, with 52% of trees showing an increase in retention. Disease severity also saw an improvement in ratings (Δ = - 0.2), with 71% of trees showing a reduction in severity (Fig 12, Fig. 14). This suggests that foliage retention in the Cascade foothills remained relatively consistent between sampling periods despite a notable reduction in disease pressure.

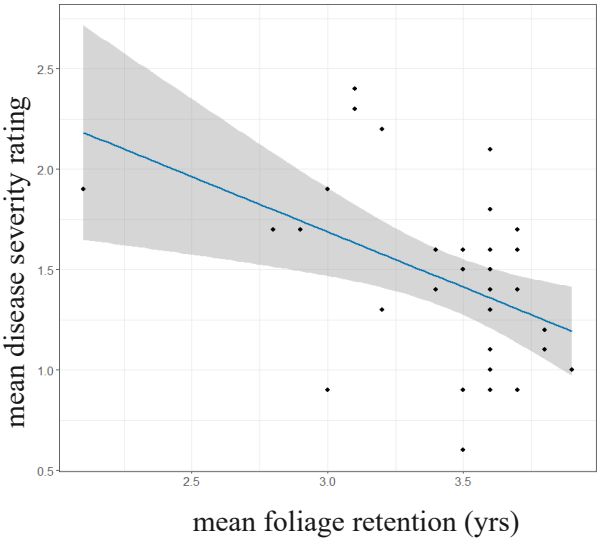

Figure 10. Scatter plot showing the relationship between mean disease severity and mean foliage retention ratings, R^2= 0.21

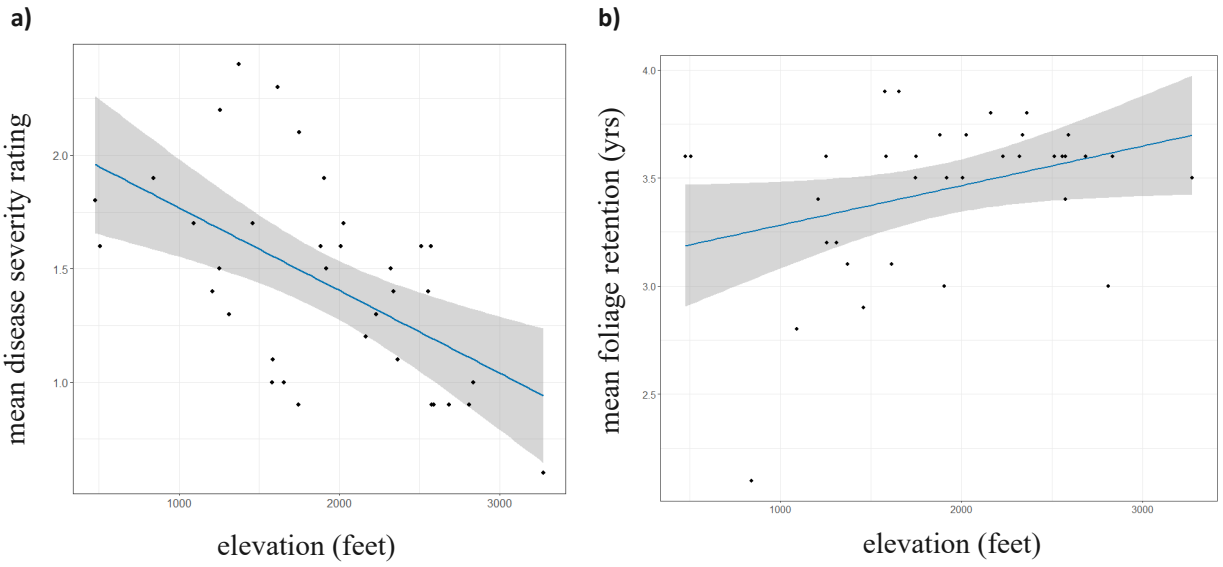

Figure 11. (a) Scatter plot showing the relationship between mean disease severity rating and elevation, R^2= 0.31; (b) mean foliage retention and elevation R^2= 0.11

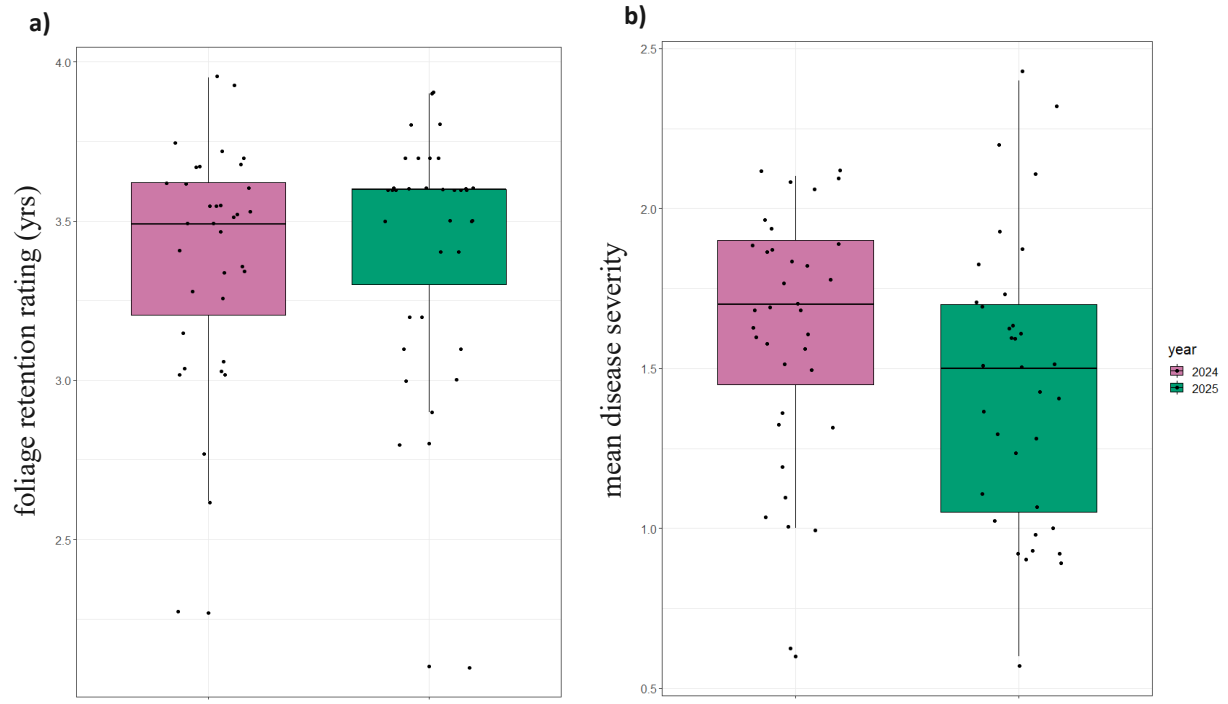

Figure 12. (a) Box and dot plot showing the mean foliage retention ratings for 2024 (left / pink) and 2025 (right / green); (b) box and dot plot showing the mean disease severity ratings for 2024 (left / pink) and 2025 (right / green)

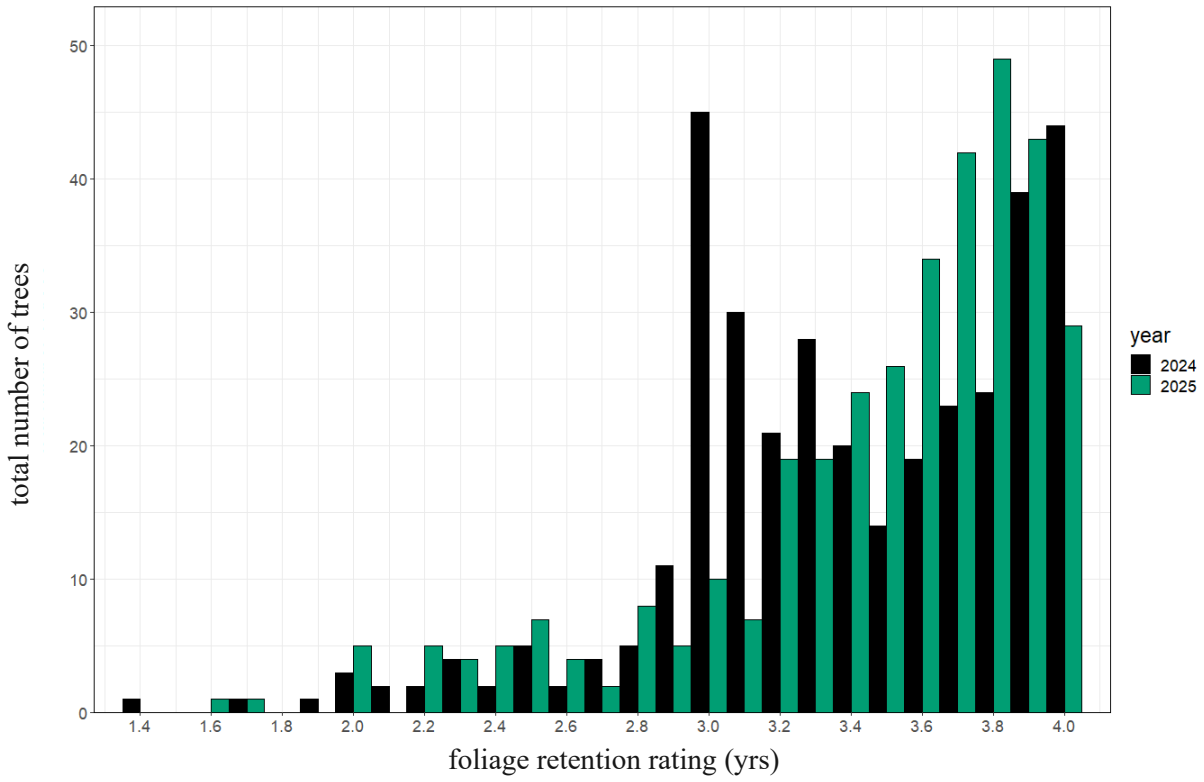

Figure 13. Bar plot showing the total number of trees rated within each foliage retention index by year. Ratings for 2024 are colored black, and the 2025 ratings are colored green

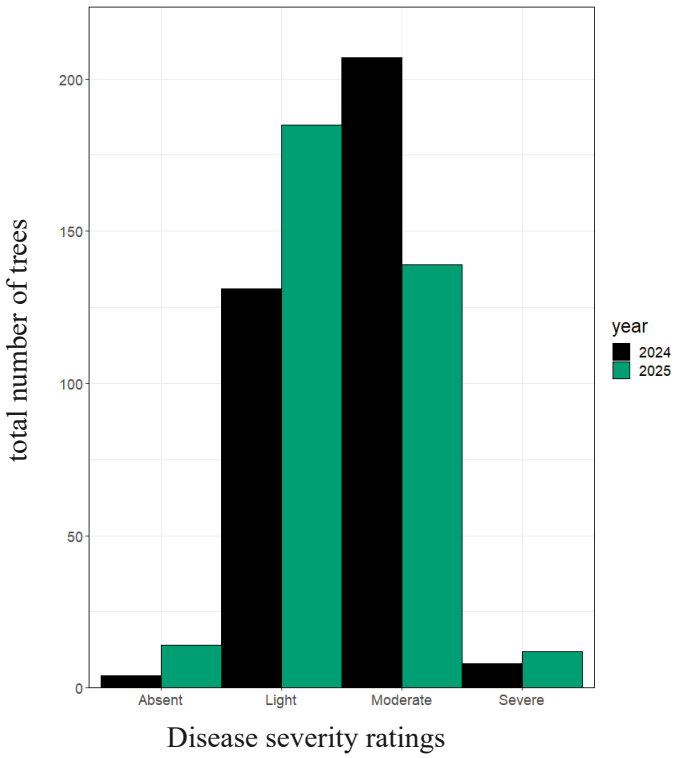

Figure 14. Bar plot showing the total number of trees rated within each foliage retention index by year. Ratings for 2024 are colored black, and the 2025 ratings are colored green

Literature Cited

Gómez-Gallego, M., LeBoldus, J. M., Bader, M. K. F., Hansen, E., Donaldson, L., & Williams, N. M. (2019). Contrasting the pathogen loads in co-existing populations of *Phytophthora pluvialis* and *Nothophaeocryptopus gaeumannii* in Douglas fir plantations in New Zealand and the Pacific Northwest United States. *Phytopathology, 109*(11), 1908-1921.

Maguire, D. A., Mainwaring, D. B., & Kanaskie, A. (2011). Ten-year growth and mortality in young Douglas-fir stands experiencing a range in Swiss needle cast severity. *Canadian Journal of Forest Research*, *41*(10), 2064-2076.

Mainwaring, D., Maguire, D., Ritóková, G., & Shaw, D. Volume growth losses within Swiss Needle Cast Infected Douglas-fir plantations, 2013-2020. *Swiss Needle Cast Cooperative*, *1*, 24.

Ritóková, G., Mainwaring, D. B., Shaw, D. C., & Lan, Y. H. (2021). Douglas-fir foliage retention dynamics across a gradient of Swiss needle cast in coastal Oregon and Washington. *Canadian Journal of Forest Research*, *51*(4), 573-582.

Screening for Swiss Needle Cast Tolerance in Douglas-fir Seedlings

2025 Research Activities of the Swiss Needle Cast Cooperative

Cristian González [1], Adam Carson[1], Jared LeBoldus[1,2]

[1] Swiss Needle Cast Cooperative, Forest Engineering, Resources, and Management, Oregon State University, [2] Department of Botany and Plant Pathology, Oregon State University
*Corresponding author: cristian.gonzalez@oregonstate.edu

Abstract

Swiss needle cast (SNC), caused by *Nothophaeocryptopus gaeumannii*, is a major foliar disease affecting Douglas-fir (*Pseudotsuga menziesii*) in the Pacific Northwest. Management strategies to reduce disease severity include silvicultural practices such as thinning to improve canopy airflow, site selection to avoid high-risk environments, and the identification of tolerant Douglas-fir families through tree breeding programs. Additionally, breeding programs have aimed to identify families with greater tolerance to SNC. However, effective screening for disease tolerance faces several technical hurdles, including developing efficient inoculum production and reproducible inoculation protocols that consistently induce infection under controlled conditions. In this study, we optimized a host-derived liquid culture medium for producing inoculum. We tested multiple inoculation methods to establish a reliable, standardized framework for screening Douglas-fir families for SNC tolerance. A needle extract broth (NEB) was developed using Douglas-fir needles and compared with malt yeast extract (MYE) for mycelial growth across various isolates. Growth in NEB was significantly faster than in MYE, reducing culture time by about 50% while maintaining similar biomass levels. We conducted controlled inoculation assays using localized branch inoculation with a temporary high-humidity enclosure, and whole-plant inoculation in greenhouse or high-humidity-chamber environments. Fungal colonization was quantified by qPCR at 3- and 6-month post-inoculation. Significant differences among inoculation methods were observed at 3 months, with localized branch inoculation showing stronger early colonization signals. By 6 months, Cq values decreased across treatments, indicating ongoing increases in fungal biomass, and differences among treatments diminished. Disease incidence ranged from 10% to 20% at 6 months, likely affected by sampling intensity and tissue relocation limitations. Because *N. gaeumannii* is a slow-developing pathogen, extended monitoring is necessary to connect early molecular detection with eventual symptom development.

Introduction

Douglas-fir (*Pseudotsuga menziesii*) is the most economically important tree species in Oregon, accounting for more than 70% of the harvest volume (Oswalt et al., 2019). *Nothophaeocryptopus gaeumannii*, an ascomycete fungus native to the Pacific Northwest, causes the foliar disease Swiss Needle Cast (SNC) in Douglas-fir. SNC blocks the stomata of needles, impairing gas exchange and causing premature needle loss and growth decline (Kelsey & Manter, 2004; Shaw et al., 2021). A recent economic analysis estimated that Swiss needle cast reduces the aggregate land expectation value of Oregon's current Douglas-fir plantations by $206.5–$430 million.

Field progeny trials evaluating Douglas-fir full-sib families for tolerance to SNC showed increased growth in the breeding population compared to Wood's run seedlots, along with genetic evidence supporting the effective use of additive genetic variation in tree breeding (Northwest Tree Improvement Cooperative, 2024). Previous research has demonstrated that early testing of seedlings can eliminate poorly performing families at the seedling stage, allowing rapid screening of large numbers of already selected families and enabling the selection of the most SNC-tolerant individuals for seed orchards (Temel et al., 2005). Additionally, Montwé et al. (2021) concluded that screening for Swiss needle cast tolerance in the coastal BC Douglas-fir breeding population is feasible if needle retention can be assessed. However, achieving this requires overcoming technical barriers, including efficient inoculum production, the inoculation method, and the assessment of disease damage.

Regarding the inoculum, previous work showed that *N. gaeumannii* grows very slowly on artificial culture media such as PDA, malt agar, or CMA, requiring approximately 2 to 16 weeks to produce sufficient mycelial biomass for DNA extraction (Graham et al., 2025). Traditionally, growing *N. gaeumannii* on solid media produces insufficient amounts of mycelium, requiring a large number of replicate growth plates. This increases workload, time, and space usage, as well as increasing the risk of contamination due to prolonged incubation in culture incubators. These limitations motivate the development of alternative inoculum production approaches that enable large-scale production in short periods.

Among the various culture media available for working with fungal pathogens, many are based on artificial carbon and nitrogen sources; however, all depend on artificial reagents that may not be ideal for fungal growth. Many fungi are difficult to isolate and exhibit slow growth in culture, often requiring the use of natural ingredients that better mimic their natural growing conditions. Studies with

Phytophthora have shown that mixed culture media, containing both artificial reagents and natural ingredients such as leaves and sterile plant material, can promote greater growth than artificial media (Guo & Ko, 1993; Guo et al., 2025). Host plant tissue extracts, such as those from celery stems or oakleaf goosefoot leaves, have been shown to support stronger sporulation and higher average growth rates compared to V8 medium, indicating that host plant tissues can be effectively used for pathogen culture (Guo et al., 2025). Similarly, liquid cultures, as alternatives to solid media, increase biomass production because fungi have more space for growth in a suitable, favorable environment (Hansen et al., 2013; Jackson et al., 2016).

Furthermore, another major challenge in developing tolerance to *N. gaeumannii* is establishing a successful inoculation protocol that ensures foliar infection and the development of fungal propagules within the needles. Several inoculation protocols have been developed for other plant–pathogen systems, particularly for controlled environments, and have been used to screen plant germplasm. These include detached leaf or stem assays, intact leaf assays, cotyledon screening, and petiole or leaf axil inoculation (Zalewska et al., 2025).

Therefore, the objectives of this work were: (1) to develop a host-based liquid culture medium from Douglas-fir needles for laboratory cultivation of *N. gaeumannii*; and (2) to develop an efficient inoculation and screening methods for evaluating SNC tolerance in Douglas-fir families.

Materials and Methods

Fungal inoculum production

Fungal inoculum of *Nothophaeocryptopus gaeumannii* was produced using a needle extract broth (NEB). A total of eleven genetically distinct *N. gaeumannii* isolates were used to account for isolate-level variability in mycelial growth and culture performance. Isolates were maintained on potato dextrose agar (PDA) prior to liquid culture assays. Healthy, symptomless Douglas-fir needles were collected from disease-free trees, weighed (15 g per 500 mL of final medium), and surface sterilized by sequential immersion in 70% ethanol for 1 min and 1–2% sodium hypochlorite for 1–2 min. Needles were rinsed three times with sterile distilled water, dried under laminar flow, and finely macerated using a handheld homogenizer.

The macerated material was transferred to 1-L Schott bottles, sterile distilled water was added to a final volume of 500 mL, and the suspension was gently boiled for 30 min. The resulting extract was filtered through sterile cheesecloth to remove coarse debris. Yeast extract (0.5%, w/v) and dextrose (2%, w/v) were added, and the medium was sterilized by autoclaving at 121 °C for 20 min.

After cooling, NEB was dispensed into 250-mL Erlenmeyer flasks (50 mL per flask) and inoculated with 5-mm mycelial plugs taken from the actively growing margins of *N. gaeumannii* colonies cultured on potato dextrose agar (PDA). Growth assays were conducted using multiple *N. gaeumannii* isolates to account for isolate-level variability in mycelial growth. Cultures were incubated in the dark at 20–22 °C with orbital shaking (100–150 rpm) for 4–6 weeks until sufficient mycelial biomass developed. For comparison, isolates were also cultured in malt yeast extract broth (MYE) under identical incubation conditions.

Mycelial biomass was harvested by filtration through sterile cheesecloth, and fresh weight was determined. For inoculum preparation, 20 g of fresh mycelium was homogenized for 2–3 min in a sterile blender and suspended in 1 L of sterile distilled water containing 0.01% (v/v) Tween 80. The inoculum suspension was used within 2 h of preparation.

Differences in mycelial growth rate between culture media were analyzed using Welch's t-test, which is robust to unequal variances and unbalanced sample sizes. Assumptions of normality and homogeneity of variance were evaluated using Shapiro–Wilk and Levene's tests, respectively. A non-parametric Mann–Whitney U test was additionally performed to confirm the robustness of the observed differences.

Inoculation treatments and experimental design

A total of 250 Douglas-fir seedlings (1–2 years old) were maintained under uniform greenhouse conditions and assigned to seven treatment groups following a completely randomized design (Table 1). Treatments included three inoculated treatments (T1, T2, and T3), two procedural controls (C1 and C2), and one absolute control (C3) (Table 1).

Treatment T1 consisted of localized inoculation of a single branch per seedling (n = 80) with macerated mycelium (20 g/L), applied twice at a 7-day interval. Following each application, the inoculated branch was individually enclosed in a pollination bag for 48–72 h to maintain high local humidity. Treatment T2 consisted of whole-plant inoculation conducted under high-humidity chamber conditions (>95% relative humidity with intermittent mist irrigation). It included two sub-treatments: T2A, which received a single

inoculation (n = 40), and T2B, which received two inoculations spaced 7 days apart (n = 40). Treatment T3 consisted of a single whole-plant inoculation, with seedlings maintained under standard greenhouse mist irrigation without an additional humidity enclosure (n = 40). The inoculated branch on each seedling was marked with flagging tape to facilitate identification of the inoculation point as branches elongated during growth.

Control treatment C1 followed the same localized branch-level procedure as T1, including pollination bag enclosure, but plants were sprayed with sterile distilled water containing 0.01% (v/v) Tween 80 only (n = 20). Control treatment C2 followed the same whole-plant procedure and high-humidity chamber conditions as T2 but received no fungal inoculum (n = 20). Absolute control plants (C3; n = 10) received no inoculation and no humidity manipulation.

Inoculations were performed using a fine-mist sprayer, applying 5–10 mL of suspension per plant to ensure complete needle wetting. For treatments receiving two applications (T1 and T2B), inoculations were repeated after 7 days. All experiments were conducted at 20 ± 2 °C under a 12-h photoperiod.

Table 1. Summary of inoculation treatments and post-inoculation environmental conditions.

Inoculum	Treatment	No. of plants	No. of applications	Post-inoculation conditions
Macerated mycelium (20 g/L)	T1	80	2	Pollination bags (48–72 h)
	T2A	40	1	Humidity chamber (>95% RH) with intermittent mist
	T2B	40	2	
	T3	40	1	Greenhouse mist irrigation only
Sterile distilled water	C1	20	1	Pollination bags (48–72 h)
	C2	20	1	Humidity chamber (>95% RH) with intermittent mist
	C3	10	1	Greenhouse mist irrigation only

Disease assessment and molecular detection

Fungal colonization was measured through quantitative PCR (qPCR) at 3- and 6-month post-inoculation. At each time point, four needles were collected from the previously inoculated area of the youngest fully expanded foliage, immediately frozen at −80 °C, and processed for DNA extraction using the NucleoSpin Plant II kit (Macherey-Nagel) in a 96-well format, with an increased lysis volume (975 µL PL2 buffer + 25 µL RNase A). DNA purity was evaluated with a NanoDrop spectrophotometer.

Simplex qPCR assays were performed in 20-µL reactions containing 5 µL of template DNA, 10 µL of PerfeCTa qPCR ToughMix (Quantabio), 400 nM of each primer, and 150 nM TaqMan probe. Thermal cycling conditions were 50 °C for 10 min, 95 °C for 5 min, followed by 40 cycles of 95 °C for 15 s and 60 °C for 1 min.

Quantification of *N. gaeumannii* was based on the β-tubulin gene using primers PGBT308F and PGBT429R and a FAM-labeled TaqMan probe (amplicon size: 122 bp). Standard curves, positive controls, and no-template controls were included in all runs. Fungal abundance was expressed as the ratio of *N. gaeumannii* DNA to *P. menziesii* host DNA to normalize for variation in DNA extraction and tissue input.

Results

Growth of *N. gaeumannii* in NEB vs MYE

Growth of *Nothophaeocryptopus gaeumannii* varied significantly between culture media. Across 11 isolates, mycelial growth in needle extract broth (NEB) consistently showed higher growth rates compared to malt yeast extract (MYE). In NEB, isolates produced 3.4–12.0 g of fresh mycelium within 25 days, corresponding to growth rates of 0.14–0.48 g day^{-1} (Fig. 1). In contrast, growth in MYE required 53 days to produce comparable biomass (4.2–12.6 g), with lower growth rates ranging from 0.08 to 0.24 g day^{-1}. Mean growth rate in NEB (0.31 ± 0.10 g day^{-1}) was significantly higher than in MYE (0.18 ± 0.05 g day^{-1}; Welch's t-test, $p < 0.0001$) a pattern that was also supported by a non-parametric Mann–Whitney U test ($p = 0.0016$). Despite occasional higher final biomass in MYE, NEB enabled significantly faster biomass accumulation, reducing culture time by approximately 50% (Fig. 2).

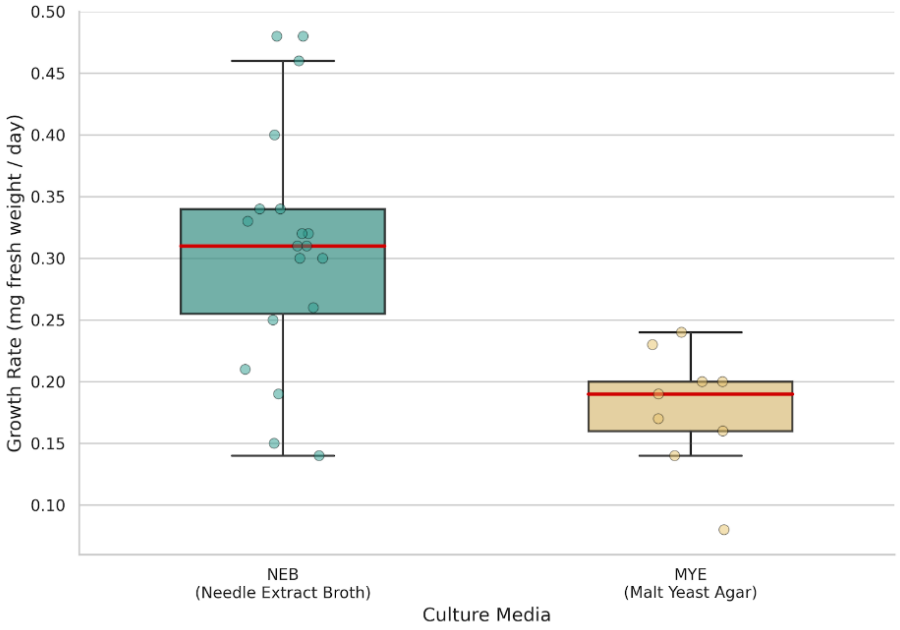

Figure 1. Comparison of mycelial growth rates of *N. gaeumannii* in needle extract broth (NEB) and malt yeast extract (MYE). Growth rate calculations were based on biomass accumulation over the culture period.

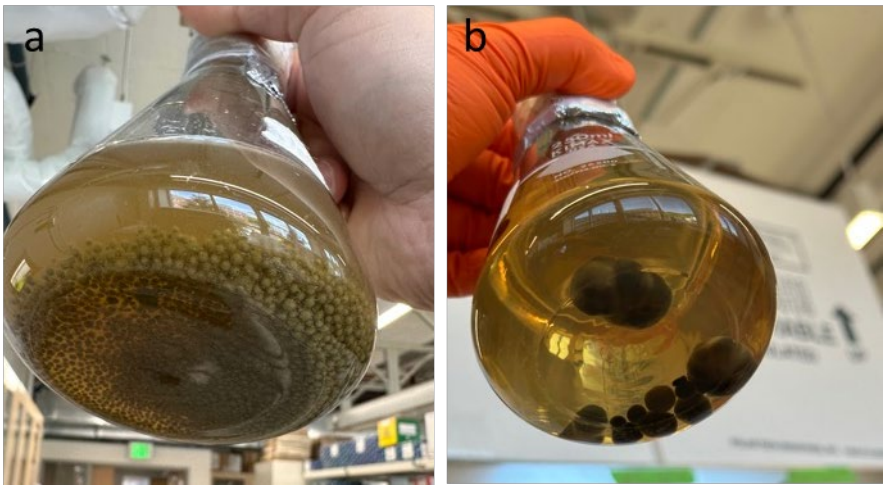

Figure 2. Mycelial growth of *Nothophaeocryptopus gaeumannii* in liquid culture: a) NEB after 25 days, b) MYE after 53 days.

Disease incidence

Infection by *Nothophaeocryptopus gaeumannii* was successfully established in all inoculated treatments at both evaluation time points (Fig 3). At 3 months post-inoculation, disease incidence ranged from 5% to 15% among treatments. T3 showed the highest incidence (15%), followed by T1 (12.5%) and T2A (10%), whereas T2B exhibited the lowest incidence (5%).

At 6 months post-inoculation, incidence increased in most treatments. T1 reached 20%, representing the highest infection frequency observed in the study. T2B increased markedly from 5% at 3 months to 17.5% at 6 months. T2A remained stable at 10%, while T3 slightly decreased to 10%. Overall, incidence across treatments at 6 months ranged between 10% and 20%.

Although infection frequencies remained moderate, all inoculated treatments consistently showed positive detections, confirming successful pathogen establishment and persistence over time.

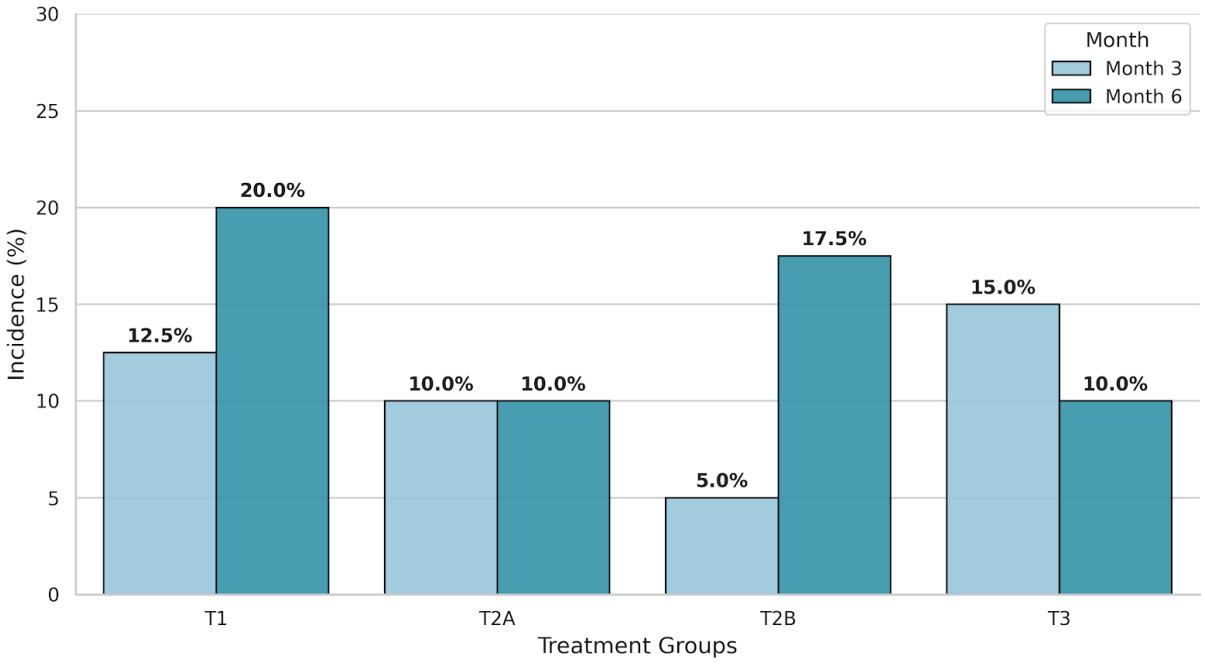

Figure 3. Disease incidence (%) of *Nothophaeocryptopus gaeumannii* across inoculation treatments at 3- and 6-month post-inoculation.

Fungal colonization quantified by qPCR

Quantitative PCR analysis provided a detailed assessment of fungal colonization dynamics. At 3 months post-inoculation, mean Cq values differed significantly among treatments ($F_{3,18} = 11.02$, $p < 0.001$). Treatment T1 exhibited a mean Cq of 33.19 (± 1.36 SD), with values ranging from 30.91 to 35.57, indicating relatively strong early colonization. T2A showed a higher mean Cq of 34.85 (± 0.63), while T3 presented a mean of 35.40 (± 1.16). T2B displayed the highest mean Cq at 37.93 (± 0.65), reflecting the lowest early fungal DNA accumulation among treatments. The relatively low standard deviation in T1 and T2A at 3 months suggests consistent colonization responses within those treatments, whereas T2B showed uniformly high Cq values, indicating delayed establishment.

At 6 months post-inoculation, Cq values decreased across most treatments, reflecting increased accumulation of fungal biomass over time. T2A showed a reduction from 34.85 to 31.53 (± 3.23), and T2B exhibited a pronounced decrease from 37.93 to 31.35 (± 3.90). T3 decreased from 35.40 to 30.66 (± 5.57), showing the lowest mean Cq at 6 months among treatments. In contrast, T1 showed a slight increase in mean Cq from 33.19 to 33.74 (± 2.94), although its distribution widened considerably, with values ranging from 25.25 to 37.34. This increased variability at 6 months suggests heterogeneous colonization intensity among individual seedlings.

Although differences among treatments at 6 months were not statistically significant ($F_{3,27} = 1.33$, $p = 0.284$), the downward shift in mean Cq values in T2A, T2B, and T3 indicates progressive fungal colonization. Because Cq values are inversely proportional to fungal DNA concentration, the reduction observed between 3 and 6 months confirms increasing mycelial accumulation within needle tissues over time. The substantial decline observed in T2B, from the highest mean Cq at 3 months (37.93) to one of the lowest at 6 months (31.35), suggests delayed but pronounced colonization under this treatment regime.

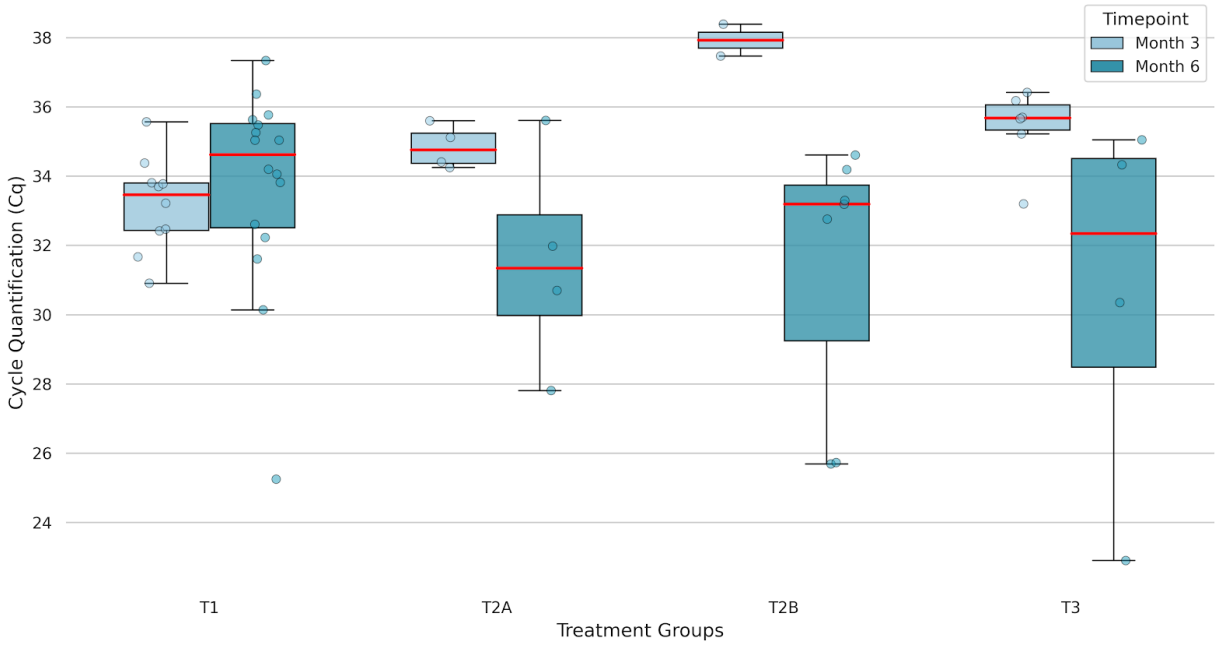

Figure 4. Quantification cycle (Cq) values of *Nothophaeocryptopus gaeumannii* across inoculation treatments at 3- and 6-month post-inoculation.

Overall, these results demonstrate a clear temporal progression of infection intensity. Early differences among inoculation methods were evident at 3 months, particularly with stronger early colonization under localized branch inoculation (T1). However, by 6 months, colonization levels converged among treatments, accompanied by increased within-treatment variability. The consistent reduction in Cq values across most treatments confirms the successful establishment of infection and the progressive development of the fungus within Douglas-fir needles.

Discussion

This study shows that controlled inoculation of *Nothophaeocryptopus gaeumannii* in greenhouse conditions reliably establishes infection and enables quantitative tracking of colonization over time, aligning with previous controlled infection research in Douglas-fir and other disease systems (Garg et al., 2008; Shaw et al., 2021). The decreasing Cq values between 3- and 6-months post-inoculation provide strong evidence of increasing fungal biomass within needle tissues, consistent with the slow, endophytic

growth typical of *N. gaeumannii*, in which fungal colonization occurs before visible symptoms appear (Kelsey & Manter, 2004; Stone et al., 2008).

Significant differences among inoculation methods were observed at 3 months post-inoculation, with localized branch inoculation combined with temporary high-humidity enclosure (T1) producing lower Cq values than other treatments. This indicates that maintaining high localized humidity during the early infection phase enhances initial fungal establishment, a pattern widely documented for foliar pathogens that require free moisture for successful penetration and early colonization (Garg et al., 2008; Zalewska et al., 2025). In contrast, whole-plant inoculation treatments showed higher Cq values at 3 months, suggesting less initial colonization. However, by 6 months post-inoculation, differences among treatments were no longer statistically significant, and Cq distributions overlapped considerably. This temporal convergence suggests that although the inoculation method significantly affects early infection success, long-term colonization is likely influenced primarily by host–pathogen interactions and the microenvironment within the needles rather than by initial environmental conditions.

Disease incidence remained moderate across treatments, ranging from 10% to 20% at 6 months. Although these values may seem lower than those observed under field epidemic conditions (Stone et al., 2008; Shaw et al., 2021), several methodological factors likely contributed to underestimations of infection frequencies. Sampling was limited to four needles per seedling at each evaluation time point. Because of the spatially heterogeneous, patchy colonization pattern typical of *N. gaeumannii* within needle cohorts (Kelsey & Manter, 2004; Shaw et al., 2021), limited sampling intensity reduces the likelihood of detecting infection when fungal distribution within a branch is uneven. Increasing the number of needles sampled per plant would likely improve detection sensitivity and provide more accurate incidence estimates.

Sampling accuracy may also have varied among treatments due to variations in methods for marking inoculation sites. In T1, the inoculated branch was enclosed in a pollination bag, allowing precise relocation of the treated tissue during later evaluations. In contrast, whole-plant treatments (T2 and T3) depended on manual marking of inoculated branches. Because Douglas-fir seedlings exhibited rapid vegetative growth during the experiment, the initial markings became less distinct over time. As a result, it cannot be fully confirmed that sampled needles at later time points came solely from tissue directly exposed to the inoculum. This possible mismatch between inoculated and sampled tissues may have led to lower apparent incidence and greater variability within treatments, especially at 6 months.

The observed decrease in Cq values from 3 to 6 months across most treatments indicates a progressive buildup of fungal DNA in needles. Because Cq values are inversely related to fungal biomass, this change confirms that infection intensifies over time. Notably, treatments like T2B and T3, which had relatively high Cq values at 3 months, showed significant reductions by 6 months, suggesting delayed yet notable colonization. These results imply that early fungal establishment and subsequent proliferation may follow different temporal paths depending on environmental conditions during the initial infection phase, which are heavily influenced by moisture availability and temperature regimes in both nursery and field settings (Stone et al., 2008; Shaw et al., 2021).

Collectively, these results suggest that early evaluation (3 months) is more sensitive for distinguishing differences in inoculation efficiency, while later evaluation (6 months) better captures cumulative fungal development and variability across treatments. For screening purposes, localized branch inoculation combined with a temporary humidity enclosure seems to provide the most consistent early colonization signal. However, since *N. gaeumannii* is a slow growing fungus under both controlled and field conditions, extended monitoring over time remains essential to understand infection dynamics fully and to observe the eventual appearance of visible signs and symptoms of disease. Molecular detection at early stages can reveal internal colonization. However, long-term assessments are necessary to link early fungal establishment to later disease expression (i.e., foliage retention, and pseudothecial occlusion~~)~~ as highlighted in field-based tolerance evaluations (Temel et al., 2005; Montwé et al., 2021). Future screening protocols should therefore consider increasing needle sampling, implementing more permanent tissue-labeling systems for tracking over time, and combining molecular quantification with physiological metrics, such as needle retention. Thahora debo ese improvements would enhance the accuracy of infection detection and the reliability of controlled SNC tolerance tests.

References

CoAdapTree. (2020). *Disease resistance*. University of British Columbia. https://coadaptree.forestry.ubc.ca/about/research-progress-highlights/disease-resistance/

Garg, H., Li, H., Sivasithamparam, K., Kuo, J., & Barbetti, M. J. (2008). The infection processes of *Sclerotinia sclerotiorum* in cotyledon tissue of a resistant and susceptible genotype of *Brassica napus*. *Annals of Botany, 103*(5), 733–744. https://doi.org/10.1093/aob/mcn255

Guo, L. Y., & Ko, W. H. (1993). Two widely accessible media for the growth and reproduction of *Phytophthora* and *Pythium* species. *Applied and Environmental Microbiology, 59*(7), 2323–2325.

Guo, L., Yang, M., Zhang, Q., Wang, S., Gao, R., Shi, X., Ma, C., Li, Q., & Zhang, H. (2025). A new method for *Phytophthora cactorum* culturing using host plant materials to prepare agar medium. *Scientific Reports, 15*, 1756.

Hansen, B. M., Venturi, V., Sørensen, J., & Nielsen, T. H. (2013). Glass bead cultivation of fungi: Combining the best of liquid and agar media. *Journal of Microbiological Methods, 94*(3), 234–239.

Jackson, M., Jaronski, S., & Dunlap, C. (2016). Liquid culture production of fungal microsclerotia. In S. S. Merlin (Ed.), *Methods in molecular biology* (Vol. 1477, pp. 275–284). Humana Press.

Kelsey, R. G., & Manter, D. K. (2004). Metabolic changes in Douglas-fir after infection with *Phaeocryptopus gaeumannii*. *Phytochemistry, 65*(17), 2423–2432. https://doi.org/10.1016/j.phytochem.2004.06.017

Montwé, D., Elder, B., Socha, P., Wyatt, J., Noshad, D., Feau, N., Hamelin, R., Stoehr, M., & Ehlting, J. (2021). Swiss needle cast tolerance in British Columbia's coastal Douglas-fir breeding population. *Forestry, 94*(2), 193–203. https://doi.org/10.1093/forestry/cpaa041

Shaw, D. C., Ritóková, G., Lan, Y. H., Omdal, D. W., Ramsey-Kroll, A., Comeleo, R., Cooley, T., & Filip, G. M. (2021). Swiss needle cast in Douglas-fir plantations of the Pacific Northwest: From nursery to mature plantations. *Forests, 12*(3), 298. https://doi.org/10.3390/f12030298

Stone, J. K., Coop, L. B., & Manter, D. K. (2008). Predicting the effects of climate change on severity of Swiss needle cast disease in Pacific Northwest forests. *Canadian Journal of Plant Pathology, 30*(2), 169–176. https://doi.org/10.1080/07060660809507518

Susaeta, A., Lal, P., Carter, D. R., & Alavalapati, J. R. R. (2024). Economics of forest disease: Swiss needle cast in Douglas-fir plantations of the US Pacific Northwest. *Journal of Environmental Management, 327*, 116913.

Temel, F., Johnson, G. R., & Adams, W. T. (2005). Early genetic testing of coastal Douglas-fir for Swiss needle cast tolerance. *Silvae Genetica, 54*(1–6), 9–14.

Zalewska, A., Gladysiak, A., & Kierzek, R. (2025). Inoculum and inoculation techniques: Key steps in studying pathogenicity and resistance to Sclerotinia stem rot in oilseed rape. *Frontiers in Plant Science, 16*, 1610049. https://doi.org/10.3389/fpls.2025.1610049

Pre-Commercial Thinning Experiment in Mixed Douglas-fir / Western Hemlock Stands

2025 Research Activities of the Swiss Needle Cast Cooperative

Cristian González [1], Adam Carson[1], Jared LeBoldus[1,2]

[1] Swiss Needle Cast Cooperative, Forest Engineering, Resources, and Management, Oregon State University, [2] Department of Botany and Plant Pathology, Oregon State University
*Corresponding author: cristian.gonzalez@oregonstate.edu

Abstract

Swiss needle cast (SNC), a foliage disease caused by the fungus *Nothophaeocryptopus gaeumannii*, has significantly affected Douglas-fir plantations in the Pacific Northwest by reducing growth and volume production, particularly in areas with moderate-to-high disease severity. In mixed Douglas-fir–western hemlock (Tsuga heterophylla) plantations, this reduction in Douglas-fir growth may influence species performance and has important implications for species selection during pre-commercial thinning (PCT). This project aims to identify effective pre-commercial thinning (PCT) prescriptions for maximizing stand volume production in mixed Douglas-fir and western hemlock plantations within the SNC impact zone. To address this objective, the Swiss Needle Cast Cooperative is establishing a network of experimental plots in young mixed~~-species~~ Douglas-fir-western hemlock plantations. The experiment will evaluate six thinning treatments representing different retention ratios of Douglas-fir and western hemlock. Candidate stands were identified using inventory data provided by participating forest companies and screened based on species composition and tree density thresholds to determine treatment suitability. Evaluations of candidate stands began in 2025, with experimental plot establishment scheduled for the 2026 field season.

Introduction

Swiss needle cast (SNC), a foliar disease caused by the fungus *Nothophaeocryptopus gaeumannii,* is a significant threat to Douglas-fir (*Pseudotsuga menziesii*) plantations in the Pacific Northwest. The pathogen reduces foliar retention and volume growth in Douglas fir, effects that are exacerbated in mixed-species systems with western hemlock (Tsuga

heterophylla). The infection pressure on Douglas-fir gives Western hemlock a competitive edge, reducing the silvicultural yield of Douglas-fir. Studies by Zhao et al. (2014) used the Swiss Needle Cast Cooperative (SNCC) GIS datasets, together with pre-commercial thinning (PCT) and control treatment data, to develop a diameter-growth model for western hemlock. Their results showed that western hemlock diameter increases with increasing SNC disease pressure, indicating a competitive advantage over Douglas-fir in infected stands. However, their analysis relied on stand conditions not directly applicable to early PCT decision-making. The average trees included in their study had a diameter at breast height (DBH) of approximately 15 cm and a crown ratio of 68%, and western hemlock heights were largely unavailable. Consequently, long-term differences in species growth trajectories under early thinning conditions remain poorly understood.

Many plantations within the SNC impact zone currently contain both Douglas-fir and western hemlock, either through natural regeneration or mixed planting, allowing managers to maintain flexibility under variable disease pressure. However, the optimal species retention strategies during pre-commercial thinning remain uncertain. A controlled silvicultural experiment using young, high-density mixed stands is therefore needed to better quantify competitive dynamics and provide more robust guidance for PCT management in SNC-affected forests.

Material and Methods

Experimental Design

The study will be conducted in young mixed plantations of Douglas-fir (*Pseudotsuga menziesii*) and western hemlock (*Tsuga heterophylla*) located within the Swiss needle cast (SNC) impact zone of western Oregon and Washington. Candidate stands were selected according to several criteria to ensure suitability for experimental thinning treatments and long-term monitoring.

Plantations were required to meet the following conditions: (1) stand age between 8 and 13 years, (2) high stand density (≥450 trees per acre, TPA), and (3) presence of both Douglas-fir and western hemlock. In addition, stands had to exhibit sufficient species composition and density to support multiple thinning treatments. These criteria ensured that selected stands would

allow meaningful comparisons among different strategies of species-retention under varying levels of SNC severity.

Each selected plantation will contain six experimental plots, each measuring 0.1 acres and surrounded by a 20-ft buffer to minimize edge effects. Each plot will be assigned to one of six pre-commercial thinning (PCT) treatments, each representing a different retained species composition and a target post-thinning density of 300–350 trees per acre (TPA) (Table 1). These treatments were designed to evaluate how species composition influences stand development under varying levels of Swiss needle cast disease pressure.

Table 1. Pre-commercial thinning (PCT) treatments evaluated in the experiment.

Treatment	Description	Target density (TPA)	Species composition
T1	Control (no thinning)	—	No trees removed
T2	Western hemlock only	300–350	100% western hemlock
T3	Douglas-fir only	300–350	100% Douglas-fir
T4	Mixed stand	300–350	75% western hemlock / 25% Douglas-fir
T5	Mixed stand	300–350	50% western hemlock / 50% Douglas-fir
T6	Mixed stand	300–350	25% western hemlock / 75% Douglas-fir

All thinning prescriptions will follow a best-tree selection approach, retaining the largest and healthiest individuals to promote optimal stand development.

A minimum of nine plantations will be selected and distributed across three SNC-severity classes defined by Douglas-fir foliage retention. These classes include lightly infected stands (≥2.75

years of foliage retention), moderately infected stands (2.0–2.5 years), and severely infected stands (≤1.75 years).

Tree measurements will be collected at Year 0 (pre-treatment baseline) and again at 3 and 6 years after thinning. Measurements will include diameter at breast height (DBH), total tree height, and height to live crown base for all trees. Foliage retention will be assessed on the five largest Douglas-fir trees per plot at each measurement interval to track changes in SNC severity relative to stand development.

The original study design specified a minimum stand density of 600 TPA. However, preliminary field survey and database screening indicated that this threshold was overly restrictive for available plantations. As a result, the minimum density threshold was revised to 450 TPA for the combined density of Douglas-fir and western hemlock. A 1.25× density buffer was maintained to ensure that post-thinning targets of 300–350 TPA could still be achieved through best-tree selection.

Stand Dataset and Filtering

Stand inventory data provided by participating companies were compiled into a screening database to evaluate treatment feasibility across candidate plantations. The selection process followed a stepwise filtering approach. First, a minimum density threshold of 450 TPA for the combined density of Douglas-fir and western hemlock was applied. This filter ensured that stands would retain sufficient stocking after thinning to meet experimental design requirements. Second, stands were evaluated for treatment feasibility based on species composition and density. To provide sufficient experimental flexibility, stands were required to support at least three of the six potential thinning treatments defined in the experimental design.

Finally, candidate stands will be verified during field survey visits to confirm stand structure, species composition, accessibility, and operational feasibility for plot establishment. If field verification reveals that some candidate stands do not meet the expected conditions, the selection criteria may be expanded to include stands capable of supporting at least two treatments, ensuring adequate replication within the experimental network.

Analysis

Stand-level responses to pre-commercial thinning will be evaluated by analyzing basal area (BA) growth under different levels of SNC severity. Tree-level diameter increment models will be developed separately for western hemlock and Douglas-fir. These models will incorporate the competitive effects of neighboring trees, distinguishing between intraspecific competition (same species) and interspecific competition (other species).

The resulting growth models will be used to evaluate how different thinning prescriptions influence species growth trajectories and competitive dynamics under varying levels of disease pressure. Height growth patterns for both species will also be incorporated to support silvicultural recommendations for pre-commercial thinning in mixed species stands affected by SNC to maximize volume production.

Results

Stand Screening and Selection

Inventory data from participating forestry companies were aggregated into a comprehensive database containing 337 candidate plantations located within the Swiss needle cast impact zone of western Oregon and Washington. The stand selection process was conducted in two sequential phases to ensure the long-term experimental feasibility of the study.

A primary filter applied a minimum density threshold of ≥450 trees per acre (TPA), considering only the two focal species of this study: western hemlock (WH) and Douglas-fir (DF). This step excluded stands dominated by non-target species or those with insufficient stocking to support the experimental design. After applying this filter, 263 stands (78% of the initial dataset) met the density requirement and were retained for further evaluation.

Figure 1 illustrates the distribution of all candidate stands included in the screening process, showing the relationship between Douglas-fir and western hemlock density across the dataset. The dashed diagonal line represents the 450 TPA density threshold, corresponding to the minimum combined density of the focal species required for experimental consideration. Stands falling below this threshold, indicated in red (n = 113), were excluded from further consideration

due to insufficient stocking to support the experimental design. Stands above the threshold were further classified according to their treatment versatility. High priority stands, shown in green (n = 42), met the density requirement and exhibited species compositions capable of supporting at least three of the six proposed pre-commercial thinning (PCT) treatments. In contrast, gray points (n = 111) represent stands that met the density threshold but were strongly dominated by a single species, limiting the number of feasible treatment combinations. Application of this filter reduced the candidate pool to 42 high-priority plantations, representing 12.5% of the original dataset, and prioritized them for field verification.

The distribution of points along the axes indicates a strong tendency toward single-species dominance, highlighting the relative scarcity of balanced, high-density mixed stands within the coastal plantation inventory.

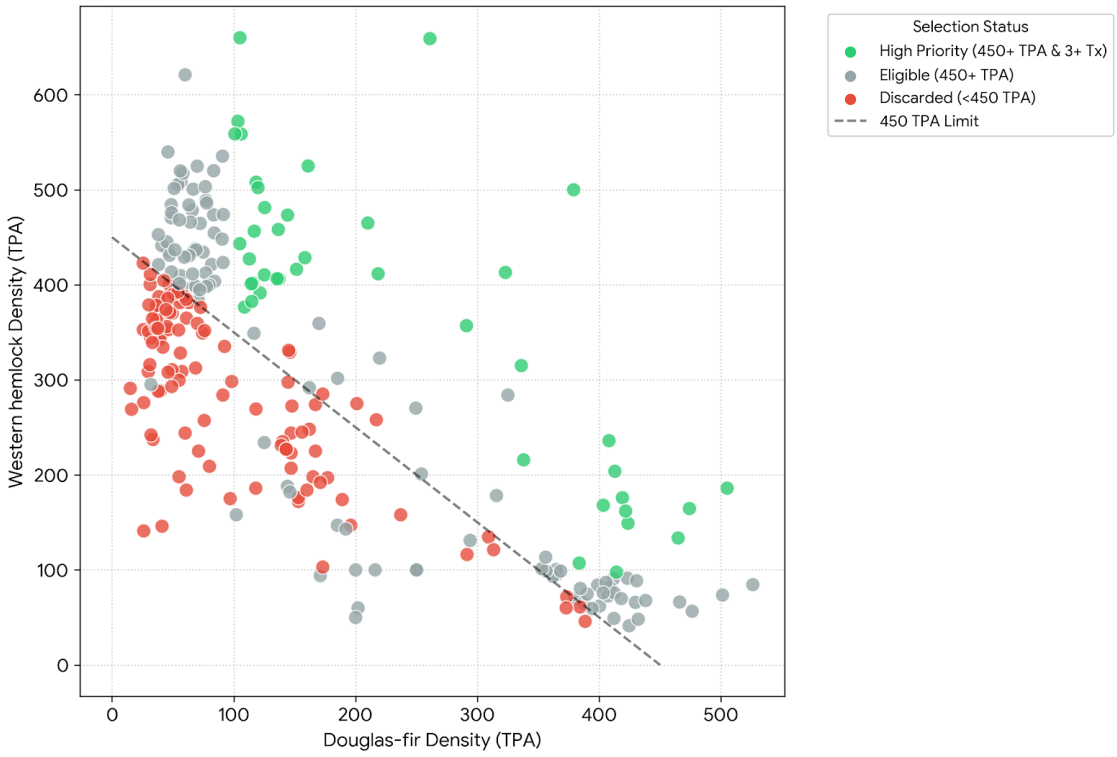

Figure 1. Stand composition and selection eligibility based on a minimum density threshold of 450 TPA and treatment versatility.

Treatment Feasibility and Distribution

The treatment feasibility analysis showed that most candidate stands exhibited strong single-species dominance, which limited the number of possible thinning prescriptions. Only 42 stands (12.5% of the original dataset) met the high-priority criterion by possessing the density and species composition necessary to support at least three of the six experimental treatments.

Eligibility varied considerably among treatments (Figure 2). The control treatment (T1) was the most widely supported, with 55 candidate stands. Treatments favoring western hemlock retention were also relatively common, including the western hemlock-only treatment (T2) and the 75% WH / 25% DF mixture (T4), each supported by 29 stands. In contrast, treatments requiring higher proportions of Douglas-fir were less frequent. The Douglas-fir-only treatment (T3) was feasible in 12 stands, while the balanced 50/50 mixture (T5) and the 25% WH / 75% DF mixture (T6) were feasible in 14 stands each.

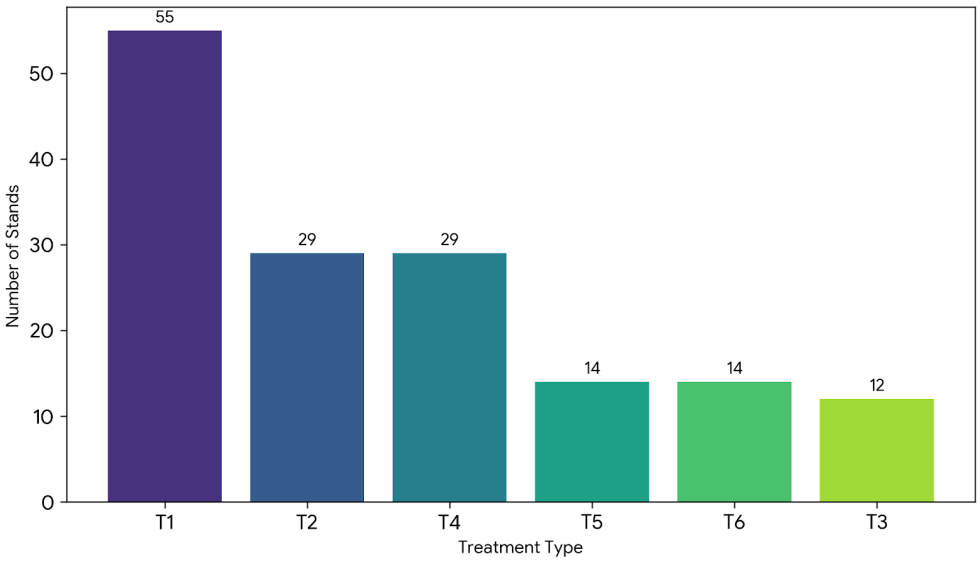

Figure 2. Frequency of candidate stands capable of supporting each pre-commercial thinning treatment.

The geographic distribution of candidate stands shows a clear regional pattern (Figure 3). Stands located in coastal Washington tend to be dominated by western hemlock, whereas plantations along the Oregon coast more frequently contain higher proportions of Douglas-fir. Because the experimental design requires representation across light, moderate, and severe Swiss needle cast severity classes, the final number of eligible sites may be further reduced once foliage retention levels are confirmed.

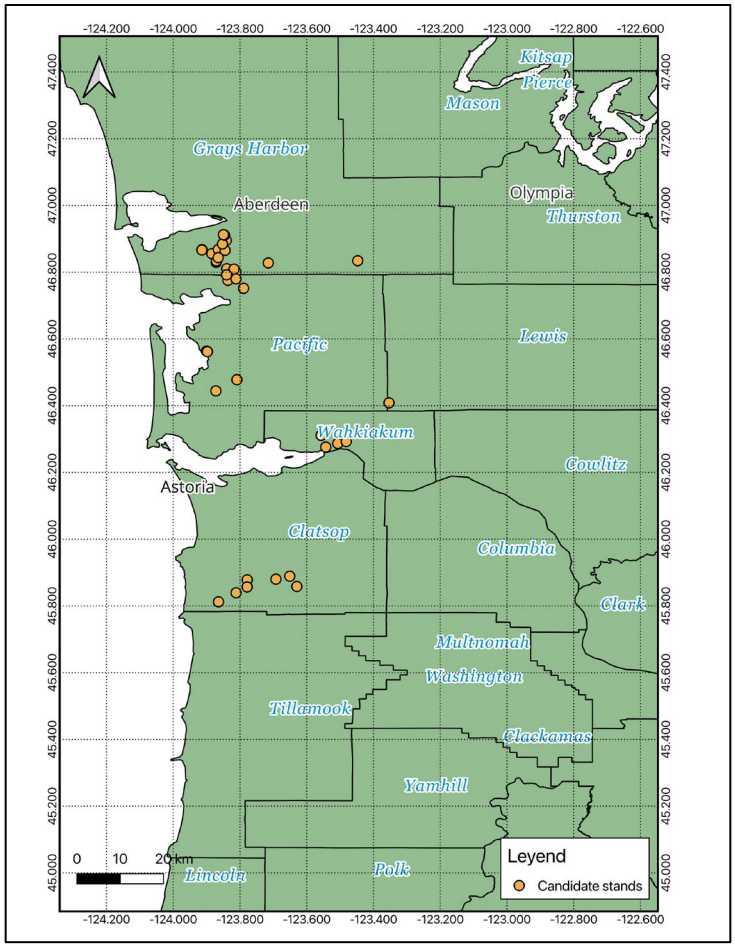

Figure 3. Geographic distribution of candidate stands selected for field verification.

Discussion

The initial phase of this study revealed a substantial discrepancy between the broad availability of young plantations and those that meet the technical requirements for the experimental design. Although the consolidated database initially included 337 candidate stands, the filtering process reduced this pool to 42 high-priority sites capable of supporting the experimental treatments. This reduction highlights the difficulty of identifying plantations with sufficient stocking and an appropriate mixture of Douglas-fir and western hemlock to support mixed-species silvicultural plots.

The application of the 25% density buffer (TPA × 1.25) proved to be the most restrictive, yet essential, component of the filtering process. This buffer is necessary because pre-commercial thinning (PCT) fundamentally relies on best-tree selection. Without an initial density substantially higher than the desired residual density (300–350 TPA), the opportunity to select trees based on superior stem form, vigor, and health is greatly reduced. Stands that already approach the target density cannot effectively remove suppressed or diseased individuals, which would compromise the long-term productivity and comparability of the experimental plots.

The number of viable candidate stands may decrease further as the study moves into the next stage of filtering based on Swiss needle cast (SNC) severity. The experimental design requires representation across light, moderate, and severe foliage retention classes. Consequently, stands that meet the density and species composition criteria may still be excluded if they do not exhibit the appropriate level of disease severity required for the experimental matrix. This potential severity bottleneck reinforces the importance of maintaining a large initial pool of candidate stands to ensure that the final network adequately represents the range of disease conditions present across the SNC coastal region.

A clear regional pattern also emerged from the screening process. Candidates in coastal Washington tend to be dominated by western hemlock, while plantations along the Oregon coast often feature a larger Douglas-fir component. Despite these differences in species dominance, nearly all viable candidates are located within the SNC coastal impact zone, confirming that disease pressure remains an important ecological factor influencing competitive dynamics between these species.

Next Steps

The immediate priority of the project is to complete field validation of the remaining 17 priority stands. These survey visits will evaluate spatial uniformity within stands to ensure that species are sufficiently intermixed to support the planned treatment ratios. Operational factors, including road access, terrain conditions, and topographic uniformity, will also be assessed before final site selection.

Once the final nine experimental sites are selected, formal establishment of the 0.1-acre experimental plots will begin. A comprehensive Year 0 baseline inventory will be conducted, including measurements of diameter at breast height (DBH), total tree height, and height to live crown base for all trees within each plot. In addition, foliage retention will be quantified on the largest Douglas-fir trees to characterize SNC severity at the beginning of the experiment.

These baseline measurements will define the pre-treatment conditions of each stand and will serve as the reference point for evaluating how different thinning prescriptions and species compositions influence basal area growth, competitive dynamics, and stand resilience over the six-year monitoring period. All plots will then be remeasured at year 3 and 6 post establishment.

References

Zhao, W., Mainwaring, D. B., Maguire, D. A., Kanaskie, A., & Meek, P. (2014). Western hemlock growth response to Swiss needle cast severity in coastal Oregon plantations. Forest Ecology and Management, 318, 78–87. https://doi.org/10.1016/j.foreco.2014.01.013

Journal of Forestry
https://doi.org/10.1007/s44392-025-00054-9

ORIGINAL PAPER

Forum Article: Why a Network of Old-Growth and Mature Forests Across the Douglas-Fir Region is Good for the Timber Industry

David C. Shaw[1]

Received: 24 April 2025 / Accepted: 28 July 2025
© The Author(s) 2025

Abstract

The Douglas-fir region of the Pacific Northwest is one of the most productive forestry regions in the world, combining sustainable timber production with native species management, particularly Douglas-fir. This landscape also supports a network of old-growth and mature forests that sustain the biodiversity of these regional forests, including beneficial biota such as fungi and other microbes, insects and other invertebrates, vertebrates, and lichens and other plants. I believe it is in the interests of the timber industry to protect these remaining old-growth and older mature forests because they contain a reservoir of beneficial biota that aids in protection and health of managed plantations. Beneficial invertebrates include parasitoid wasps, predaceous insects and spiders, pollinators, and decomposers, while beneficial microbes include mycorrhizal fungi, decomposers, and biocontrol agents. Beneficial vertebrates, especially the insect gleaning birds and bats are also important, as well as many plants and lichens. These organisms enhance forest resilience by protecting younger trees from pests and pathogens and contributing to nutrient cycling and soil health. Although forest plantations necessarily simplify forest structure and composition, potentially excluding this biodiversity, older forests help maintain this critical beneficial biota. Contrary to a common belief that old-growth forests are a source of pests and pathogens, their above- and below-ground complexity often provides habitat for organisms that moderates the influence of pests and pathogens. Therefore, on

Study Implications

Old-growth and mature forests of the Douglas-fir region have an important role in sustaining the biodiversity of beneficial biota that protect younger trees from pests and pathogens and contribute to nutrient cycling and soil health. Beneficial biota, in the context of forestry, are organisms that support tree health directly by preventing pest attack and indirectly by enhancing tree vigor. These organisms are generally most diverse in older stands. Although forest plantations necessarily simplify forest structure and composition, potentially excluding this biodiversity, older forests help maintain this critical beneficial biota. I believe it is in the interest of the timber industry to protect the remaining old-growth and older mature forests that currently exist in the Douglas-fir region because they directly benefit the health of younger Douglas-fir forests.

Extended author information available on the last page of the article

Published online: 18 October 2025

balance, I believe that protecting old-growth and mature forests across the region is essential for maintaining forest health and supporting the long-term productivity of Douglas-fir plantations.

Keywords Forest health · Beneficial biota · Old-growth · Plantations · Douglas-fir

Introduction

The Douglas-fir region (western Oregon and Washington) (Franklin 1981) is a productive forest region that produces timber for homes and buildings through a system of sustainable forestry built on native species, particularly Douglas-fir. This same landscape also includes a network of old-growth and mature forests that sustain regional biodiversity (Thomas et al. 2006; Spies et al. 2019). Increasingly, I have come to believe that this biodiversity contributes to the health of younger forests and expansive plantations and provides a reservoir of beneficial biota that can aid in protection of younger forests from pests and pathogens. And for this reason, it is in the interests of the timber industry to protect the remaining old-growth and older mature forests in the Douglas-fir region.

I define beneficial biota, in the context of forestry, as organisms that support tree health directly – such as parasitoid wasps that kill defoliating caterpillars or symbiotic mycorrhizal fungi that provide nutrients to the tree – and indirectly by enhancing tree vigor – such as microbiota enhancing nutrient cycling and improving soil conditions. Beneficial biota is critical to the health of individual trees in plantations and naturally regenerated forests, and include fungi and other microbes, insects and other invertebrates, vertebrates, and lichens and other plants. Diversity of these organisms is generally greatest in older stands (Ruggiero et al. 1991; Lattin 1993; Carey et al. 1996; Schowalter 2017; Spies et al. 2018).

As the intensity of forest management increases, biodiversity decreases (Demarais et al. 2017; Tomao et al. 2020). Therefore, it is natural that older, more complex stands would be more biodiverse. Long-standing ecological principles and field observations suggest that old forests with diverse species composition, complex vertical structure, rich understory vegetation, large snags and down woody debris, spatial heterogeneity, and old, well-developed tree crowns and root systems support higher biodiversity than young homogeneous plantations (Mannan et al. 1980; Ruggiero et al. 1991; Lattin 1993; McCune 1993; Michel and Winter 2009; Schowalter 2017; Spies et al. 2018).

Young Douglas-fir forest pests and pathogens are now becoming a key feature of regional Douglas-fir forest health (Agne et al. 2018), while I am not aware of any evidence that a lack of beneficial biota is affecting productivity and health of industrial plantations. However, I contend that it is likely that today's plantations benefit from the broader regional mosaic of forest age classes, particularly the remaining old-growth and mature stands that serve as refugia for beneficial biota (FIGURE 1). As of 2018, approximately 40.7% of the forests in western Oregon and Washington were under 50 years old, 52.7% were between 50 and 250 years

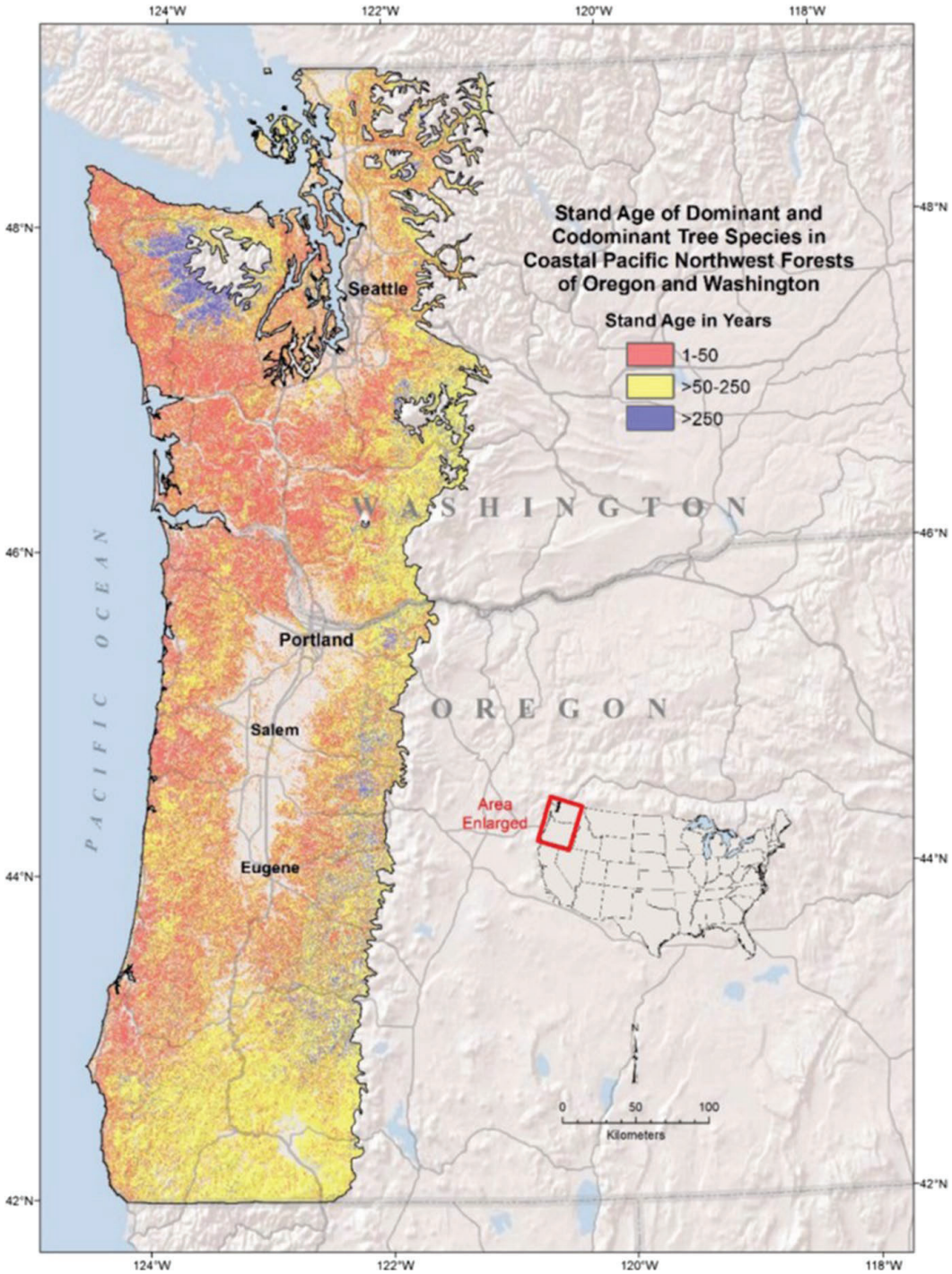

Fig. 1 Stand age classes in 2018 in the Douglas-fir region. Color codes indicate three age classes for dominant and codominant tree species; red = 1–50 year-old stands (4.12 million ha, 40.7%), yellow = 50–250 year-old stands (5.34 million ha, 52.7%), and blue ≥ 250 years old (0.67 million ha, 6.6%). (Source: GNN maps for Washington, Oregon, and California, 2012, https://lemma.forestry.oregonstate.edu/data/ download/?file=/export/grids/sppsz/r2/gnn_sppsz_2014_08_28.zip). Map from Agne et al. 2018)

old, and 6.6% were over 250 years old (Agne et al. 2018). Mature forests appear to be widely distributed through the intensively managed landscape, while old-growth stands are concentrated in the Olympics and western Cascade mountains and scattered in the Oregon Coast Range.

I have been working for over four decades in the field studying forest biology, ecology, tree health, and silviculture, with a focus on forest pathology and forest entomology in old-growth, mature, and plantation systems across the Douglas-fir region from the Klamath-Siskiyou Mts. in Oregon to the North Cascades of Washington. I have spent the last 20 years working in Oregon as a state-wide extension forest health specialist, a Professor of forest health, and as Director of a research cooperative focused on health of Douglas-fir plantations. I previously worked at field stations for 14 years on the western Olympic Peninsula and at the Wind River Experimental Forest in Washington, while my dissertation work concerned root disease of young-growth plantation trees on the western Olympic Peninsula and Willapa Hills, Washington. I worked on the Mt. Baker-Snoqualmie and Olympic National Forests doing forest vegetation classification surveys, did my Master's thesis in the North Cascades, Washington, and I've been involved in long-term tree demography and mortality monitoring in natural forests of western Oregon and Washington, with a focus on the H.J. Andrews (western Cascades Oregon), Wind River (western Cascades Washington), and Cascade Head (Oregon Coast Range) Experimental Forests. I fully understand the causes and consequences of tree mortality and tree health in both managed and unmanaged forests across the breadth of the Douglas-fir Region.

From my perspective on forest health, I believe there is a story here concerning the relevance of older age classes of trees and the role they play in the health of younger stands: in particular, how the current network of old-growth and mature forests helps sustain the biotic communities that benefit younger trees in forest plantations. In this Forum, I briefly summarize the diversity of beneficial biota found in Douglas-fir forests. I then discuss the principal forest pests of Douglas-fir plantation systems and some of their epidemiology in old-growth. I conclude that older Douglas-fir forests, despite common misconceptions, are a net benefit to plantation forest health management and that maintaining a landscape mosaic that includes these legacy stands is essential for the long-term health and productivity of Douglas-fir forestry.

This Forum piece is not a review of how old-growth and older mature forests should be integrated into landscapes to enhance biodiversity (e.g. Lindenmayer and Franklin 2002; Betts et al. 2021), nor is it a review of how biota can move from old-growth to younger stands (e.g. Amaranthus et al. 1994; Schowalter 1995), but this is a call to protect the remaining old-growth and older mature forests that currently exist on the landscape because once we lose this beneficial biodiversity, it is gone. I'm certainly not telling industry how to manage their lands. However, I believe that it is in the interest of the timber industry for these remaining old-growth and older mature forests to be protected because it is essential for the maintenance of the biodiversity necessary for sustainable plantation tree health.

Beneficial Biota

Beneficial biota occurs across the spectrum of forest age classes and are not limited to old-growth forests. However, old-growth and older mature forests have rich biodiversity of these groups which have important ecological functions and benefits to forest plantations in the region. In natural and planted forests of the Douglas-fir region, biodiversity peaks prior to canopy closure (~ 10–12 years in plantations), and then declines, as the site becomes completely dominated by conifer trees (Swanson et al. 2010, Harris and Betts 2021, Rivers and Betts 2021). Although somewhat dependent on whether any mid-rotation harvesting takes place, structural complexity, tree species composition, and spatial heterogeneity increase with stand age (Franklin et al. 2002) which is linked to increasing biodiversity, including beneficial biota (Ruggiero et al. 1991; Michel and Winter 2009; Schowalter 2017). On the eastern side of Vancouver Island, British Columbia a chronosequence approach was taken to study how forest management influences biodiversity in Douglas-fir forests (Trofymow et al. 2003). They found that regenerating forests (5–10 yrs), were most distinct from the closed canopy older forests, that many attributes of biodiversity recovered by 75–95 years, and that old-growth was most diverse, but was not always so for specific biotic groups.

Beneficial Fungi and Other Microbes

Beneficial fungi and other microbes include decomposers, and microbial biocontrol agents of the microbiome, as well as symbiotic mycorrhizae. Microbial decomposition of organic material is an essential component of forest productivity and nutrient cycling in the Douglas-fir region (Fogel and Hunt 1983; Edmonds 1991; Molina et al. 1999). Though plantation forests are apparently not limited by decomposers, old-growth forests have greater biodiversity due to a wider variety of substrates such as large snags, large down logs, and diverse wood sizes and ages (Franklin et al. 1981; Lattin 1993; Molina et al. 1999). Literature reviews in global forests indicate a variety of woody debris maintain higher diversity of these microbes (Abrego and Salcedo 2013; Tomao et al. 2020).

The plant microbiome, comprising microbes that are on, in, and surrounding roots, stems, bark, and leaves, is increasingly recognized for its role in promoting plant health (Trivedi et al. 2020). These microbes can contribute to growth, enhance nutrient uptake, increase stress tolerance, and aid resistance to pathogens. For example, some plant endophytes (fungi that live within live plant parts such as needles, stems and wood) are thought to produce chemicals that are antagonistic to insect herbivores (Carroll 1991; Stone et al. 1996). However, the microbiome may also include pathogens and latent pathogens such as *Nothophaeocryptopus gaeumannii*, cause of Swiss needle cast. The interaction of biota within the microbiome, and how some microbes are biocontrol agents of pathogens, is an active area of scientific discovery (Trivedi et al. 2020). Recently, Graham et al. (2025), have demonstrated that some metabolite extracts from endophytes of

Douglas-fir foliage suppress growth of *N. gaeumannii*, indicating the potential for biocontrol. While Kiser et al. (2019) suggest that Douglas-fir endophytes may have potential for natural pharmaceuticals in human medicine.

Old-growth trees support a diversity of microbes due to their complex structure, age of substrates, complex microenvironments, epiphytic lichens and mosses, and diversity of live and dead woody material in the crown (Caldwell et al. 1979; Carroll et al. 1980; Stone et al. 1996). Gervers et al. (2022) recently investigated the biodiversity of endophytic fungi in foliage of six old-growth trees in the western Oregon Cascade Mts. and found 218 Operational Taxonomic Units (OTUs). OTUs are unique groups of DNA sequences, implying different species. This indicates a very high level of diversity of fungi within needles of Douglas-fir and individual needles typically have numerous fungal species within them. Gervers et al. (2022) relate this diversity to the complex microenvironment within tree crowns and the age classes of retained needles. Older Douglas-fir trees consistently have higher foliage retention than nearby young plantation trees (Lan et al. 2019). Because microbiome biodiversity increases with diversity of plant species (Dastogeer et al. 2020) and in large old tree crowns (Stone et al. 1996), old-growth forests may generally have higher diversity than plantations.

Mycorrhizae (Fig. 2) are symbiotic fungi that assist trees with nutrient and water uptake and are part of the microbiome (Trivedi et al. 2020; Dastogeer et al. 2020). To be classified as mycorrhizal, the fungal hyphae must both penetrate the root and extend into the surrounding substrate, acquiring carbon from the host plant while supplying it with soil-derived resources (Allen et al. 2003). Conifer trees, including Douglas-fir, require mycorrhizal associations for normal growth and development (Trappe and Strand 1969), while mycorrhizae aid in protecting root tips from pathogens (Sylvia and Sinclair 1983). Plantation forests are generally not limited by mycorrhizal fungi, but old-growth forests tend to have more unique species (Smith et al. 2002) and one study in mature (180 year-old) Douglas-fir forest fragments and adjacent plantations found that hypogeous mycorrhizal fungi (truffles) were more numerous and had higher biomass in the mature forest (Amaranthus et al. 1994). A recent review of the literature suggests that

Fig. 2 Ectomycorrhizal root tip on a conifer. Photo Robert L. Anderson, USDA Forest Service, Bugwood.org

ectomycorrhizal fungi diversity decreases with increasing intensification of forest management (Tomao et al. 2020).

Beneficial Insects, Spiders and Other Invertebrates

Arthropod communities are significantly more diverse and compositionally distinct in natural old and mature Douglas-fir forests compared to young plantation forests (Lattin 1993; Schowalter 2017). This heightened diversity is driven by diverse tree species composition, well developed understory vegetation, diversity of dead wood age classes and sizes, diversity of live tree sizes and conditions, variation in vertical habitat stratification in tall trees, and complex soil and litter layers. Simple manipulative studies of needle density and branching complexity in Douglas-fir canopies have shown that canopy complexity increases the diversity of predaceous spiders (Halaj et al. 2000). Schowalter (2017) suggests that a value of old-growth forests lies in their role as a reservoir of native species that are capable of colonizing young forests where they contribute to essential ecological functions that support forest health, such as by aiding in suppression of insect outbreaks of herbivorous insects.

Among the most important beneficial invertebrates are parasitoid wasps and flies, predaceous insects, spiders and mites, decomposers, fungivores, and pollinators. Parasitoid wasps (Fig. 3) and flies lay eggs on or in other insects and their larvae consume the host, ultimately killing it (Burke and Sharanowski 2024). The parasitoid wasps affect nearly all insect groups, especially defoliators, and are thus vital biocontrol agents of insect pests (Burke and Sharanowski 2024). Some are generalists, while others are highly specialized. In one study from forests of New Zealand, their biodiversity was associated with the diversity of vegetation types, plant diversity and coarse woody debris (Kendall and Ward 2016). Predaceous insects, along with spiders and mites, also play major roles in insect pest biocontrol (Schowalter 2017), and old-growth forests are known sources of these predators for plantations (Schowalter 1995). Arthropods are key components of decomposer communities

Fig. 3 *Bracon* species (Coleoptera: Braconidae), a parasitoid wasp of defoliators. Photo Oregon State Arthropod Collection

that teem with mites and other invertebrates (Moldenke 1999). Their biodiversity is typically greater in old-growth forests where substrate is diverse (Lattin 1993). Pollinators are obviously not necessary for Douglas-fir, but they are crucial to understory shrubs and herbaceous plants in older forests, and are diverse in young early seral stands before canopy closure (Rivers and Betts 2021; Ulyshen et al. 2024).

Beneficial Vertebrates

Beneficial vertebrates that directly aid tree health include insect-eating birds that glean and probe the entire tree for insect prey, as well as swoop and flit to pick off flying insects. Chickadees, kinglets (Fig. 4), nuthatches, creepers, flycatchers, swallows, warblers, woodpeckers and other insectivorous birds spend much of their waking hours eating insects. I've observed red-breasted nuthatches consistently bringing geometrid caterpillars (inch worms, Lepidoptera: Geometridae) to their cavity 55 m up in the dead top of an old Douglas-fir tree. Geometrids are important herbivores. In western Oregon and Washington, year-round residents glean the tree all year, regional migrants move locally and harvest insects seasonally, while neotropical migrants come and harvest the spring and summer emergence of insects in our forests.

Mammals, amphibians and reptiles also feed on insects and other invertebrates, and bats are important insectivores in Douglas-fir forests (Christy and West 1993) as well as important consumers of pest species around the globe (Tuneu-Corral et al. 2023). Bat activity and roosting is greater in old-growth forests than in mature and young forests (Thomas 1988; Thomas and West 1991; Christy and West 1993). However, the bats apparently forage in a variety of habitats, not exclusively in old-growth where they roost. Reductions in old-growth forest habitat could have an impact on breeding bat populations (Thomas 1988; Thomas and West 1991). Another important forest health benefit of mammals includes dispersal of the spores of mycorrhizal fungi that fruit below-ground (truffles) and require mammals, such as flying squirrels, to dig them up and disperse their spores (Maser and Maser 1988;

Fig. 4 Golden-crowned kinglet. An important year-round resident insectivore

Luoma et al. 2003). Vertebrate predators also prey on plantation pest vertebrates such as deer and gophers (Ingles 1965).

The relationship of vertebrates to forest composition, structure, complex habitat features, and forest age has been especially well studied in the Douglas-fir region (Thomas et al. 1988; Ruggiero et al. 1991; Christy and West 1993; Blaustein et al. 1995; McGarigal and McComb 1995; Hansen et al. 1995; McComb et al. 2007; Spies et al. 2018; Phalan et al. 2019). All these studies support the notion that old-growth forests are important to wildlife in the Douglas-fir region. Although not all wildlife requires older forests (Brunnell 1999), there are many species that prefer older stands (Spies et al. 2018) and old-growth forests may be particularly important for cavity nesting species and some insectivorous bats because the structure of older forests includes snags and complex old trees with broken tops, dead tops, heart and butt rot, and dead wood (Mannan et al. 1980; Christy and West 1993; Parks and Shaw 1996). Old-growth forest habitat varies seasonally, and may be particularly important to year-round resident songbirds in winter (Huff et al. 1991) while understory temperature is moderated during summer (Betts et al. 2018).

Wildlife populations respond to changing landscapes in ways that may not reflect local stand structure, but abundance of habitat across landscape scales (McGarigal and McComb 1995; Betts et al. 2007; McComb et al. 2007) which complicates concepts of how forest structure at the stand scale will influence wildlife. Demarais et al. (2017) reviewed the impact of intensive forest management on terrestrial vertebrates and found that diversity decreases with intensification of management practices. They noted that although such practices can reduce vertebrate abundance, landscape-level strategies can help conserve vertebrate populations.

Beneficial Plants and Lichens

Plantation management often aims to fully occupy the site with crop trees. This includes using herbicides to control competing vegetation during planting and early stand growth. Therefore, the benefits provided by associated plants and lichens may be necessarily minimized in forest plantations. Nonetheless, certain plants and lichens offer important ecosystem services. For example, hardwoods slow the spread of conifer root disease because they are immune and break up the below-ground pathways of root disease movement (Thies and Sturrock 1995). Nitrogen fixation is another important ecosystem function of some plants and lichens. Red alder (*Alnus rubra*) forms nodules with nitrogen-fixing actinomycetes (a type of bacteria) and contributes nitrogen to early successional forest systems (Hibbs et al. 1994). The epiphytic lichen, *Lobaria oregana* is also a nitrogen fixer, and in old-growth forests of western Oregon and Washington, *L. oregana* may contribute between 1.5–16.5 kg/ha/yr of plant-available nitrogen to the forest (Antoine 2004). An often-under-appreciated role of understory flowering plants is that their flower nectar is an important source of food for adult parasitoid wasps before they attack their prey (Zemenick et al. 2019; Damien et al. 2020). The nectar sources may be necessary and lack of this important resource may limit the success of parasitoid wasps (Damien et al. 2020).

In natural and plantation forests, plant diversity is high in early seral habitats where control of competing vegetation is not done, and this diversity abruptly decreases with canopy closure (Halpern and Spies 1995; Swanson et al. 2010). As the forest stand ages, the understory vegetation begins to develop again, and is generally well-developed and most diverse in old-growth forests (Halpern and Spies 1995). Similarly, epiphytic lichens increase in abundance and diversity with stand age and are particularly rich in old-growth forests (McCune 1993). *Lobaria oregana*, a nitrogen fixing cyanolichen (lichen harboring N-fixing cyanobacteria), takes around 200 years before occurring in upland Douglas-fir forests (McCune 1993).

Forest Pests and Pathogens

Spending time in the field with foresters and loggers, I get the impression that there is a general opinion that old-growth forests are a source of insect pests and microbial pathogens. However, I believe that old-growth forests are not a significant source of pests and pathogens. In fact, the structural complexity and biodiversity found above and below ground often mitigate the impacts of pests (Shea 1971; Schowalter 2017). In 1971, Keith Shea, a prominent forest pathologist who worked for Weyerhaeuser Corporation and USDA Forest Service (Forest Service) Research, noted in a report for the International Union of Forest Research Organizations that heterogenous natural forests moderate the spread of insect pests and pathogens due to their mixed species composition, multiple age classes of trees, and natural openings that form barriers to insect pest and pathogen spread (Shea 1971).

This insight is supported by Schowalter (2017) concerning arthropod pests in old-growth where he notes that the complex food webs and abundant predators and parasitoids help mitigate outbreaks of pest insects. Recent reviews have also confirmed that forests with multiple tree species experience less insect (Jactel et al. 2017, Jactel and Brockerhoff 2007) and pathogen (Field et al. 2025) damage than single species forests. Although tree species composition can be increased in young forests to diversify plantations, in my discussions with foresters, it is avoided due to issues with log handling, marketing, and negative effects on efficiency.

I believe the most important pests of Douglas-fir plantations in western Oregon and Washington are laminated root rot (caused by *Coniferiporia sulphurascens*), black stain root disease of Douglas-fir (caused by *Leptographium pseudotsugae*), and Swiss needle cast (caused by *Nothophaeocryptopus gaeumannii*). Defoliating insects and bark beetles are generally not a major issue in Douglas-fir Region plantation management (personal observation). The lack of major defoliating insect outbreaks in Douglas-fir of western Oregon and Washington is curious since the drier inland forests are well known for major defoliating insect outbreaks in Douglas-fir (Perry and Pitman 1983; Torgersen 2001).

Laminated root rot is estimated to occupy 5–13% of the land area within the Douglas-fir forest region (Washington State Academy of Sciences 2013). The fungus spreads below-ground and rarely by spores (Thies and Sturrock 1995; Hansen and Goheen 2000). Its spread is facilitated in plantations managed as single-species Douglas-fir stands, whereas the diverse structure and composition of old-growth

forests slow the spread (Thies and Sturrock 1995). However, it is important to acknowledge that the composition and structure of Douglas-fir forests, including old-growth, is at least partially driven by native root diseases (Hansen and Goheen 2000). Black stain root disease of Douglas-fir, typically associated with disturbance and thinning in young Douglas-fir plantations, mainly attacks Douglas-fir (Hessburg et al. 2001; Choi et al. 2023). Tree mortality and spread slows significantly after tree age ~ 35 years (Hessburg et al. 1995). While Swiss needle cast, a foliage disease specific to Douglas-fir, is most important along the coast and in wet inland valleys (Shaw et al. 2021), the disease is consistently more severe in young rather than old stands (Lan et al. 2019). Regional aerial detection surveys in the Oregon Coast Range indicate private lands are more likely to show visible symptoms (Fig. 5) (Mildrexler et al. 2019).

I believe that old-growth forests are not a significant threat to forest plantations as a source of pests and pathogens. This is not to say that some insect pests and pathogens don't move from old-growth into adjacent plantations or visa-versa. Older stands are typically a source for dwarf mistletoe, which can spread from taller, older trees onto nearby younger trees along plantation edges (Hawksworth and Wiens 1996; Muir and Geils 2002). However, the common dwarf mistletoe of the Douglas-fir Region is hemlock dwarf mistletoe (*Arceuthobium tsugense*) which does not occur on Douglas-fir (Mathiasen 2021). Douglas-fir dwarf mistletoe (*A. douglasii*) is not present in the Douglas-fir region, except in SW Oregon (Mathiasen 2021).

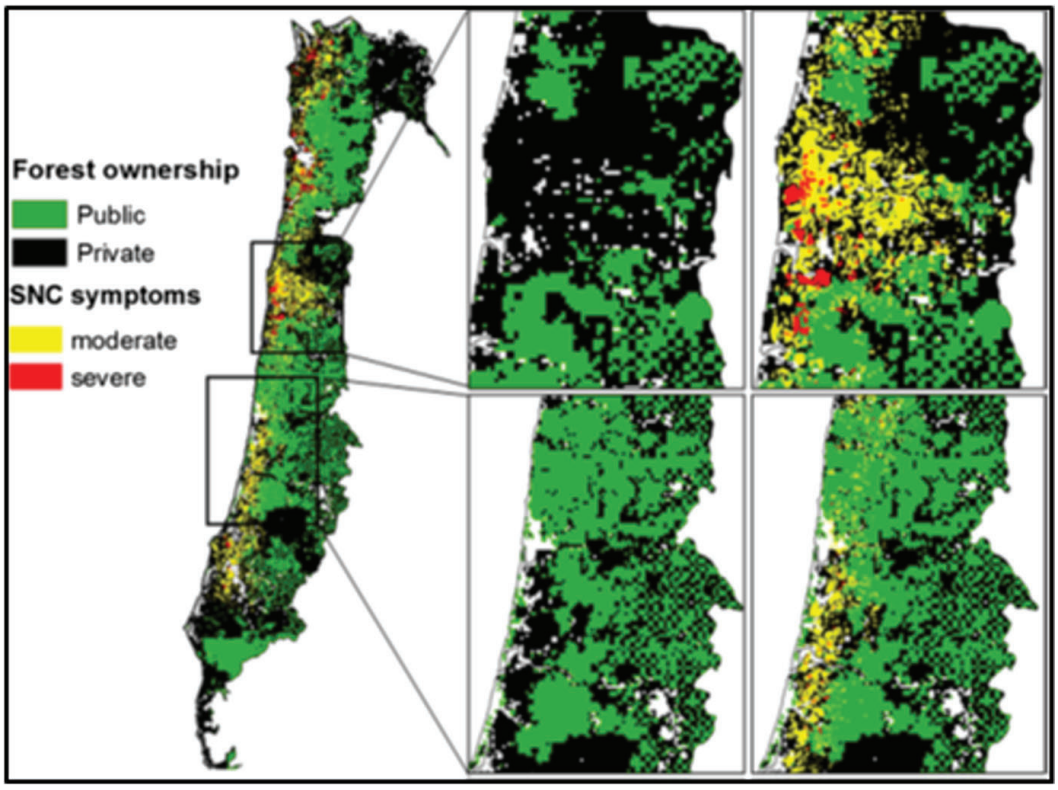

Fig. 5 Oregon coast range map showing public land (green), private land (black) with Swiss needle cast (SNC) aerial detection survey overlain in yellow (visible symptoms) and red (visible symptoms that look especially severe). From Mildrexler et al. 2019

Weevils (*Steremnius carinatus* and *Pissodes faciatus* (Coleoptera: Curculionidae)) and the root feeding bark beetle (*Hylates nigrinus* (Coleoptera: Curculionidade) may vector black stain root disease between plantation forests and older stands. Typically, these insects attack the roots of freshly cut stumps following thinning and harvesting as well as wounded and damaged live trees along roadsides and skid trails (Hansen et al. 1988; Hessburg et al. 2001). The insects can vector the fungus on their bodies and the fungus will colonize the xylem of the stumps and wounded trees. After precommercial thinning, the fungus can spread from stumps to nearby live trees across root contacts (Hansen et al. 1988; Hessburg et al. 1995). If there are adjacent older stands with black stain root disease present, it is possible the insects could vector the fungus into the plantations. However, whether this directly impacts spread of black stain root disease in plantations, or whether plantations spread infections to older stands, is not well documented.

The Douglas-fir beetle (*Dendroctonus pseudotsugae*, Coleoptera: Curculionidae) is associated with older forests on the landscape in the western Oregon Cascades (Powers et al. 1999). Typically, increased activity is associated with windthrow events or drought, while endemic activity is associated with root disease or generally low-vigor trees in the Douglas-fir region (Powers et al. 1999, Furniss 2014a, 2014b; Goheen and Willhite 2021). If a major windthrow event occurs in older stands, it is possible the bark beetle population will significantly increase after breeding in windthrown trees (Furniss 2014a). These beetles can move from windthrow into nearby healthy stands containing trees of sufficient size (Powers et al. 1999, Goheen and Willhite 2021). The Douglas-fir beetle rarely attacks trees less than 12 inches in diameter in the Douglas-fir region (Goheen and Willhite 2021) and I have not observed any significant outbreaks in westside Douglas-fir plantations under 40 years old, which is about when many stands are harvested. This may be because there is such a short window of susceptibility and the trees are vigorous.

Conclusions

I conclude that old-growth and mature forests are important in providing a reservoir of beneficial biota and do not pose a threat to plantations from pests and pathogens. From a policy perspective, I contend that Douglas-fir region foresters should support the protection of the old-growth and older mature forests designated in the Northwest Forest Plan of the Pacific Northwest Region of the Forest Service (Davis et al. 2022). Plantation management, by design, simplifies forest structure and biodiversity, increasing vulnerability to pests and pathogens (Shea 1971; Schowalter 2017). Maintaining a network of old-growth and mature forests across the region provides a long-term source of beneficial organisms that can potentially bolster the resilience and productivity of Douglas-fir plantations. If we convert the remaining old-growth and older mature forests to younger plantations we could lose much of this biodiversity. I fear this would create a large region of homogeneous plantations where pests and pathogens could become an overwhelming negative factor in forest health.

This is not an argument against plantations. I support the timber industry and recognize the value of plantation management in providing a renewable source of

wood products and sustaining rural economies. Small woodland owners also rely on robust logging and milling infrastructure to manage their lands effectively. My goal is to promote productive, healthy plantations that are part of a sustainable forest economy, which I believe requires a diversity of age classes on the regional landscape, including the existing old-growth. It is in the interests of the timber industry to protect the remaining old-growth and older mature forests of the Douglas-fir region because these forests are living repositories of the biodiversity that help maintain individual tree health and broader forest resilience. By protecting these legacy stands, we ensure beneficial biota are maintained on the landscape.

Acknowledgements Special thanks to the reviewers.

Authors' Contributions These are my ideas, I asked one person to help with edits, a graduate student I work with.

Funding Retired/NA.

Data Availability N/A.

Declarations

Competing Interests I'm retired, and have no financial interests.

Open Access This article is licensed under a Creative Commons Attribution-NonCommercial-NoDerivatives 4.0 International License, which permits any non-commercial use, sharing, distribution and reproduction in any medium or format, as long as you give appropriate credit to the original author(s) and the source, provide a link to the Creative Commons licence, and indicate if you modified the licensed material. You do not have permission under this licence to share adapted material derived from this article or parts of it. The images or other third party material in this article are included in the article's Creative Commons licence, unless indicated otherwise in a credit line to the material. If material is not included in the article's Creative Commons licence and your intended use is not permitted by statutory regulation or exceeds the permitted use, you will need to obtain permission directly from the copyright holder. To view a copy of this licence, visit http://creativecommons.org/licenses/by-nc-nd/4.0/.

References

Abrego, N., and I. Salcedo. 2013. Variety of woody debris as the factor influencing wood-inhabiting fungal richness and assemblages: Is it a question of quantity or quality? *Forest Ecology and Management* 291:377–385. https://doi.org/10.1016/j.foreco.2012.11.025.

Agne, M. C., P. A. Beedlow, D. C. Shaw, D. R. Woodruff, E. H. Lee, S. Cline, and R. L. Comeleo. 2018. Interactions of predominant insects and diseases with climate change in Douglas-fir forests of western Oregon and Washington, U.S.A. *Forest Ecology and Management.* 409:317–332.

Allen, M. F., W. Swenson, J. K. Querejeta, L. M. Egerton-Warburton, and K. K. Treseder. 2003. Ecology of Mycorrhizae: A conceptual framework for complex interactions among plants and fungi. *Annual Review of Phytopathology* 41:271–303.

Amaranthus, M., J. M. Trappe, L. Bednar, and D. Arthur. 1994. Hypogeous fungal production in mature Douglas-fir forest fragments and surrounding plantations and its relations to coarse woody debris and animal mycophagy. *Canadian Journal of Forest Research*. https://doi.org/10.1139/x94-278.

Antoine, M. E. 2004. An ecophysiological approach to quantifying nitrogen fixation by *Lobaria oregana*. *The Bryologist* 107:82–87.

Betts, M. G., G. J. Forbes, and A. W. Diamond. 2007. Thresholds in songbird occurrence in relation to landscape structure. *Conservation Biology* 21:1046–1058. https://doi.org/10.1111/j.1523-1739.2007.00723.x.

Betts, M. G., B. Phalan, S. J. K. Frey, J. S. Rousseau, and Z. Yang. 2018. Old-growth forests buffer climate-sensitive bird populations from warming. *Diversity and Distributions* 24 (439–447): 525. https://doi.org/10.1111/ddi.12688.

Betts, M. G., B. T. Phalan, C. Wolf, S. C. Baker, C. Messier, K. J. Puettmann, R. Green, S. H. Harris, D. P. Edwards, D. B. Lindenmayer, and A. Balmford. 2021. Producing wood at least cost to biodiversity: Integrating Triad and sharing-sparing approaches to inform forest landscape management. *Biological Reviews* 96:1301–1317. https://doi.org/10.1111/brv.12703.

Blaustein, A. F., J. J. Beatty, D. H. Olson, and R. M. Storm. 1995. *The biology of amphibians and reptiles in old-growth forests in the Pacific Northwest*. USDA Forest Service, Gen. Tech. Rep. PNW-GTR-337. Portland, Oregon: Pacific Northwest Research Station.

Brunnell, F. L. 1999. What habitat is an island? In *Forest Fragmentation. Wildlife and Management Implications*, ed. J.A. Rochelle, L.A. Lehmann, and J. Wisniewski, 1–31. Leiden, The Netherlands: Brill.

Burke, G. R., and B. J. Sharanowski. 2024. Parasitoid wasps. *Current Biology*. https://doi.org/10.1016/j.cub.2024.03.038.

Caldwell, B. A., C. Hagedorn, and W. C. Denison. 1979. Bacterial ecology of an old-growth douglas fir canopy. *Microbial Ecology* 5 (2): 91–103. https://doi.org/10.1007/BF02010500.

Carey, A. B., D. R., Thysell, L. J., Villa, T. M., Wilson, S. M., Wilson, J. M., Trappe, W., Cogan, III, E. R., Ingham, and M. Holmes. 1996. Foundations of biodiversity in managed Douglas-fir forests. In *The role of restoration in the ecosystem, ed. DL Peterson and CV Klimas. Proceedings of the 2 Symposium for Ecological Restoration Sept 14–17, 1995*. Seattle, WA: Society of Ecological Restoration, Madison WI.

Carroll, G. C., Pike, L. H., Perkins, J. R., and M. Sherwood. 1980. Biomass and distribution patterns of conifer twig microepiphytes in a Douglas-fir forest. Canadian Journal of Botany 58. https://doi.org/10.1139/b80-078

Carroll, G. C. 1991. Fungal associates of woody plants as insect antagonists in leaves and stems. In Microbial Mediation of Plant- Herbivore Interactions. ed. P. Barbosa, V. A. Krischik, C. G. Jones, Chapter 9, John Wiley and Sons, Inc.

Choi, D., T. C. Harrington, D. C. Shaw, J. E. Stewart, N. B. Klopfenstein, D. R. Kroese, and M.-S. Kim. 2023. Phylogenetic analyses allow species-level recognition of *Leptographium wageneri* varieties that cause black stain root disease of conifers in western North America. *Frontiers in Plant Science*. https://doi.org/10.3389/fpls.2023.1286157.

Christy, R. E., and S. D. West. 1993. *Biology of Bats in Douglas-fir Forests. USDA Forest Service, Gen*. Tech. Rep. PNW-GTR-308,. Portland, Oregon, USA: Pacific Northwest Research Station.

Damien, M., S. Llopis, N. Desneux, J. Van Baaren, and C. Le Lann. 2020. How does floral nectar quality affect life history strategies in parasitic wasps? *Entomologia Generalis* 40:147. https://doi.org/10.1127/entomologia/2020/0906.

Dastogeer, K. M. G., F. H. Tumpa, A. Sultana, M. A. Akter, and A. Chakraborty. 2020. Plant microbiome-an account of the factors that shape community composition and diversity. *Current Plant Biology*. https://doi.org/10.1016/j.cpb.2020.100161.

Davis, R. J., Bell, D. M., Gregory, M. J, Yang, Z., Gray, A. N., Healey, S. P., and A. E. Stratton. 2022. Northwest Forest Plan—the first 25 years (1994–2018): status and trends of late-successional and old-growth forests. Gen. Tech. Rep. PNW-GTR-1004. Portland, OR: USDA Forest Service, Pacific Northwest Research Station. 82 p. https://doi.org/10.2737/PNW-GTR-1004

Demarais, S., J. P. Verschuyl, G. J. Roloff, D. A. Miller, and T. B. Wigley. 2017. Tamm review: Terrestrial vertebrate biodiversity and intensive forest management in the US. *Forest Ecology and Management* 385:308–330. https://doi.org/10.1016/j.foreco.2016.10.006.

Edmonds, R. L. 1991. Organic matter decomposition in western United States forests. Pages 118–128. In *Proceedings-Management and Productivity of Western Montane Soils*. ed. A. E. Harvey and L.F. Neuenschwander, USDA Forest Service Gen. Tech. Rep. INT-280. Ogden, Utah: Intermountain Research Station.

Field, E., A. Hector, N. Barsoum, and J. Koricheva. 2025. Tree diversity reduces pathogen damage in temperate forests: A systematic review and meta analysis. *Forest Ecology and Management* 578 (2025): 122398. https://doi.org/10.1016/j.foreco.2024.122398.

Fogel, R., and G. Hunt. 1983. Contribution of mycorrhizae and soil fungi to nutrient cycling in a Douglas-fir ecosystem. *Canadian Journal of Forest Research*. https://doi.org/10.1139/x83-031.

Franklin, J. F. 1981. Vegetation of the Douglas-fir Region. In *Forest Soils of the Douglas-fir Region*, ed. P.E. Heilman, H.W. Anderson, D.M. Baumgartner, and I.V. Chapter. Pullman, Washington, USA: Washington State University Cooperative Extension.

Franklin, J. F., K. Cromack Jr., W. Denison, A. McKee, C. Maser, J. Sedell, F. Swanson, and G. Juday. 1981. *Ecological characteristics of old-growth Douglas-fir forests*. USDA Forest Service, Gen. Tech. Rep. PNW-GTR-118. Portland, Oregon.

Franklin, J. F., T. A. Spies, R. Van Pelt, A. B. Carey, D. A. Thornburgh, D. R. Berg, D. B. Lindenmayer, M. E. Harmon, W. S. Keeton, D. C. Shaw, K. Bible, and J. Chen. 2002. Disturbances and structural development of natural forest ecosystems with silvicultural implications, using Douglas-fir forests as an example. *Forest Ecology and Management* 155:399–423.

Furniss, M. M. 2014a. The Douglas-fir beetle in western forests. A Historical Perspective Part 1. *American Entomologist. Summer* 60:84–96.

Furniss, M. M. 2014b. The Douglas-fir beetle in western forests. A Historical Perspective Part 2. *American Entomologist. Fall.* 60:166–181.

Gervers, K. A., D. C. Thomas, B. A. Roy, J. W. Spatafora, and P. E. Busby. 2022. Crown closure affects endophytic leaf mycobiome compositional dynamics over time in Pseudotsuga menziesii var. menziesii. *Fungal Ecology*57–58. https://doi.org/10.1016/j.funeco.2022.101155.

Goheen, E. M., and E. A. Willhite. 2021. *Field Guide to Common Diseases and Insect Pests of Oregon and Washington Conifers. USDA Forest Service, R6-FHP-RO-2021–01*. Portland, OR: Pacific Northwest Region.

Graham, H. R., E. Hayward, J. Ehlting, P. Y. de la Bastide, T. J. Avis, N. Feau, R. Hamlin, J. Bérubé, D. R. McMullin, and J. B. Tanney. 2025. In vitro suppression of the Swiss needle cast pathogen Nothophaeocryptopus gaeumannii by metabolite extracts from endophytes of Douglas-fir. *Phyto-Frontiers*. https://doi.org/10.1094/PHYTOFR-07-24-0085-R.

Halaj, J., D. W. Ross, and A. R. Moldenke. 2000. Importance of habitat structure to the arthropod food-web in Douglas-fir canopies. *Oikos* 90:139–152.

Halpern, C. B., and T. A. Spies. 1995. Plant species diversity in natural and managed forests. *Ecological Applications* 5:913–934. https://doi.org/10.2307/2269343.

Hansen, E. M., and E. M. Goheen. 2000. *Phellinus weirii* and other native root pathogens as determinants of forest structure and process in western North America. *Annual Review of Phytopathology* 38:515–539. https://doi.org/10.1146/annurev.phyto.38.1.515.

Hansen, A. J., W. C. McComb, R. Vega, M. G. Raphael, and M. Hunter. 1995. Bird habitat relationships in natural and managed forests in the west Cascades of Oregon. *Ecological Applications* 5:555–569. https://doi.org/10.2307/1941966.

Hansen, E. M., D. J. Goheen, P. F. Hessburg, J. J. Witcosky, and T. D. Schowalter. 1988. Biology and management of black-stain root disease in Douglas-fir. In *Leptographium Root Diseases on Conifers*, ed. T.C. Harrington and F.W. Cobb Jr., 63–80. St. Paul, Minnesota, USA: APS Press.

Harris, S. H., and M. G. Betts. 2021. Bird abundance is highly dynamic across succession in early seral tree plantations. *Forest Ecology and Management* 483. https://doi.org/10.1016/j.foreco.2020.118902.

Hawksworth, F. G., and D. W. Wiens. 1996. Dwarf Mistletoes: Biology, Pathology and Systematics. *USDA Forest Service Agriculture Handbook 709*. Washington DC.

Hessburg, P. F., D. J. Goheen, and H. Koester. 2001. Association of black stain root disease with roads, skid trails and precommercial thinning. *Western Journal of Applied Forestry* 16:127–135.

Hessburg, P. F., D. J. Goheen, and R. V. Bega. 1995. Black Stain Root Disease of Conifers. In *USDA Forest Service Forest Insect and Disease Leaflet (FIDL) 145* Washington D.C.

Hibbs, D. E., D. S. DeBell, and R. F. Tarrant, eds. 1994. *The biology and management of red alder*, 256. Corvallis, OR: Oregon State University Press.

Huff, M. H., D. A., Manual, and J. A. Putera. 1991. Winter bird communities in the Southern Washington Cascade Range. In *Wildlife and vegetation of unmanaged Douglas-fir forests*. ed. L.F. Ruggiero, K. B. Aubry, A. B. Carey, M. H. Huff. 207–218, USDA Forest Service Gen. Tech. Rep. PNW-GTR-285. Pacific Northwest Research Station, Portland, Oregon, USA.

Ingles, L. G. 1965. *Mammals of the Pacific States*. Stanford, California, USA: Stanford University Press.

Jactel, H., and E. G. Brockerhoff. 2007. Tree diversity reduces herbivory by forest insects. *Ecology Letters* 10 (9): 835–848. https://doi.org/10.1111/j.1461-0248.2007.01073.x.

Jactel, H., J. Bauhus, J. Boberg, D. Bonal, B. Castagneyrol, B. Gardiner, and E. G. Brockerhoff. 2017. Tree diversity drives forest stand resistance to natural disturbances. *Current Forestry Reports* 3 (3): 223–243. https://doi.org/10.1007/s40725-017-0064-1.

Kendall, L. K., and D. F. Ward. 2016. Habitat determinants of the taxonomic and functional diversity of parasitoid wasps. *Biodiversity and Conservation* 2016 (25): 1955–1972. https://doi.org/10.1007/s10531-016-1174-y.

Kiser, J., H. Daniels, and Scrivani. 2019. Isolation of endophytic fungi from Douglas-fir (*Pseudotsuga menziesii*) foliage with bioprospecting potential for natural pharmaceuticals. *Current Trends in Forest Research* 3:1035. https://doi.org/10.29011/2638-0013.101035.

Lan, Y.-H., D. C. Shaw, P. A. Beedlow, E. H. Lee, and R. S. Waschmann. 2019. Severity of Swiss needle cast in young and mature Douglas-fir forests in western Oregon, USA. *Forest Ecology and Management* 442:79–95.

Lattin, J. D. 1993. Arthropod diversity and conservation in old-growth Northwest Forests. *American Zoologist.* 1993 (33): 578–587.

Lindenmayer, D. B., and J. F. Franklin. 2002. *Conserving Forest Biodiversity*. A Comprehensive Multiscaled Approach: Island Press, Washington.

Luoma, D. L., J. M. Trappe, A. W. Claridge, K. M. Jacobs, and E. Cazares. 2003. Relationship among fungi and small mammals in forested ecosystems. In *Mammal community dynamics: management and conservation in the coniferous forests of western North America*, ed. C.J. Zabel and R.G. Anthony, 343–373. Cambridge, United Kingdom: Cambridge University Press.

Mannan, R. W., E. C. Meslow, and H. M. Wight. 1980. Use of snags by birds in Douglas-fir forests, western Oregon. *Journal of Wildlife Management* 44:787–797.

Maser, M., and Z. Maser. 1988. Interactions among squirrels, mycorrhizal fungi, and coniferous forests in Oregon. *The Great Basin Naturalist* 48:358–369.

Mathiasen, R. L. 2021. *Mistletoes of the Continental United States and Canada*. Fort Worth, Texas, USA: Britt Press.

McComb, B. C., T. A. Spies, and K. A. Olsen. 2007. Sustaining biodiversity in the Oregon Coast Range: potential effects of forest policies in a multi-ownership province. *Ecology and Society* 12:29 http://www.ecologyandsociety.org/vol12/iss2/art29/. Accessed 8/1/2025.

McCune, B. 1993. Gradients in epiphyte biomass in three Pseudotsuga-Tsuga forests of different ages in western Oregon and Washington. *The Bryologist* 96:405–411.

McGarigal, K., and W. C. McComb. 1995. Relationships between landscape structure and breeding birds in the Oregon Coast Range. *Ecological Monographs* 65:235–260. https://doi.org/10.2307/2937059.

Michel, A. K., and S. Winter. 2009. Tree microhabitat structures as indicators of biodiversity in Douglas-fir forests of different stand ages and management histories in the Pacific Northwest, U.S.A. *Forest Ecology and Management* 257:1453–1464. https://doi.org/10.1016/j.foreco.2008.11.027.

Mildrexler, D. J., D. C. Shaw, and W. B. Cohen. 2019. Short-term climate trends and the Swiss needle cast epidemic in Oregon's public and private coastal forestlands. *Forest Ecology and Management* 432:501–513.

Moldenke, A. R. 1999. Soil-dwelling arthropods: their diversity and functional roles. In Proceedings: Pacific Northwest Forest and Rangeland Soil Organism Symposium; 1998 March 17–19; Corvallis, OR. ed. R. T. Meurisse, W. G. Ypsilantis, C. Seybold, 33–44, USDA Forest Service Gen. Tech. Rep. PNW-GTR-461. Pacific Northwest Research Station, Portland, OR, USA.

Molina, R., O'Dell, T., Dunham, S., and D. Pilz. 1999. Biological diversity and ecosystem functions of forest soil fungi: management implications, 45–58. In *Proceedings: Pacific Northwest Forest and Rangeland Soil Organism Symposium: 1998 March 17-19; Corvallis OR*. eds. R. T. Meurisse, W. G. Ypsilantis, and C. Seybold, 33-44. USDA Forest Service Gen. Tech. Rep. PNWGTR-461. Portland, OR: Pacific Northwest Research Station

Muir, J. A., and B. W. Geils. 2002. Management strategies for dwarf mistletoe: silviculture. In *Mistletoes of North American Conifers*, ed B. W. Geils, J. C. Tovar, B. Moody B, Chapter 8. USDA Forest Service, Gen. Tech. Rep. RMRS-GTR-98. Rocky Mountain Research Station, Ogdon, Utah, USA.

Parks, C. G., and D. C. Shaw. 1996. Death and decay: a vital part of living canopies. *Northwest Science* 70:46–53 (**Special Issue**).

Perry, D. A., and G. B. Pitman. 1983. Genetic and environmental influences in host resistance to herbivory: Douglas-fir and the western spruce budworm. *Journal of Applied Entomology* 96:217–228. https://doi.org/10.1111/j.1439-0418.1983.tb03662.x.

Phalan, B. T., J. M. Northrup, Z. Yang, R. L. Deal, J. S. Rousseau, T. A. Spies, and M. G. Betts. 2019. Impacts of the Northwest Forest Plan on forest composition and bird populations. *Proceedings of the National Academy of Sciences (PNAS)* 116:3322–3327. https://doi.org/10.1073/pnas.1813072116.

Powers, J. S., P. Sollins, M. E. Harmon, and J. A. Jones. 1999. Plant-pest interactions in time and space: A Douglas-fir bark beetle outbreak as a case study. *Landscape Ecology* 14:105–120. https://doi.org/10.1023/A:1008017711917.

Rivers, J. W., and M. G. Betts. 2021. Postharvest bee diversity is high but declines rapidly with stand age in regenerating Douglas-fir forest. *Forest Science* 67:275–285. https://doi.org/10.1093/forsci/fxab002.

Ruggiero, L. F., K. B., Aubry, A. B., Carey, and M. H. Huff (tech. eds.) 1991. *Wildlife and vegetation of unmanaged Douglas-fir forests*. USDA Forest Service Gen. Tech. Rep. PNW-GTR-285. Pacific Northwest Research Station, Portland, Oregon.

Schowalter, T. D. 1995. Canopy arthropod communities in relation to forest age and alternative harvest practices in western Oregon. *Forest Ecology and Management* 78:115–125. https://doi.org/10.1016/0378-1127(95)03592-4.

Schowalter, T. 2017. Arthropod diversity and functional importance in old-growth forests of North America. *Forests* 8:97. https://doi.org/10.3390/f8040097.

Shaw, D. C., G. Ritóková, Y.-H. Lan, D. B. Mainwaring, A. Russo, R. L. Comeleo, S. Navarro, D. Norlander, and B. Smith. 2021. Persistence of the Swiss Needle Cast Outbreak in Oregon Coastal Douglas-fir, and New Insights from Research and Monitoring. *Journal of Forestry.* 119:407–421.

Shea, K. R. 1971. Disease and Insect activity in relation to intensive culture of forests. In *Proceedings of the XV International Union of Forestry Research Organizations (IUFRO), March 1971*. ed. USDA Forest Service. Washington D.C., USA: U.S Department of Agriculture.

Smith, J. E., R. Molina, M. M. P. Huso, D. L. Luoma, D. McKay, M. A. Castellano, T. Lebel, and Y. Valachovic. 2002. Species richness, abundance, and composition of hypogeous and epigeous ectomycorrhizal fungal sporocarps in young, rotation-age, and old-growth stands of Douglas-fir (Pseudotsuga menziesii) in the Cascade Range of Oregon, U.S.A. *Canadian Journal of Botany* 88:186–204. https://doi.org/10.1139/b02-003.

Spies, T. A., J. W. Long, S. Charnley, P. F. Hessburg, B. G. Marcot, G. H. Reeves, D. B. Lesmeister, M. J. Reilly, L. K. Cerveny, P. A. Stine, and M. G. Raphael. 2019. Twenty-five years of the Northwest Forest Plan: What have we learned? *Frontiers in Ecology and the Environment* 17:511–520.

Spies, T. A., P. A., Stine, R., Gravenmier, J. W., Long, M. J., Reilly, and R. Mazza (tech. cords). 2018. Synthesis of science to inform land management within the Northwest Forest Plan area: Executive Summary, Volume 1, and Volume 2. USDA Forest Service Gen. Tech. Rep. PNW-GTR-970. Pacific Northwest Research Station, Portland, OR, USA

Stone, J. K., M. A. Sherwood, and G. C. Carroll. 1996. Canopy microfungi: function and diversity. *Northwest Science* 70:37–45 (**Special Issue**).

Swanson, M. E., J. F. Franklin, R. L. Beschta, C. M. Crisafulli, D. A. DellaSalla, R. L. Hutto, D. B. Lindenmayer, and F. J. Swanson. 2010. The forgotten stage of forest succession: Early-successional ecosystems on forest sites. *Frontiers in Ecology and Environment* 9:117–125. https://doi.org/10.1890/090157.

Sylvia, D. M., and W. A. Sinclair. 1983. Phenolic compounds and resistance to fungal pathogens induced in primary roots of Douglas-fir seedlings by the ectomycorrhizal fungus *Laccaria laccata*. *Phytopathology* 73:390–397.

Thies, W. G., and R. N. Sturrock. 1995. Laminated root rot in Western North America. USDA Forest Service Gen. Tech. Rep. PNWGTR-349. Portland, OR: USDA Forest Service, Pacific Northwest Research Station, Portland, OR USA, in cooperation with: Natural Resources Canada, Canadian Forest Service, Pacific Forestry Centre., Victoria, B.C. Canada.

Thomas, D. W. 1988. The distribution of bats in different ages of Douglas-fir forests. *Journal of Wildlife Management* 52:619–626.

Thomas, J. W., L. F. Ruggiero, R. W. Mannan, J. W. Schoen, and R. A. Lancia. 1988. Management and conservation of old-growth forests in the United States. *Wildlife Society Bulletin* 16:252–262.

Thomas, J. W., J. F. Franklin, J. Gordon, and K. N. Johnson. 2006. The Northwest Forest Plan: Origins, components, implementation experience, and suggestions for change. *Conservation Biology* 20:277–287. https://doi.org/10.1111/j.1523-1739.2006.00385.x.

Thomas, D. W., and S. D. West. 1991. Forest age associations of bats in the Washington cascades and oregon coast ranges. In Wildlife and vegetation of unmanaged Douglas-fir forests, ed. L. F. Ruggiero,

K. B. Aubry, A. B. Carey, M. H. Huff (tech. Eds.), 291–302. USDA Forest Service Gen. Tech. Rep. PNW-GTR-285. Pacific Northwest Research Station, Portland, OR

Tomao, A., J. A. Bonet, C. Castaño, and S. de-Miguel. 2020. How does forest management affect fungal diversity and community composition? Current knowledge and future perspectives for the conservation of forest fungi. *Forest Ecology and Management* 457. https://doi.org/10.1016/j.foreco.2019.117678.

Torgersen, T. R. 2001. Defoliators in eastern Oregon and Washington. *Northwest Science* 75:11–20 (**Special Issue**).

Trappe, J. M., and R. F. Strand. 1969. Mycorrhizal deficiency in a Douglas-fir Region Nursery. *Forest Science* 15:381–389.

Trivedi, P., J. E. Leach, S. G. Trige, T. Sa, and B. K. Singh. 2020. Plant-microbiome interactions: From community assembly to plant health. *Nature Reviews Microbiology* 18:607–621. https://doi.org/10.1038/s41579-020-0412-1.

Trofymow, J. A., J. Addison, B. A. Blackwell, F. He, C. A. Preston, and V. G. Marshall. 2003. Attributes and indicators of old-growth and successional Douglas-fir forests on Vancouver Island. *Environmental Reviews* 11 (S1): S187–S204. https://doi.org/10.1139/A03-007.

Tuneu-Corral, C., X. Puig-Montserrat, D. Riba-Bertolin, D. Russo, H. Rebelo, M. Cabeza, and A. Lopez-Baucells. 2023. Pest suppression by bats and management strategies to favor it: A global review. *Biological Reviews* 98:1564–1582. https://doi.org/10.1111/brv.12967.

Ulyshen, M. D., K. M. Ballare, C. J. Fettig, J. W. Rivers, and J. B. Runyon. 2024. The value of forests to pollinating insects varies with forest structure, composition, and age. *Current Forestry Reports* 10:322–336. https://doi.org/10.1007/s40725-024-00224-6.

Washington State Academy of Sciences. 2013. *Opportunities for addressing laminated root rot caused by Phellinus sulphuracens in Washington's forests. A Report from the Washington State Academy of Sciences in cooperation with the Washington State Department of Natural Resources*. Olympia, WA. http://www.washacad.org/. https://washacad.org/projectspublications/opportunities-for-addressing-laminated-root-rot-caused-by-phellinus-sulphurascens-in-washingtons-forests/ Accessed 8/1/2025.

Zemenick, A. T., R. R. Kula, L. Russo, and J. Tooker. 2019. A network approach reveals parasitoid wasps to be generalized nectar foragers. *Arthropod-Plant Interactions* 13:239–251. https://doi.org/10.1007/s11829-018-9642-9.

Publisher's Note Springer Nature remains neutral with regard to jurisdictional claims in published maps and institutional affiliations.

Authors and Affiliations

David C. Shaw[1]

✉ David C. Shaw
dave.shaw@oregonstate.edu

[1] Department of Forest Engineering, Resources and Management, Oregon State University, Corvallis, OR 97330, USA

Check for updates

Global Change Biology

WILEY

Global Change Biology

RESEARCH ARTICLE

Extreme Heatwave Causes Immediate, Widespread Mortality of Forest Canopy Foliage, Highlighting Modes of Forest Sensitivity to Extreme Heat

Adam Sibley[1,2] | Christopher Still[1] | Matthew Gregory[1] | Constance Harrington[3] | David Shaw[1] | Nina Ferrari[1] | Alex Dye[1] | Mark Schulze[1] | Glenn Howe[1] | David E. Rupp[4] | Christopher Daly[5] | Daniel DePinte[6] | Cameron E. Naficy[1,7] | Chaney Hart[1] | David M. Bell[8]

[1]Department of Forest Ecosystems and Society, 321 Richardson Hall, Oregon State University, Corvallis, Oregon, USA | [2]Chloris Geospatial, Boston, Massachusetts, USA | [3]USDA Forest Service, Pacific Northwest Research Station, Olympia, WA, USA | [4]Oregon Climate Change Research Institute, College of Earth, Ocean, and Atmospheric Science, Oregon State University, Corvallis, Oregon, USA | [5]PRISM Climate Group, Northwest Alliance for Computational Science and Engineering, College of Engineering, Oregon State University, Corvallis, Oregon, USA | [6]USFS, PNW Forest Health Protection, Portland, Oregon, USA | [7]Ecology Program, Pacific Northwest Region, USDA Forest Service, Baker City, Oregon, USA | [8]USDA Forest Service, Pacific Northwest Research Station, Corvallis, Oregon, USA

Correspondence: Adam Sibley (adam@chloris.earth)

Received: 20 November 2024 | **Revised:** 11 September 2025 | **Accepted:** 29 September 2025

Funding: This research was funded by a U.S. Geological Survey Northwest Climate Adaptation Science Center (Award G17AC000218 to Adam Sibley), the H.J. Andrews Experimental Forest and Long-Term Ecological Research (LTER) program under the NSF (Grant LTER8 DEB-2025755), and USDA Forest Service Pacific Northwest Research Station.

Keywords: climate extremes | ecophysiology | foliage mortality | foliar pathogen | forest ecology | forest health | heat wave | plant thermal tolerance | remote sensing

ABSTRACT

In late June 2021, multiple days of record-breaking heat caused an unprecedented amount of foliage death in the forests of the Pacific Northwest, USA. Portions of tree canopies with healthy green foliage prior to the heat changed to red or orange shortly after the event. The change in foliage color could be readily seen in satellite imagery and was corroborated as foliar death (heat scorch) by aerial surveys and extensive observations on the ground. To better understand the patterns and processes driving foliar death, we used satellite imagery to identify 293,546 ha of forest, or ~4.7% of forest area, that were damaged in western Oregon and Washington by this extreme heat event. Analysis of underlying drivers of the observed heat damage indicated greater sensitivity was related to abiotic factors such as sun exposure, aspect, and microclimate, as well as biotic factors like tree species and stand age, budburst phenology, and foliar pathogens impacting tree health. Iconic, culturally and economically significant species like western redcedar, western hemlock, and Sitka spruce were disproportionately sensitive to heat damage, including in old-growth stands where they are canopy dominants. These findings highlight the multifaceted challenges posed to forests by extreme heat waves, and the need to better understand their impact on forest ecosystems in a rapidly warming climate.

1 | Introduction

Droughts and heatwaves exacerbated by anthropogenic climate change are anticipated to be a major driver of future forest change (Allen et al. 2015). As long-lived species that have evolved to tolerate periods of extreme weather, trees rarely die immediately in response to heat and drought; rather, forest mortality usually occurs from a combination of stressors acting over multiple years (Andrus et al. 2024; Franklin et al. 1987). While drought events impacting trees have been widely observed and

© 2025 John Wiley & Sons Ltd.

documented (e.g., Allen et al. 2010; Anderegg et al. 2013; Andrus et al. 2024; Bose et al. 2024; Hammond et al. 2022), studies examining the long-term impacts of short duration, extreme heat have been largely restricted to seedlings and laboratory studies (Fauset et al. 2019; Marias et al. 2016; Slot and Winter 2017). The effects of short, extreme heatwaves are poorly captured in most ecosystem models, and in some cases are not represented at all (Jiang et al. 2019; Kala et al. 2016). This is partly because there are multiple proposed mechanisms underlying heat stress and damage to leaves (Berry and Bjorkman 1980; Teskey et al. 2015).

Plant responses to heat stress affect many physiological processes and biological structures simultaneously. Rising temperatures initially increase photosynthesis rates until an optimum is reached, beyond which photosynthesis declines with increasing mitochondrial respiration, photorespiration, and decreasing active Rubisco and electron transport (O'Sullivan et al. 2016; Scafaro et al. 2023). Rising temperatures also limit CO_2 availability because increases in vapor pressure deficit (VPD) induce stomatal closure (Grossiord et al. 2020). Finally, direct cellular damage increases the permeability of thylakoid membranes, which disrupts photosynthetic electron transport (Sharkey 2005) and causes damage associated with oxidative bursts (Hüve et al. 2011; Zhu et al. 2024). Substantial cellular damage leads to tissue necrosis shortly after exposure to extreme heat (Colombo and Timmer 1992; Hüve et al. 2011; Javad et al. 2025; Krause et al. 2010; Marchin et al. 2022; Neuner and Buchner 2023). The connections between heat stress and tree foliar damage have been studied in controlled settings but rarely in natural environments.

Between June 25–29, 2021, an extreme heat wave occurred in the Pacific Northwest (PNW) of the United States and southwestern Canada (Loikith and Kalashnikov 2023; Mass et al. 2024; Thompson et al. 2022), which caused widespread damage to tree foliage. During this event, daily maximum air temperatures exceeded 40°C for at least three consecutive days, anomalies in maximum daily air temperature exceeded 15°C across much of the region, and all-time high temperatures were recorded in Canada (49.6°C), Washington (48.8°C), and Oregon (48.3°C) (Fleishman et al. 2025). Maximum land surface temperatures exceeded 40°C in many forested areas and exceeded 47°C in many nonforested areas (Figure 1). This heat wave was unprecedented regionally in the modern instrumentation record and had among the most extreme temperature anomalies ever recorded globally (Thompson et al. 2022). Observation and climate model-based estimates of the probability of such a heat wave occurring under the recent historical climate range widely: from 0.001% to 1.8% per year (100,000 to 56-year return interval, respectively) (Fleishman et al. 2025).

The 2021 heat wave had unprecedented effects on PNW forests. A few days after the heat wave ended, trees with dead or "scorched" foliage (Figure 2, Figures S1 and S2) appeared on the landscape as far south as Roseburg, Oregon (latitude: 43.215° N) and as far north as southern British Columbia (latitude ~49.5° N, ~700 km range). Foliage "scorch" occurs when healthy green leaves turn red, orange, or brown as living tissues die and chlorophyll is degraded due to a variety of causes. Hereafter, we use the terms foliage scorch, foliar death, leaf death, and foliar mortality interchangeably. The death of tree leaves causes an acute stress that may lead to short-term or long-term reductions in tree growth, declines in defenses, or even tree mortality, particularly if combined with stresses from other biotic and abiotic factors like co-occurring drought and pathogens.

In response to widespread reports of foliar death, the USDA Forest Service Aerial Detection Survey (ADS) conducted aerial surveys of coastal forests in northern Oregon and southern Washington. They documented ~92,000 ha of damaged forest in only a portion of the affected range (U.S. Forest Service-PNW Forest Health Protection 2023). Ground-level and aerial observations in the months after the heat wave indicated that foliar mortality was widespread but affected some forest stands more than others (Still et al. 2021). Foliar death was in some cases accompanied by mortality of branches and entire trees, with seedlings and saplings being the most sensitive (Still et al. 2021). Although it is important to understand forest sensitivity to extreme heat (Allen et al. 2015; Hammond et al. 2022; Teskey et al. 2015), to date, there has been no systematic analysis of which forests, species, or landscape positions were affected by this heatwave and why.

Initial assessments of the 2021 extreme heat wave associated forest sensitivity with biophysical factors that vary across the landscape. For example, observations suggested that temperature anomalies were important and varied geographically, that more leaf death occurred on south- and west-facing slopes, that sensitivity varied among tree species, and that vegetative phenology seemed to relate to the amount of damage (Still et al. 2023). Spatial variations in temperature anomalies during the event have been widely documented (e.g., White et al. 2023), and it is known that heat stress may be amplified or dampened by canopy position, canopy structure, aspect, and topographic position (De Frenne et al. 2021; Dobrowski 2011). The condition of the forest should also affect sensitivity to heat, especially tree water status, as well as species-specific differences in heat tolerance, tree age, and biotic stressors like foliar pathogens (Allen et al. 2015). Finally, interactions among weather, topography, and forest condition affect fine-scale variation in forest microclimate (De Frenne et al. 2019; Frey et al. 2016; Wolf et al. 2021), which could cause differentiated impacts over relatively short distances.

Our primary aim in this study was to quantify the effects of the 2021 heat event on foliar mortality in the forests of Oregon and Washington west of the Cascade mountains. First, we developed a robust, straightforward method for detecting heat-killed foliage using machine learning and satellite images acquired immediately before and after the heat wave. Next, we used geospatial datasets to determine which biophysical factors were associated with sensitivity to foliar damage across the landscape. These geospatial datasets represent factors that may mediate foliage sensitivity to extreme heat and consisted of surface and air temperatures, topographic variables, dominant tree species, canopy height, and for Douglas-fir (*Pseudotsuga menziesii*), budburst phenology and the presence of a foliar pathogen. This spatially explicit approach was used to (1) examine the associations between potential contributors to extreme heat sensitivity in these temperate, conifer-dominated forests and (2) suggest future controlled experiments or simulations to test causal relationships. Next, we identified spatial "hotspots" where mapped foliar mortality was particularly intense and evaluated the ecosystem and cultural context of two of these hotspots: old-growth forests of Olympic National Park and the plantation forests of

13652486, 2025, 11, Downloaded from https://onlinelibrary.wiley.com/doi/10.1111/gcb.70571 by National Forest Service Library, Wiley Online Library on [20/11/2025]. See the Terms and Conditions (https://onlinelibrary.wiley.com/terms-and-conditions) on Wiley Online Library for rules of use; OA articles are governed by the applicable Creative Commons License

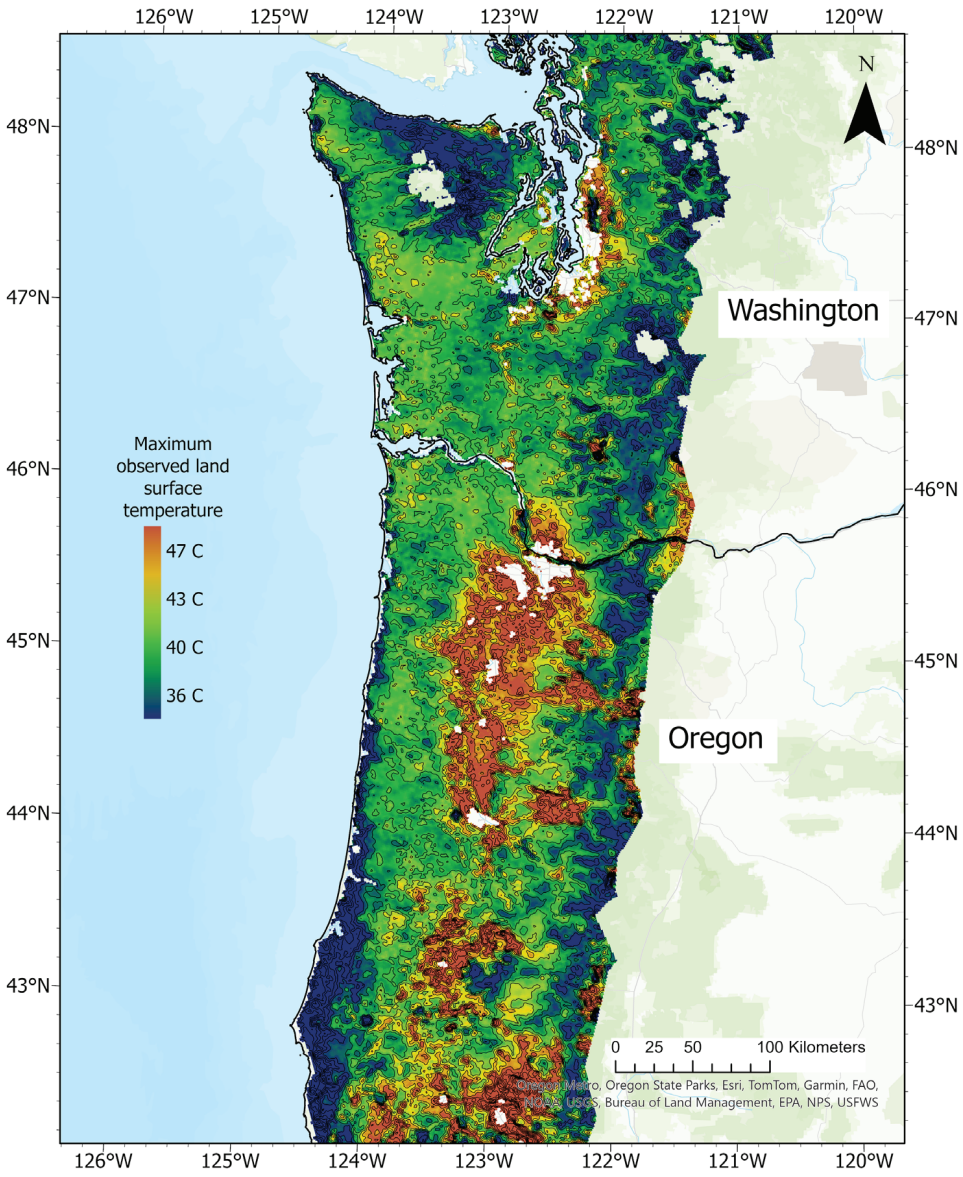

FIGURE 1 | Maximum land surface temperatures in the study area during the heatwave (June 25–29, 2021), derived from the MODIS (Moderate Resolution Imaging Spectroradiometer) daily daytime land surface temperature product (MYD11A1, Hulley and Hook 2021). Hotspots > 47°C include urban areas, agricultural valleys, and burn scars from the 2020 Oregon wildfires. Isotherm line intervals are 2°C and begin at 36°C. Map lines delineate study areas and do not necessarily depict accepted national boundaries.

the Oregon Coast Range. These analyses allowed us to describe how specific heat sensitivities could lead to large future changes in forest species composition, structure, function, carbon storage, and ecosystem services if extreme heat waves become more common. Finally, we place the response of PNW forests to the 2021 heat wave in a global context and provide recommendations for further research.

2 | Materials and Methods

2.1 | Study Area

Based on communications with researchers and forestry professionals about the regional extent of canopy damage related to the 2021 heat event (Figure 2), this study focused on forested lands in the western portions of Oregon and Washington, USA (Figure 3). Forests of this area are primarily temperate coniferous forests (Franklin and Dyrness 1973). At lower elevations, dominant canopy tree species include Douglas-fir (*Pseudotsuga menziesii*), western hemlock (*Tsuga heterophylla*), and western redcedar (*Thuja plicata*). At higher elevations, dominant canopy tree species include Pacific silver fir (*Abies amabilis*) and noble fir (*Abies procera*). Deciduous tree species like Oregon white oak (*Quercus garryanna*), red alder (*Alnus rubra*), and bigleaf maple (*Acer macrophyllum*) are common in wetter valley bottoms and at the margins of non-forest ecosystems that were historically maintained by frequent fire. Other forests are locally dominated by other tree species due to particular environmental conditions, such as moisture limitation (e.g., Pacific madrone, *Arbutus menziesii*), and disturbance history, such as the presence or absence of past logging activity. By percentage of the study area where a given species has the plurality of basal area (scale: 900 m^2 grid cells, see "forest condition" section),

13652486, 2025, 11, Downloaded from https://onlinelibrary.wiley.com/doi/10.1111/gcb.70571 by National Forest Service Library, Wiley Online Library on [20/11/2025]. See the Terms and Conditions (https://onlinelibrary.wiley.com/terms-and-conditions) on Wiley Online Library for rules of use; OA articles are governed by the applicable Creative Commons License

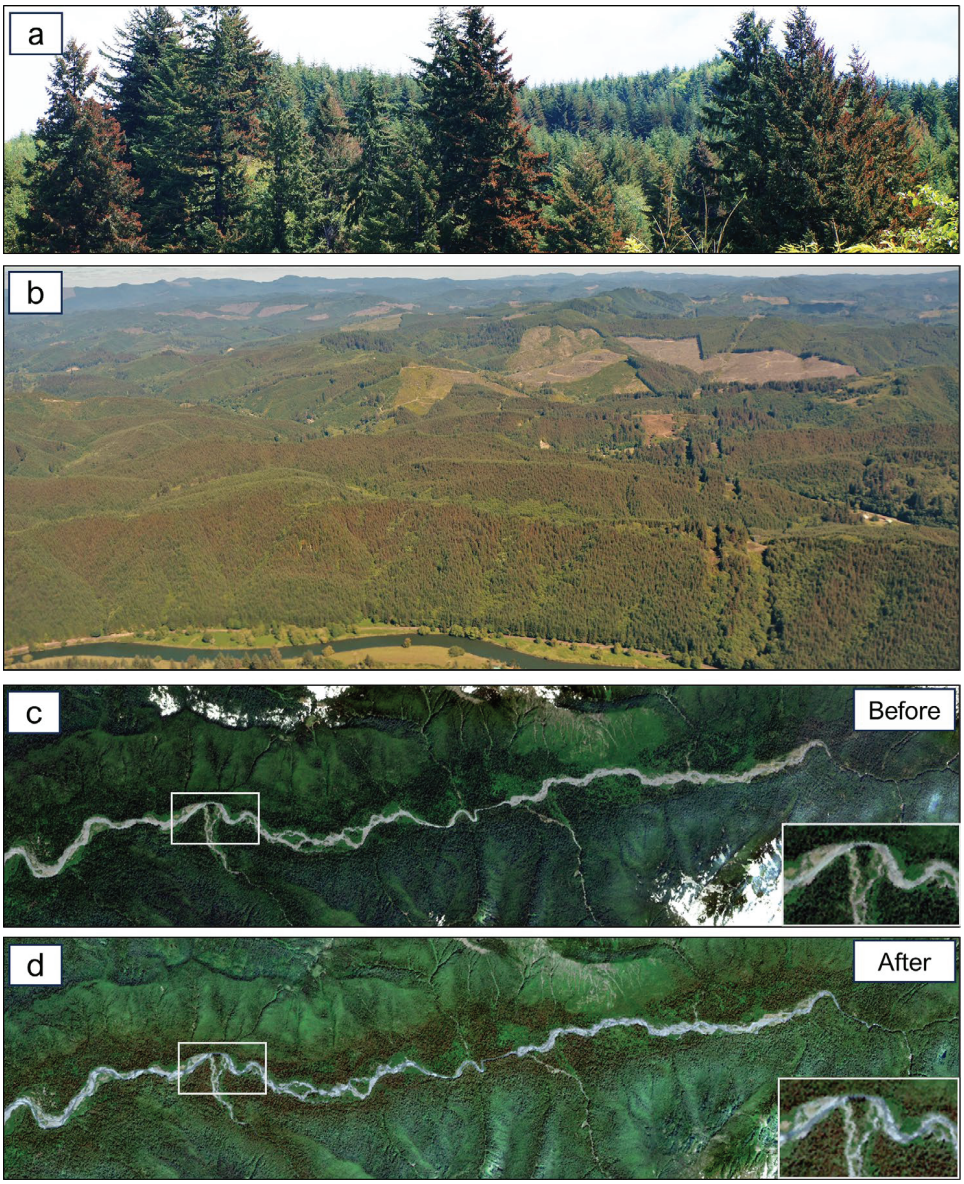

FIGURE 2 | Photographic evidence of foliar death on the landscape. (a) Douglas-fir trees near Logsden, OR (latitude: 44.74°N) with scorched foliage on west-facing branches. (b) Aerial photograph of Douglas-fir dominated hillsides near Newport, OR (credit: Daniel DePinte, latitude: 44.61°N). (c) True-color imagery composite of an upper stretch of the Hoh River on the Olympic Peninsula, WA (composite of Sentinel-2 imagery between June 1 and 24, 2021.) (d) The same stretch of the Hoh River, composite dates July 4–21, 2021. Insets in lower right show zoomed-in imagery from white boxes in the center left of the images. Notable species in this valley include Sitka spruce, bigleaf maple, western hemlock, western redcedar, red alder, and Douglas-fir.

the five most common species in the study area are Douglas-fir (*Pseudotsuga menziesii*, 65% of forest area), western hemlock (*Tsuga heterophylla* , 12.1%), red alder (*Alnus rubra* , 7.7%), western redcedar (*Thuja plicata, 3.6%*), and bigleaf maple (*Acer macrophyllum* , 3.6%) (Ohmann 2012; Bell et al. 2023). All other tree species made up the remaining 9.2% of forested area (Table 2).

2.2 | Mapping Scorch

To map forests that exhibited heat killed, or "scorched" upper-canopy foliage (that which is visible to a satellite), we gathered multispectral remote sensing data for the entire study region, collected reference data for forested pixels (scorched vs. unscorched pixels), developed a model for classifying forested pixels as scorched, and applied masking techniques to the resulting prediction maps to exclude nonforest pixels and pixels with spectral properties consistent with scorch prior to the heat event.

The imagery that we used to map scorched foliage was 10-m spatial resolution pre- and postheat wave composites of surface reflectance (SR) data from the Sentinel-2 L2A product (Copernicus Sentinel-2 (processed by ESA) 2022). We used a median composite and approximately 3 weeks of data for pre- and postheat wave intervals (June 1–24 and July 4–30, respectively), which was the minimum time range that resulted in relatively cloud-free composites and was sufficiently near in time to the event to minimize the inclusion of changes in foliage associated with other agents and/or phenological changes. Before compositing, we masked pixels that contained clouds

13652486, 2025, 11, Downloaded from https://onlinelibrary.wiley.com/doi/10.1111/gcb.70571 by National Forest Service Library, Wiley Online Library on [20/11/2025]. See the Terms and Conditions (https://onlinelibrary.wiley.com/terms-and-conditions) on Wiley Online Library for rules of use; OA articles are governed by the applicable Creative Commons License

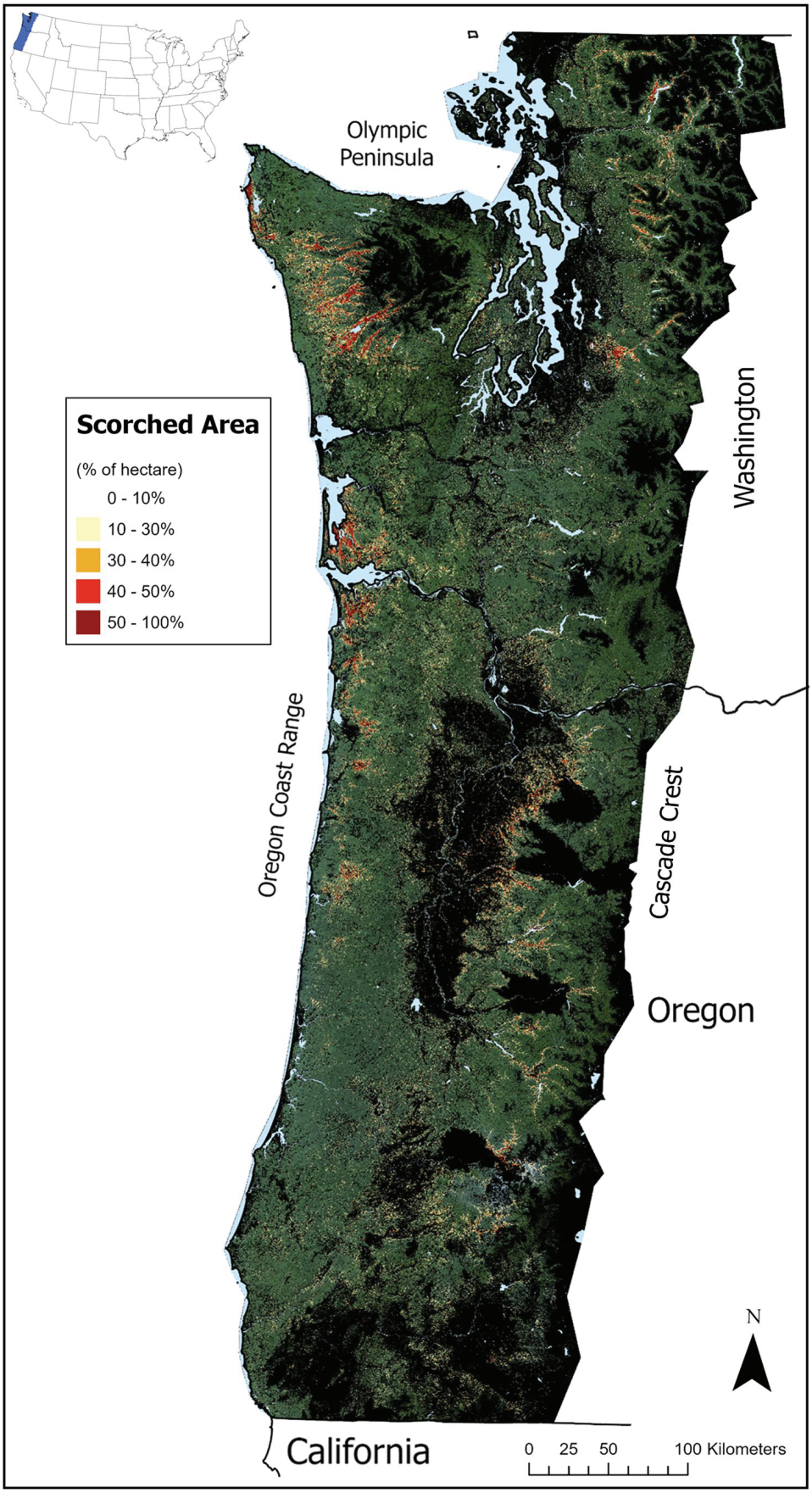

FIGURE 3 | Legend on next page.

13652486, 2025, 11, Downloaded from https://onlinelibrary.wiley.com/doi/10.1111/gcb.70571 by National Forest Service Library, Wiley Online Library on [20/11/2025]. See the Terms and Conditions (https://onlinelibrary.wiley.com/terms-and-conditions) on Wiley Online Library for rules of use; OA articles are governed by the applicable Creative Commons License

FIGURE 3 | Map of scorched foliage, highlighting regional hotspots. Classification of scorch produced at 100 m^2 resolution was averaged over a 10,000 m^2 footprint and expressed as percent of hectare scorched. Black background represents areas that were masked out of the analysis. Green background represents areas within the study area that had < 10% canopy scorch (transparent value in legend). Inset in upper left shows study region in blue. Map lines delineate study areas and do not necessarily depict accepted national boundaries.

or cloud shadows using the "S2 Cloud Probability" layer in Google Earth Engine (GEE; Gorelick et al. 2017). Briefly, we used a cloud probability threshold of 30%, above which a pixel was excluded from consideration if its cloud displacement index was also greater than −0.5 (calculated using the GEE operator ee.Algorithms.Sentinel2.CDI) or if it had a value greater than 0.01 in Sentinel-2 band 10 (the "cirrus" band). Pixels were also masked if projected shadows intersected with low reflectance in the NIR band (band 8). We also masked pixels that had reflectance values higher than 0.035 in Sentinel-2 band 1 (the "aerosols" band) to exclude observations that were contaminated by smoke or haze, primarily from fires smoldering in southern Oregon.

To assemble a data set of training points, we used a two-stage approach. For the first stage, points of each class were chosen using Planet imagery. For areas of the Oregon Coast where substantial foliage scorch was documented in ground observations, we obtained five scene pairs of single-date (one pre-June 24, one post-July 4), high-resolution image acquisitions from Planet Scope 2 Superdove satellites (Planet Labs). These 3-m spatial resolution, true-color images from pre- and postheat wave were uploaded into GEE for training point selection. Scorch points were chosen as the centroid of a $\geq 3 \times 3$ pixel area of forest that transitioned from visibly green before the heat wave to visibly orange/red after. For a point to be labeled "unscorched," the center pixel and surrounding 3×3 area needed to be visibly green both before and after the heat wave. 971 points were selected in this way (528 scorch, 443 unscorched).

For the second stage of training data collection, an additional 354 training points were selected. Selection was done via visual inspection of true-color composites made from the pre- and postheatwave Sentinel-2 imagery described previously. We applied the same criteria of selecting the centroid of 3×3 pixel areas of either pure scorch or unscorched pixels, in this case, to avoid pixels that may be influenced by edge effects. Damaged points were selected within areas that were verified by ground observations as hotspots of canopy scorch. There were a greater number of unscorched examples selected in this round of point selection (52 scorch, 302 unscorched) as extra examples were included of locations where scorch did not occur but visible haze was present in the post-heatwave imagery near smoldering fires in southern Oregon. These points were included to improve the classification of pixels as "unscorched" when their spectral signature was influenced by haze and not tree canopy damage.

To train a random forest classifier (ee.Classifier.smileRandomForest in GEE) using these points, we extracted blue (B), green (G), red (R), and near infrared (NIR) bands from both pre- and postheat wave Sentinel image composites. For predictors, we used postheat wave composite values in the R, G, and B bands, the red to green ratio (red–green index, RGI), an index of vegetation greenness (enhanced vegetation index, EVI; Huete et al. 2002), an index of whiteness (normalized saturation-value difference index, NSVDI; Ma et al. 2008), and the difference between pre- and postheatwave composites in RGI and EVI. NSVDI was used to help counterbalance changes in band values that were caused by haze/smoke and not scorch. The classifier was configured with 50 decision trees, 3 variables per split, a minimum leaf population of 1, and a bag fraction of 0.5, which are the default settings in Google Earth Engine. Classification was done using a probability threshold of 0.5 to mimic the expectation for a binomial process.

After producing a classified map of scorch/unscorched, we applied a series of masks to ensure that further analysis only included forested areas and forest pixels which did not show signs of previous damage. To develop a mask to exclude non-forested pixels from our analysis, we used the Dynamic World near real-time land use/land cover product (Brown et al. 2022). For every pixel and every date of Sentinel-2 imagery used in our study, the Dynamic World product provided the probability that a pixel belonged to each of nine possible land cover classes. We made a preheat wave median composite of class probability values and then classified each pixel as forest or nonforest. We tested probability thresholds between 30% and 80% in increments of 10% for the "tree" class and between 5% and 30% in 5% increments for all other classes and used combinations of these thresholds to create a series of forest masks. Based on visual inspection of the study region and judging effectiveness in discriminating nonforest from forest pixels, we determined the best performing mask used criteria where pixels were considered forest if they had a median probability of belonging to the "tree" class greater than 40% as well as a lower than 15% probability of belonging to any other class. Compared to other thresholds, this combination was particularly effective at excluding forest roads and clearcut areas containing grass and shrubs. However, there remained notable cases where pixels around the perimeter of clearcuts and those making up narrow forest roads were inappropriately included in the forest class. To ensure that these areas could not be classified as scorched forest, we added a 1-pixel (10 m) square buffer to our base mask using the focal max operator in GEE, which effectively expanded the nonforest-classified areas to include these edge cases, thus eliminating them from our forest canopy scorch analyses.

In addition to the mask of nonforested areas, we developed two masks to ensure we excluded forest pixels that were orange/red before the heat wave. The first mask used the Monitoring Trends in Burn Severity (Eidenshink et al. 2007, Picotte et al. 2020, https://www.mtbs.gov/) raster product to exclude all pixels that were within the burn perimeter of a wildfire (severity class 1 or greater) that ignited in the years 2020 or 2021. This was done to exclude any trees that had been damaged in a wildfire and still retained fire-scorched dead foliage. The second mask was developed to handle all other biotic or abiotic causes of damage preheat wave. This mask was made by training a random forest

13652486, 2025, 11, Downloaded from https://onlinelibrary.wiley.com/doi/10.1111/gcb.70571 by National Forest Service Library, Wiley Online Library on [20/11/2025]. See the Terms and Conditions (https://onlinelibrary.wiley.com/terms-and-conditions) on Wiley Online Library for rules of use; OA articles are governed by the applicable Creative Commons License

classifier on just the postheat wave composite imagery and applying it to the preheat wave composite. If a pixel was classified as "scorched" in the preheat wave imagery, it was masked from further analysis.

To validate the random forest classifier and to generate an unbiased estimate of total scorch area for our map, we used the map of scorch as a stratifier to randomly sample 349 scorch pixels and 349 unscorched pixels. The centroids of these pixels were uploaded as points to Google Earth Engine without labels. We visually interpreted change in the Sentinel-2 true-color image composites at each point location and labeled the actual scorch status for each pixel. These points were used to apply an error-adjusted area estimation approach (Olofsson et al. 2013) to generate a bias-corrected scorch area estimate with a 95% confidence interval. This approach uses an error matrix constructed for the class of interest (scorch) to quantify omission and commission rates. The total estimate of scorched area is adjusted to subtract the percentage of area represented by the commission rate and add the percentage of area represented by the omission rate. The error adjustment procedure uses a similar quantification of the omission and commission rates to quantify the standard error of the area estimate, from which the 95% confidence interval is calculated (Olofsson et al. 2013). Validation of the random forest classifier was done using the full training data set in both a hold-one-out cross-validation and a 10-fold cross-validation. Additionally, we used the training dataset together with the stratified random sample of points ($n = 1983$) to conduct a spatially blocked cross-validation using the "spatial kfold" package in Python. We used random allocation of blocks to folds, a block size of 10 km, and 15 folds to generate a mean and standard deviation of model accuracy. This method gives an accuracy estimate that is robust against spatial autocorrelation.

2.3 | Forest Scorch Related to Environmental Predictors

To quantify how the frequency of forest canopy scorch varied as a function of different potential drivers of forest sensitivity to extreme heat—specifically, geomorphology, tree species, stand height, site climatology, heat wave temperatures, and vegetative bud burst phenology—we developed a Scorch Probability Index (SPI). Within discrete intervals across the range of each data source, we calculated SPI as the proportion of mapped scorched forest area to total forest area, which demonstrates where scorch occurrence was disproportionately high relative to the existing areal coverage under a given set of conditions (e.g., for southwest-facing topographic positions). To facilitate the relevant SPI comparisons, we leveraged existing geospatial data sets to quantify terrain attributes, air and land surface temperatures, tree species dominance, forest canopy height, and tree phenology (Table 1). In the figures that present the continuous variables considered (Figures 4–7 and S4), each point in the plot represents the center value of equally sized bins that were used to discretize the continuous variable. We also delineated four "hotspots" of scorch within the study region after visual inspection of the map of canopy scorch. These hotspots were chosen based on the intensity of scorch within subregions of the study area that are biogeographically distinct (Figure S3). Scorch patterns were analyzed within these hotspots when factors specific to these biogeographic regions appeared to play a role in determining scorch severity.

2.3.1 | Terrain Features

To characterize landform types and topographically driven heat loading, we used the Ecologically Relevant Geomorphology (ERGo) data set produced by the Conservation Science Partners (CSP) (Theobald et al. 2015). This data set is available at 10-m resolution and was aggregated for analysis with other predictors to a common resolution of 30-m using nearest-neighbor resampling. From this data set, we used the Continuous Heat-Insolation Load Index (CHILI), which scales between 0 and 1 and is a "surrogate for effects of insolation and topographic shading on evapotranspiration." A CHILI value of 0 represents the coolest, most shaded landscape positions, whereas 1 indicates the most sun-exposed, warmest positions. The CHILI index was computed as a function of latitude, slope, aspect (McCune and Keon 2002), and an aspect "folding parameter" of 22°, which reflects the location of "thermal south" as 22° west of due south (the aspect where cumulative thermal loading is greatest, given that direct sun in the afternoon leads to higher maximum surface temperatures than direct sun exposure in the morning). We also used a simplified version of the CSP ERGo landforms classification to assign a descriptive characterization to landscape features (Table S1). We used a 10-m map of elevation (U.S. Geological Survey, 3D Elevation Program 10-Meter Resolution Digital Elevation Model) with the ee.Terrain.aspect function in GEE to assign aspect values to each 10-m pixel, which we resampled using nearest neighbor to 30-m resolution.

2.3.2 | Air and Land Surface Temperature

We obtained daily minimum, mean, and maximum air temperatures (T_{air}) at 800 m spatial resolution for our entire study area from the PRISM Climate Group (PRISM Climate Group, accessed 2023). Daily data for November 20, 2020, through June 31, 2021, were used to calculate maximum T_{air} during the heat wave and as input to the Douglas-fir bud burst model described in the following section. We used PRISM 30-year climate normals (1991–2020) at the same spatial resolution for the dates of the heat wave (June 25–29) to quantify the number of standard deviations above mean T_{air} maximum the daily T_{air} maximum values were during the heat wave. The daily time series and climate normals are subject to uncertainties in station data availability and spatial interpolation. As such, the PRISM gridded values should be viewed as reasonable estimates, not actual observations. Data for land surface temperature ($T_{surface}$) were obtained from the MODIS daily land surface temperature and emissivity product (Hulley and Hook 2021) and were used to examine potential maximum canopy temperatures experienced by forests during the heat wave. For each day of the heat wave, temperatures were obtained for the time points closest to midday (acquisition times across days varied between 12:00 and 13:30 local time) and only values with a quality flag of 0 ("good quality") were kept. Daily $T_{surface}$ grids were reduced to a single estimate of the highest $T_{surface}$ experienced across the duration of the heat wave.

13652486, 2025, 11, Downloaded from https://onlinelibrary.wiley.com/doi/10.1111/gcb.70571 by National Forest Service Library, Wiley Online Library on [20/11/2025]. See the Terms and Conditions (https://onlinelibrary.wiley.com/terms-and-conditions) on Wiley Online Library for rules of use; OA articles are governed by the applicable Creative Commons License

TABLE 1 | Description of environmental attributes to be related to canopy scorch.

Attribute group	Attribute name	Attribute description
Terrain	Aspect (degrees)	Slope direction in degrees
	Continuous Heat-Insolation Load Index (CHILI)	Surrogate for effects of insolation and topographic shading on evapotranspiration (McCune and Keon 2002)
	CSP ERgo Landform	Descriptive characterization to landscape features found in the map (Theobald et al. 2015)
Temperature	Air temperature (T_{air}) maximum (°C)	Maximum observed air temperature during June 25–29, 2021 (PRISM Climate Group 2023)
	Air temperature (T_{air}) maximum anomaly (unitless)	Number of standard deviations above the long-term mean maximum air temperature observed during June 25–29, 2021 (PRISM Climate Group 2023)
	Surface temperature ($T_{surface}$) maximum (°C)	Satellite remote sensing of land surface temperature (MODIS; Hulley and Hook 2021)
Forest condition	Budbreak date	The date of budburst as the first date when both chilling and forcing requirements are met (Ford et al. 2016)
	Canopy height (m)	Tree canopy height based on Landsat imagery and GEDI lidar acquisitions (Potapov et al. 2021)
	Dominant species	Tree species with the greatest proportion of the basal area, based on gradient nearest neighbor imputed forest structure and composition mapping (Bell et al. 2021, Davis et al. 2022)
	Swiss needle cast	Locality and severity of Swiss needle cast as observed in Aerial detection surveys (U.S. Forest Service-PNW Forest Health Protection 2023)

Spatially explicit estimates of air temperature, T_{air} normals, and $T_{surface}$ could not be directly compared with the terrain features (CHILI, landform type, aspect) because of the mismatch between spatial resolutions. At a scale of 800–1000 m (800 m for PRISM T_{air} and 1 km for MODIS $T_{surface}$), a variety of aspects, landform types, CHILI values, landcover types, and tree species can exist within a given pixel. Given the spatial mismatch between terrain and vegetation features (10-m and 30-m resolution) and temperature products (800-m and 1-km resolution), when temperature relationships were analyzed, we filtered our map of damage to include only the grid cells in the T_{air} and $T_{surface}$ products that contained > 75% forest cover and compared foliar scorch as a function of temperature within species (see following section) to get a relative sense of species sensitivity to high temperatures.

2.3.3 | Forest Condition

The distribution of tree species was characterized using the 2021 version of the gradient nearest neighbor (GNN; Ohmann and Gregory 2002) forest attribute maps for Oregon and Washington (Bell et al. 2021). As applied in Oregon, Washington, and California, GNN imputes measurements from USDA Forest Service Forest Inventory and Analysis—a national forest inventory of USA forests (Burrill et al. 2024)—to all forested 30-m pixels based on the similarity between plots and pixels in terms of climate, topography, and Landsat multispectral satellite imagery (Bell et al. 2021; Davis et al. 2022). For each pixel in the map (30-m resolution), tree species are assigned using the species with the greatest proportion of the basal area as measured on the plot imputed as the nearest neighbor. Though pixel-level uncertainty of relative abundance, and thus dominance, of tree species for these maps can be high, analyses at landscape to regional levels like ours are well supported (Bell et al. 2023). Still, over- or underrepresentation of some species could bias our results. Canopy height was obtained from a global forest canopy height map (Potapov et al. 2021) produced at 30-m spatial resolution, using Global Ecosystem Dynamics Investigation (GEDI) spaceborne LIDAR data and Landsat multispectral imagery.

To test the effect of the timing of Douglas-fir spring budburst (leaf phenology) on sensitivity to damage, we used a budburst prediction model (Ford et al. 2016), which predicts the date of budburst as the first date when both chilling and forcing requirements are met. Chilling and forcing were calculated as a function of hourly temperature, beginning November 1, 2020, and running through the beginning of the heat wave (June 24, 2021). Spatially explicit estimates of daily minimum and maximum T_{air} from PRISM (see previous section) were disaggregated to hourly values using the MEteoroLOgical observation DISaggregation Tool (MELODIST) (Förster et al. 2016). Within

13652486, 2025, 11, Downloaded from https://onlinelibrary.wiley.com/doi/10.1111/gcb.70571 by National Forest Service Library, Wiley Online Library on [20/11/2025]. See the Terms and Conditions (https://onlinelibrary.wiley.com/terms-and-conditions) on Wiley Online Library for rules of use; OA articles are governed by the applicable Creative Commons License

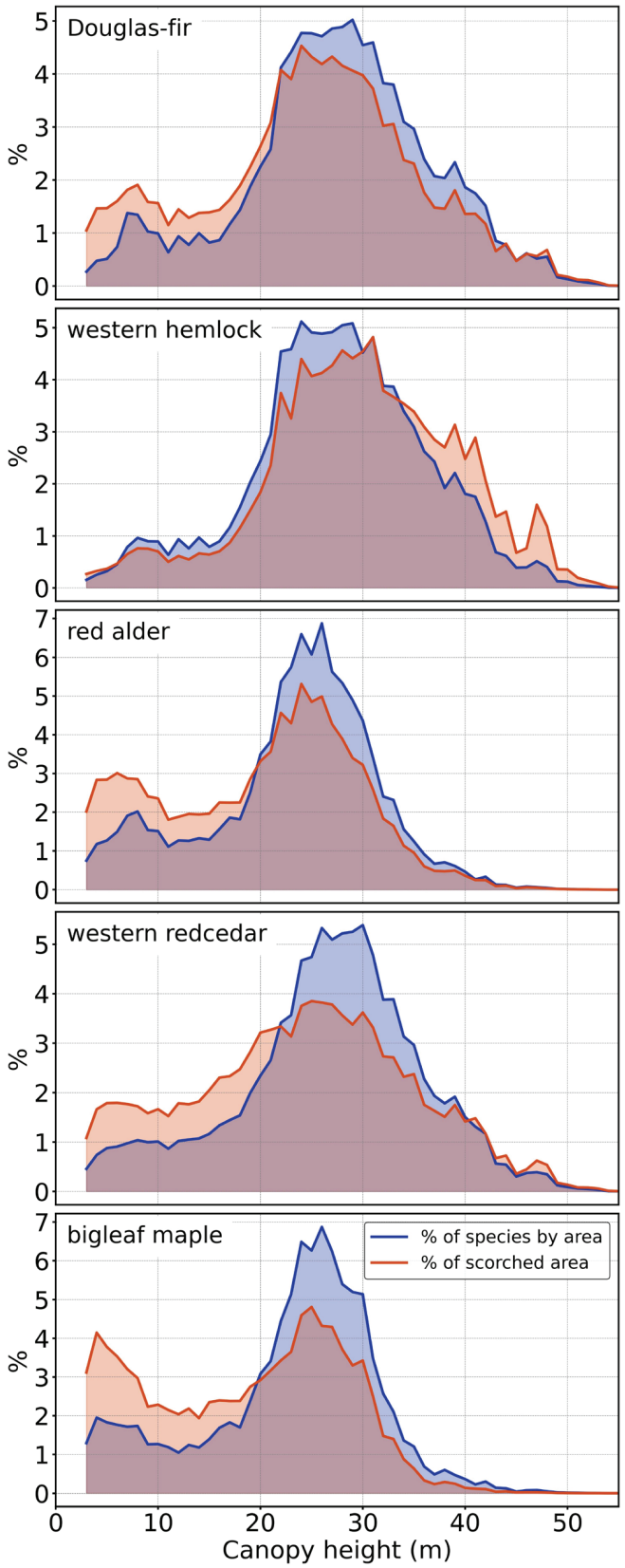

FIGURE 4 | Relationship between stand height, percent of a given species on the landscape, and percent of the scorch damaged forest within the five most common species in the study area. Canopy heights are binned at an interval of 1 m. Species labels are assigned to pixels based on the species with the greatest proportion of the basal area within the stand that the pixel represents (900 m^2 footprint).

each pixel, the first date when both chilling and forcing requirements were met was assigned to the pixel as the estimated date of budburst.

To examine the potential role of a foliar pathogen, Swiss needle cast (SNC, *Nothophaeocryptopus gaeumannii*), we incorporated into this study a map of SNC visible symptoms produced during an Aerial Detection Survey (ADS) campaign in 2018 (US Forest Service-PNW Forest Health Protection 2023). Survey flights were flown in late April to early June covering 2.7 million hectares of forest in western Oregon and Washington. Observers aboard the aircraft identified stands of Douglas-fir with yellow-brown foliage discoloration, which is a symptom of SNC infection. Polygons were drawn around affected stands and labeled as either moderately or severely infected. Both infection classes are used in this study to identify the near-coast zone of widespread SNC infection in the Coast Range (Figure 3). No explicit spatial analysis was done with these data because visible symptoms can vary from year to year within a given stand and the mapping methodology used in the survey can result in variation in mapped polygon locations between survey dates. The 2018 ADS survey was the nearest in time to the heat wave and was used in this study to identify the general zone of widespread SNC infection (Shaw et al. 2021).

2.4 | Statistical Analysis

To test the significance of relationships between scorch occurrence and potential drivers of sensitivity, we drew a spatially stratified sample of observations from the study area and used them to conduct two analyses: logistic regression and effect size quantification using Hedges' *g*. A sampling grid with ~950 m spacing was used to draw an initial sample ($n = 400{,}000$ points), within which there were 72,370 forested points. From the pool of forested pixels, we selected every dominant species type with at least 2000 points ($n = 5$) in the data set and analyzed: (1) the relationship between covariates and the probability of scorch occurrence and (2) effect sizes between the distribution of covariates for scorched and unscorched forest pixels. We did not apply denser sampling, which would have provided a sufficient sample size to examine all dominant tree species, to avoid spatial autocorrelation in the sample that could bias these statistical tests.

To quantify whether potential drivers were significantly related to increases or decreases in the probability of scorch, we fit multiple logistic regressions (using the glm function, "stats" package, R Core Team (2024)) between scorch occurrence and a single covariate for each regression: canopy height, CHILI, maximum heatwave $T_{surface}$, heatwave $T_{air\text{-}max}$, $T_{air\text{-}max}$ anomaly, and the number of standard deviations heatwave $T_{air\text{-}max}$ was above normal $T_{air\text{-}max}$. Relationships between each of these covariates and scorch within species were deemed significant if the 95% confidence interval for the estimated slope of scorch probability in logit space with respect to the covariate did not include 0.

To quantify effect sizes we calculated Hedges' g for the same covariates listed above, using the hedges_g function in the

13652486, 2025, 11, Downloaded from https://onlinelibrary.wiley.com/doi/10.1111/gcb.70571 by National Forest Service Library, Wiley Online Library on [20/11/2025]. See the Terms and Conditions (https://onlinelibrary.wiley.com/terms-and-conditions) on Wiley Online Library for rules of use; OA articles are governed by the applicable Creative Commons License

TABLE 2 | Landscape representation and scorch damage in stands where the given species has the greatest proportion of the basal area (stand scale 900 m^2).

Species		Presence in forest		Presence in scorched forest		Scorch proportionality Index
Common name	Scientific name	Area (ha)	Percent	Area (Ha)	Percent	% of scorch: % of forest
Douglas-fir	*Pseudotsuga menziesii*	4,096,873	65.3	138,187	56.5	0.9
Western hemlock	*Tsuga heterophylla*	760,174	12.1	44,970	18.4	1.5
Red alder	*Alnus rubra*	481,115	7.7	15,719	6.4	0.8
Western redcedar	*Thuja plicata*	225,972	3.6	13,332	5.5	1.5
Bigleaf maple	*Acer macrophyllum*	225,706	3.6	9814	4.0	1.1
Pacific silver fir	*Abies amabilis*	130,631	2.1	1177	0.5	0.2
Grand fir	*Abies grandis/concolor*	52,087	0.8	1954	0.8	1.0
Sitka spruce	*Picea sitchensis*	49,261	0.8	4624	1.9	2.4
Black cottonwood	*Populus balsamifera ssp. Tric.*	32,423	0.5	1801	0.7	1.4
Oregon ash	*Fraxinus latifolia*	25,332	0.4	1882	0.8	1.9
Tanoak	*Lithocarpus densiflorus*	22,832	0.4	952	0.4	1.1
Pacific madrone	*Arbutus menziesii*	20,827	0.3	1660	0.7	2.0
Noble fir	*Abies procera/shas./magn.*	17,950	0.3	207	0.1	0.3
Umbellularia	*Umbellularia californica*	16,733	0.3	446	0.2	0.7
Lodgepole pine	*Pinus contorta*	15,807	0.3	1200	0.5	1.9
Oregon white oak	*Quercus garryana*	14,196	0.2	2501	1.0	4.5
All other species		82,034	1.3	3969	1.6	1.2
Total		6,269,953	100	244,395	100	1.0

Note: Listed species are the 16 most common species by forest area, with all remaining species grouped in "All other species". Color coding shows which species had a scorch proportionality index below 1 (blue) or above 1 (red).

"effectsize" package in R (Ben-Shachar et al. 2020). *g* values were interpreted as significant if the 95% confidence interval based on a two-tailed test did not span zero.

3 | Results

3.1 | Spatial Extent of Canopy Damage

In the 6.3 million ha of forest in our study area (western Oregon and Washington), we detected 244,395 ha of forest canopy with dead foliage (Figure 3), which is greater than 250% of the area previously reported based on spatially limited aerial surveys (U.S. Forest Service-PNW Forest Health Protection 2023). Overall accuracy of the map was 92.4% assessed using hold-one-out cross-validation, 91.2% using 10-fold cross-validation (Table S2), and 94.1% on average (standard deviation 5.5%) using spatially blocked cross-validation. Using the error-adjusted area estimation procedure given by Olofsson et al. (2013), we found that 293,546 ha were scorched (95% confidence interval = 233,674–353,418 ha), which is greater than our mapped scorch area and is consistent with omission error being greater than commission error in cross-validation results (Table S2).

3.2 | Factors Influencing Spatial Patterns of Sensitivity

The top five species by forest area—Douglas-fir (*Pseudotsuga menziesii*), western hemlock (*Tsuga heterophylla*), red alder (*Alnus rubra*), western redcedar (*Thuja plicata*), and bigleaf maple (*Acer macrophyllum)—were* also the top five species in mapped scorch area. However, the Scorch Probability Index (SPI) showed that western hemlock, western redcedar, and bigleaf maple experienced disproportionately high amounts of canopy scorch (Table 2). In contrast, Douglas-fir and red alder had an SPI below 1, indicating that the fraction of mapped scorched forest they represent is less than the fraction of total forest they represent. Notable species for their high sensitivity to heat damage were Sitka spruce (*Picea sitchensis* , SPI = 2.4), black cottonwood (*Populus trichocarpa* , SPI = 1.4), and Oregon ash (*Fraxinus latifolia* , SPI = 1.9). High-elevation species such as Pacific silver fir (*Abies amabilis* , SPI = 0.2) and noble fir (*Abies procera* , SPI = 0.3) experienced relatively little heat damage.

In addition to dominant tree species composition, forest height and phenological status also appeared to affect patterns of foliar scorch. Among four of the top five most damaged species, foliar scorch was more common in stands with shorter trees

13652486, 2025, 11, Downloaded from https://onlinelibrary.wiley.com/doi/10.1111/gcb.70571 by National Forest Service Library, Wiley Online Library on [20/11/2025]. See the Terms and Conditions (https://onlinelibrary.wiley.com/terms-and-conditions) on Wiley Online Library for rules of use; OA articles are governed by the applicable Creative Commons License

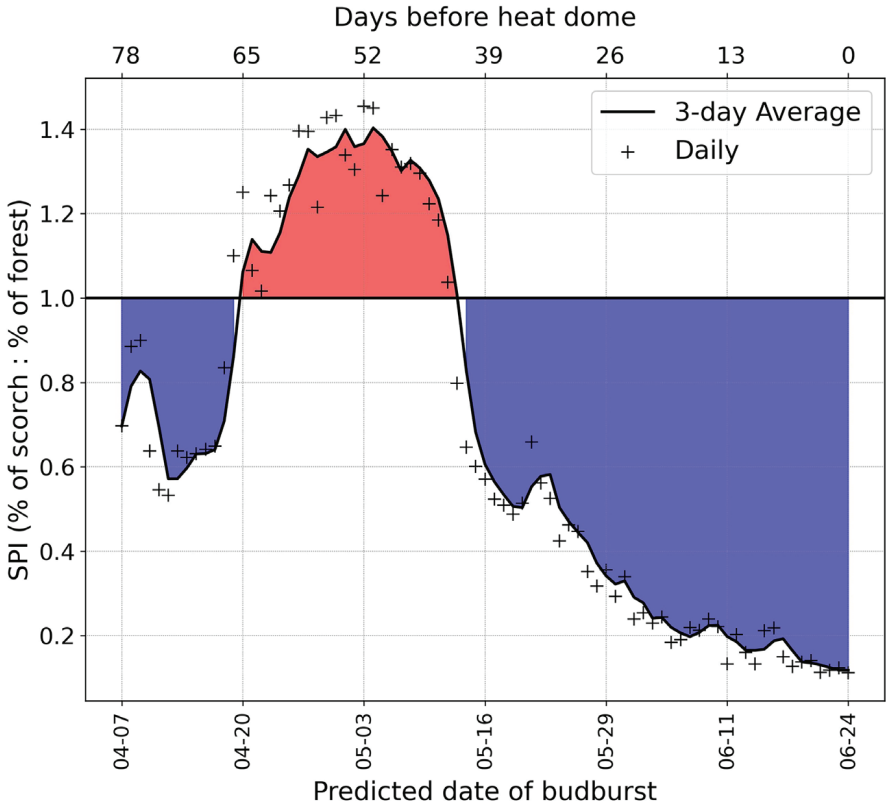

FIGURE 5 | Relationship between Scorch Proportionality Index (SPI) and predicted date of budburst in Douglas-fir.

(Figure 4). Effect sizes and logistic regression slope parameters between SPI and canopy height were negative for three of the five most common dominant tree species (Tables S3 and S4). An exception was western hemlock, which had SPI above 1 in forests with height ≥ 35 m, particularly in older forests along rivers in the western portion of the Olympic Peninsula (effect size and slope significantly positive—Tables S3 and S4). Finally, within stands dominated by Douglas-fir, trees that broke bud between April 19 and May 12 were more likely to experience damage than those that broke bud before or after those dates (Figure 5).

Across the study area, there was a tendency for higher proportions of foliar scorch (SPI > 1) on terrain positions with greater thermal loading. Specifically, mapped foliar scorch was more common when CHILI was greater than 0.63 (vertical dashed line in Figure 6a). Cooler north- and east-facing slopes largely fell under this threshold and had less scorch damage (Figure 6b,c), whereas south- and west-facing slopes were largely above this limit and made up a higher proportion of the mapped canopy scorch. CHILI values for valleys and ridge features had distinct SPI peaks at ~0.68, above the aforementioned threshold (0.63) where SPI rises above 1 (Figure 6a). Forests experiencing scorch had significantly greater CHILI values for forests dominated by three of the five most common dominant tree species (not bigleaf maple or western redcedar; Tables S3 and S4). However, valleys accounted for a larger proportion of mapped scorched forest (i.e., valleys account for 16% of the forested landscape, but 22.7% of scorched forest) than did peaks/ridges (7% of forested landscape, 6.6% of scorched forest), possibly due to the lower air temperature extremes experienced by higher elevation landscape features.

Patterns of canopy scorch within species across the range of $T_{air\text{-}max}$ and $T_{air\text{-}max}$ anomaly during the heat wave (Figure 7) showed that scorch prevalence increased above a maximum T_{air} of approximately 38°C. SPI values exceeded 1 at different thresholds for different species, with western redcedar being the most vulnerable (40°C) and bigleaf maple being the most tolerant (42.5°C). The general pattern of rising mapped scorch prevalence to SPI values greater than 1 beyond 40°C can be seen in observations of maximum $T_{surface}$ as well (Figure S4). Forests experiencing scorch had significantly greater maximum T_{air} and $T_{surface}$ for forests dominated by four of the five most common dominant tree species (no red alder; Tables S3 and S4). $T_{surface}$ values more closely correspond to sunlit leaf temperatures (T_{leaf}), which typically exceed air temperatures by 5°C–10°C (e.g., Still et al. 2023). In addition to apparent thresholds in maximum T_{leaf} and $T_{surface}$, the size of the maximum heat wave temperature anomaly was also relevant to foliar sensitivity. Heat wave air temperatures were at least 2.5 standard deviations above mean $T_{air\text{-}max}$ for the vast majority of forested areas, and across species the SPI exceeded 1 at anomalies of 3.7 standard deviations or greater (Figure 6). Forests experiencing scorch had significantly greater maximum T_{air} anomalies for forests dominated by the five most common dominant tree species, but no significant effects were noted for bigleaf maple when examining temperature anomalies as standard deviations above the mean (Tables S3 and S4). Western redcedar had a high proportion of scorch at relatively low absolute temperatures but high temperature anomalies, while in comparison bigleaf maple was relatively insensitive to the magnitude of anomalies. Instead, foliage disproportionately died in this species where it occupied low-lying landscape positions, such as valley bottoms and low hillslopes, where the heat wave led to overall higher $T_{air\text{-}max}$ (Figure 7).

13652486, 2025, 11, Downloaded from https://onlinelibrary.wiley.com/doi/10.1111/gcb.70571 by National Forest Service Library, Wiley Online Library on [20/11/2025]. See the Terms and Conditions (https://onlinelibrary.wiley.com/terms-and-conditions) on Wiley Online Library for rules of use; OA articles are governed by the applicable Creative Commons License

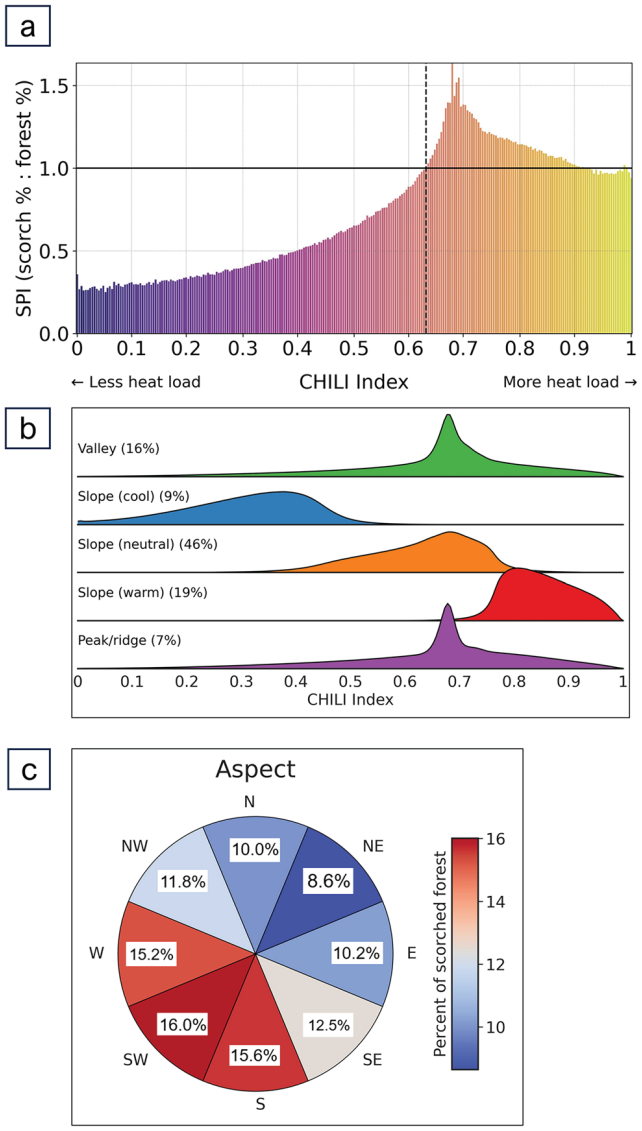

FIGURE 6 | Influence of terrain features on scorch. (a) Scorch Proportionality Index (SPI) within a given bin of the Continuous Heat-Insolation Loading Index (CHILI). Color scheme matches the scheme used in the map in Figure S6b. Distribution of CHILI values within different landform types. Percentages next to landform labels indicate the percent of the study area that falls into that landform type (see Table S1). All distributions sum to 1. (c) Percentage of scorched forest by hillslope aspect within equal area 45° slices. Nearly half of the scorched forest was within three aspects (S, SW, and W).

3.3 | Regional Variation in Canopy Scorch

Hotspots of mapped forest canopy scorch occurred in the Olympic Peninsula (49,664 ha), the Coast Range of northwest Oregon and southwest Washington (45,333 ha), and the Cascade Mountain foothills in the northern half of Oregon (35,407 ha) and in Washington (24,685 ha). Regional delineations are shown in Figure S3. On the Olympic Peninsula, damage was most extensive in Olympic National Park and Olympic National Forest, where it was conspicuously severe in the floodplain terraces and low elevation hillslopes of the river valleys west of the Olympic divide. Mapped canopy scorch was also prominent in the river valleys of the western foothills of the Cascade Mountains in both Washington and Oregon (Figure 3). In the Oregon Coast Range, which is characterized by lower elevation mountains and steeper, narrower river valleys, there was a more even balance between river valley hotspots and distributed canopy scorch on hillslopes.

4 | Discussion

The 2021 heat wave in the Pacific Northwest of North America was an uncontrolled test of the thermal tolerance of trees in their native environments. Overall, our results suggest that species distributions, species sensitivities to temperature extremes, and biotic stressors are important contributors to the unique regional hotspots of foliar mortality we observed. To our knowledge, there are no known examples of heat wave-induced foliar death at this scale in the historical record, making this event unique in the modern era. Further investigation into the specific conditions which are required to cause foliar death at this scale is merited, in anticipation of more common and more extreme future heat events.

A combination of high heat and high solar insolation can injure foliage by damaging photosystems and disrupting many aspects of photosynthesis (Teskey et al. 2015; Berry and Bjorkman 1980; Bongi and Long 1987). Foliar damage and death may also occur from membrane leakage or protein denaturation (Lancaster and Humphreys 2020; Marias et al. 2016). Because species and genotypes vary in temperature thresholds that cause foliar death (Lancaster and Humphreys 2020, Marias et al. 2016), these differences may partly explain spatial variation in foliage death. The temperature thresholds we observed (i.e., temperatures resulting in SPI >1) were close to observed thermal limits of leaf photosystems. Irreversible damage to leaf photosystems begins at leaf temperatures above 40°C–45°C for many species (Teskey et al. 2015). Future research should aim to more precisely quantify critical thresholds (in both temperature and duration of exposure) in highly sensitive species, both in the presence and absence of high solar insolation. These studies would enhance our ability to predict the extent of foliar mortality expected under a given set of heat wave conditions and topographic variables.

Of the 10 most common tree species we studied, high scorch probability index values (SPI >1) were observed for forests dominated by three shade-tolerant conifers (western hemlock, western redcedar, and Sitka spruce) and forests dominated by three riparian/wetland angiosperms (black cottonwood, Oregon ash, and bigleaf maple). This was surprising because these forests typically occupy geographic areas near the coast or topographic positions buffered from extremes in temperature and vapor pressure deficit (Davis et al. 2019; Dobrowski 2011) (Table 2). Thus, compared to species such as red alder and Douglas-fir, these species may not have had the same natural selection pressures for high heat tolerance. That is, they may have evolved a lower thermal threshold for damage to photosystems and other cellular structures, as well as a lower ability to resist wilting caused by uncontrolled transpiration. In contrast, upland forests dominated by Douglas-fir experienced extreme temperatures but were less sensitive to the heat wave (SPI <1). After disturbances such as fire, this shade-intolerant, early-seral species often regenerates in high-light environments with extreme surface temperatures. Thus,

13652486, 2025, 11, Downloaded from https://onlinelibrary.wiley.com/doi/10.1111/gcb.70571 by National Forest Service Library, Wiley Online Library on [20/11/2025]. See the Terms and Conditions (https://onlinelibrary.wiley.com/terms-and-conditions) on Wiley Online Library for rules of use; OA articles are governed by the applicable Creative Commons License

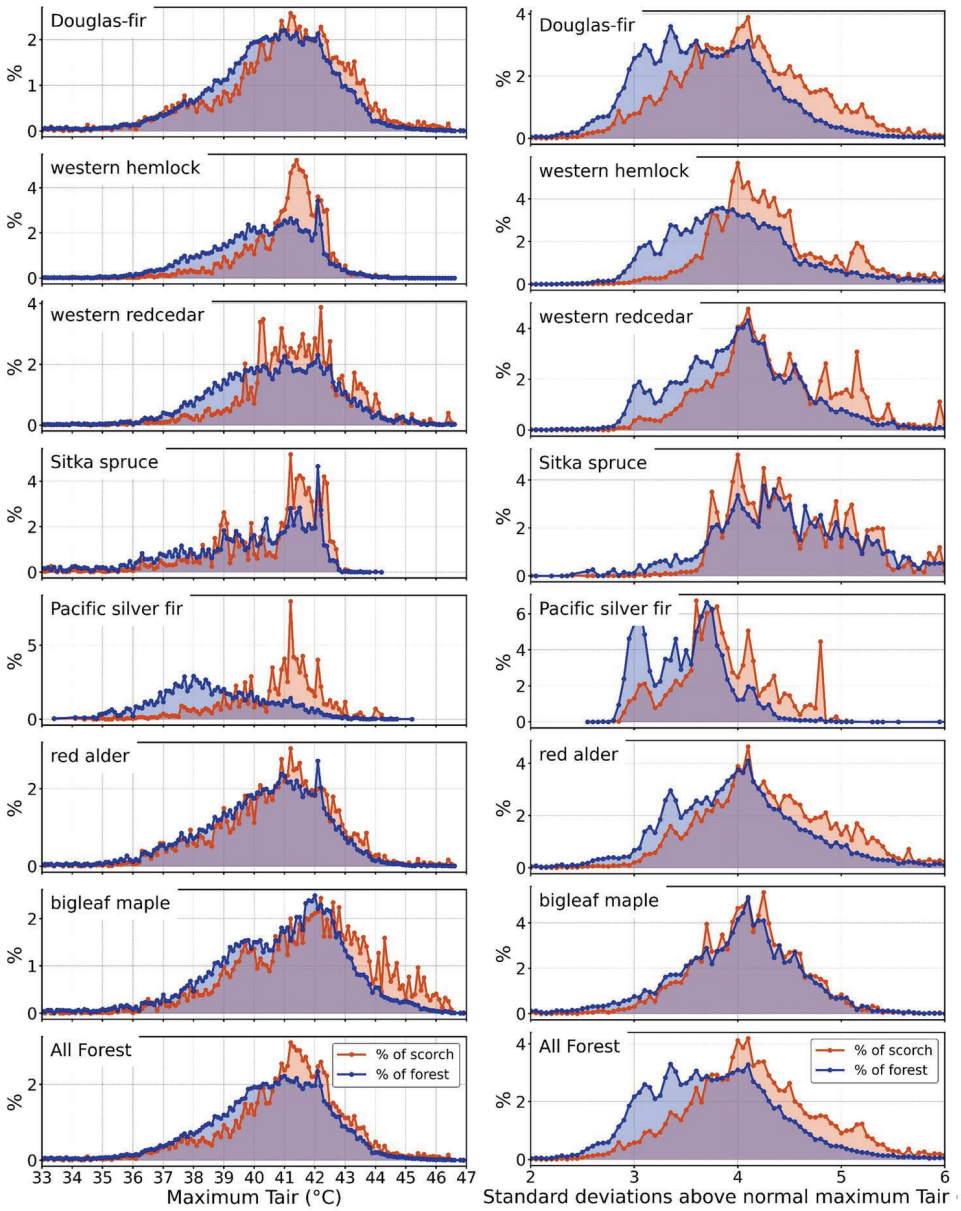

FIGURE 7 | Relationship between maximum air temperature (left column) or number of standard deviations above normal maximum T_{air} (right column) during the heat wave, the proportion of a given species on the landscape, and the proportion of the scorch damaged forest within that species. Only 800 m grid cells with > 75% forest cover were included in the analysis.

we hypothesize that low scorch resulted from natural selection for higher heat tolerance. This is also consistent with the observation that functional and morphological traits associated with leaf thermal tolerance are common in drought-tolerant tree species (Münchinger et al. 2023), since habitats that are exposed to extreme temperatures may also be drier locations. For high elevation species that also exhibited SPI < 1, canopy scorch was often observed in forests where $T_{surface\text{-}max}$ went above 40°C, but those conditions were rare for these species in our study area (see Pacific silver fir in Figure 7). Therefore, our results suggest that higher elevation species were not protected by higher thermal tolerances but rather had less exposure to high temperature extremes in the 2021 heat wave because of their topographic position (Figure 6b).

The change in canopy color due to heat-damaged foliage allowed us to explicitly map impacts across the study region. However, the heat wave may have also had negative effects on trees in areas where foliar damage was undetected (Ford et al. 2016). Heat waves that occur early in the growing season can slow growth, even when signs of stress are not apparent (Harrington et al. 2023). In Ontario, Canada, there was a spring heat wave in 2010 that coincided with leaf expansion of sugar maple trees (*Acer saccharum* Marsh.). This heat wave was associated with an earlier cessation of diameter growth, lower annual growth, and later onset of diameter growth the next year (Stangler et al. 2016). In contrast, dendrometer observations of 21 tree species across Europe showed that a late-season heat wave caused stem dehydration and temporary bole shrinkage, but no clear reduction in annual growth given that most of the seasonal growth was already completed by that time (Salomón et al. 2022). Thus, extreme heat seems to have a larger impact on tree growth when it occurs early in the growing season. In addition to reducing growth, extreme heat

13652486, 2025, 11, Downloaded from https://onlinelibrary.wiley.com/doi/10.1111/gcb.70571 by National Forest Service Library, Wiley Online Library on [20/11/2025]. See the Terms and Conditions (https://onlinelibrary.wiley.com/terms-and-conditions) on Wiley Online Library for rules of use; OA articles are governed by the applicable Creative Commons License

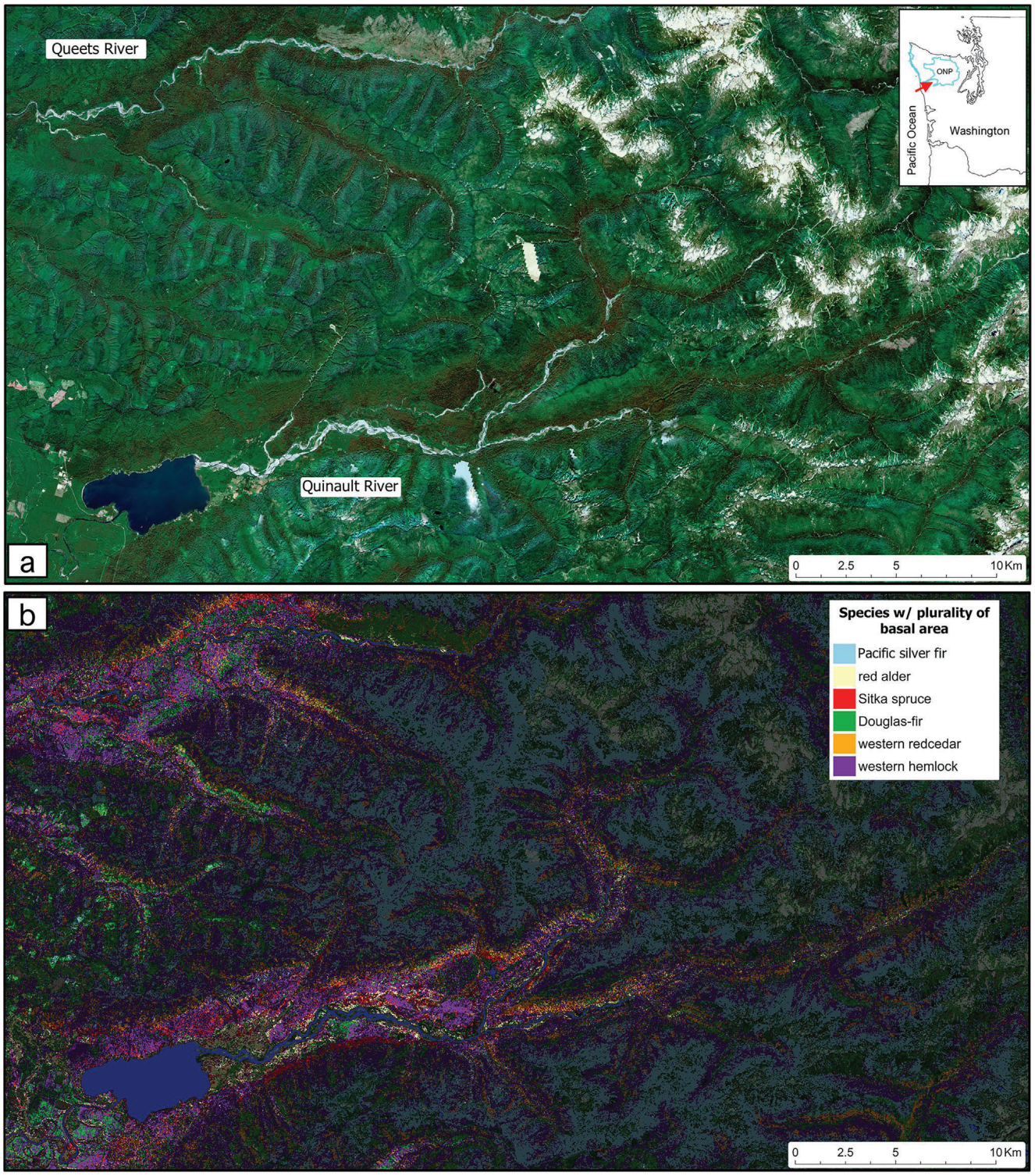

FIGURE 8 | (a) True-color median composite of the Queets and Quinault River valleys (composite period July 4–July 30), showing red/brown foliage. Inset shows Olympic National Park boundaries in blue and approximate location of image with red arrow. (b) Species map with unscorched areas partially masked with a black transparency to show contrasting species composition in scorched vs. unscorched areas.

may pre-dispose trees to damage from other biotic and abiotic stressors, ultimately leading to tree mortality after several growing seasons (Andrus et al. 2024; Franklin et al. 1987). It is still unclear whether tree mortality will increase as a result of the 2021 heat wave, or how tree growth has been impacted across the region. Future research which focuses on quantifying lasting physiological impairment or enhanced mortality rates among scorched populations of trees would lend important insight into the long-term consequences of this event.

At the local scale, species interact with unique combinations of biotic and abiotic factors that are not fully captured in regional scale analysis. In particular, tree species dominance appeared to not only play a major role in determining forest canopy scorch,

13652486, 2025, 11, Downloaded from https://onlinelibrary.wiley.com/doi/10.1111/gcb.70571 by National Forest Service Library, Wiley Online Library on [20/11/2025]. See the Terms and Conditions (https://onlinelibrary.wiley.com/terms-and-conditions) on Wiley Online Library for rules of use; OA articles are governed by the applicable Creative Commons License

but also constrained the effects of other variables, such as canopy height (Figure 3) and temperature (Figure 6). In order to better understand more localized interactions we identified two regional scorch hotspots to describe in greater detail: Olympic National Park, where old-growth trees had extensive foliage damage, and the Oregon Coast Range, where foliage damage was mostly observed in young Douglas-fir plantations and where a foliar pathogen affecting Douglas-fir is widespread.

4.1 | Canopy Scorch in Old-Growth Forests of the Olympic National Park

We found extensive areas of foliage scorch in portions of the Olympic Peninsula, WA, including portions of the Olympic National Park (ONP), a 373,000 ha World Heritage Site and International Biosphere Reserve. The ONP contains ~150,000 ha of forest, 69% of which has been classified as old growth (Bell et al. 2023; Davis et al. 2022). Forest dominated by western hemlock (53.3%), western redcedar (10.7%), and Sitka spruce (1%) accounted for 84% of the canopy heat damage within the park. These forests were concentrated in the Humptulips, Quinault, Queets, Hoh, and Bogachiel river valleys (Figures S6 and 8). Ninety-five percent of the damage to these three species happened at elevations between 33 and 655 m, where $T_{air\text{-}max}$ was 4–5 standard deviations above average. Absolute $T_{surface\text{-}max}$ was 40°C–42°C and CHILI values tended to be high, indicating high sun exposure (Figure S6). From June to July, there may be cloud cover for 40%–50% of daylight hours in this region (Dye et al. 2020). Cloud cover provides critical shielding from direct sun and mitigates the negative effects of heat waves in other summer-dry West Coast climates (Clemesha et al. 2018). In contrast to the cooler, wetter conditions of the Olympic Peninsula, the heat wave of 2021 was associated with clear skies, high temperatures, and adiabatic heating at low elevations—conditions to which western hemlock, western redcedar, and Sitka spruce may not have been acclimated or genetically adapted. The apparent sensitivity of some old-growth forests of the ONP is concerning because of their great ecological and societal importance. The ecological and societal values of these old forests include storage of large quantities of carbon (Gray and Whittier 2014), supporting biodiversity (Spies et al. 2018), providing cooler microclimates (Wolf et al. 2021; De Frenne et al. 2019; Frey et al. 2016; Kim et al. 2022; Schowalter 2017), and acting as refugia from some high-severity fires (Gavin et al. 2003; Huff 1995). If these ancient forests experience repeated events of widespread foliage death, or if scorch impacts are exacerbated by other stressors, we may lose many of the ecological and economic benefits these forests provide.

4.2 | Canopy Scorch in Plantation Forests of the Oregon Coast Range

The mountains of the Oregon Coast Range span from southern Oregon to southwest Washington, rising to a maximum elevation of 1250 m. These mountains, known for having some of the most productive forests in the world (Diaz et al. 2018), have a large component of fast-growing, even-aged stands of Douglas-fir and western hemlock, managed on short harvest rotations (35–55 years) (Table 3). Douglas-fir, which is among the most valuable timber species worldwide, is used for plantation forestry on every forested continent (Gilson and Maguire 2021; Lavender and Hermann 2014). After the 2021 heat wave, these Douglas-fir and hemlock forests had widespread foliage scorch with notable hot spots north of Florence, OR (latitude: 43.972° N), including near-coast stretches of the Necanicum, Nehalem, Nestucca, Siletz, and Yaquina Rivers, the watersheds of several rivers that drain into Tillamook Bay, and the headlands to the north and south of the mouth of the Columbia River (Figure 9a).

The OR Coast Range has a Mediterranean climate (~8-month wet season, ~4-month dry season) but also has a pronounced rain shadow that makes areas west of the Coast Range crest wetter, cloudier, and milder than the inland Willamette Valley. Therefore, it is plausible that the lack of acclimation to high temperatures and adiabatic heating at low elevations explain why damage hotspots occurred primarily west of the Coast Range crest (Figure 9a) and near the coast (Figure 9b). In addition, leaf death was associated with the timing of budburst. Using a model to predict the timing of vegetative budburst in Douglas-fir (Ford et al. 2016), we found that foliar death was more common on trees that burst bud ~6–9 weeks before the heat wave, compared to trees that burst bud earlier or later (Figure 5). This effect was corroborated by field observations in the northern half of the Coast Range. At low-elevation sites, Still et al. (2023) noted particularly strong patterns of dead first-year foliage and tissue necrosis in expanding shoots. In contrast, Douglas-fir in the southern part of the Coast Range experienced equally high temperatures, had an earlier date of bud burst (predicted), and

TABLE 3 | Landscape representation of the six most common species in the Coast Range region, as described for Table 2.

Species	Presence in forest		Presence in scorched forest		Scorch proportionality index
Common name	Area (Ha)	Percent	Area (Ha)	Percent	% of scorch: % of forest
Douglas-fir	422,100	61.0	25,758	57.3	0.94
Western hemlock	103,583	15.0	10,802	24.0	1.61
Red alder	116,962	16.9	4,686	10.4	0.62
Western redcedar	8,050	1.2	765	1.5	1.46
Bigleaf maple	9,166	1.3	392	0.9	0.66
Sitka spruce	28,144	4.1	2,219	4.9	1.20

Note: Color coding shows which species had a scorch proportionality index below 1 (blue) or above 1 (red).

13652486, 2025, 11, Downloaded from https://onlinelibrary.wiley.com/doi/10.1111/gcb.70571 by National Forest Service Library, Wiley Online Library on [20/11/2025]. See the Terms and Conditions (https://onlinelibrary.wiley.com/terms-and-conditions) on Wiley Online Library for rules of use; OA articles are governed by the applicable Creative Commons License

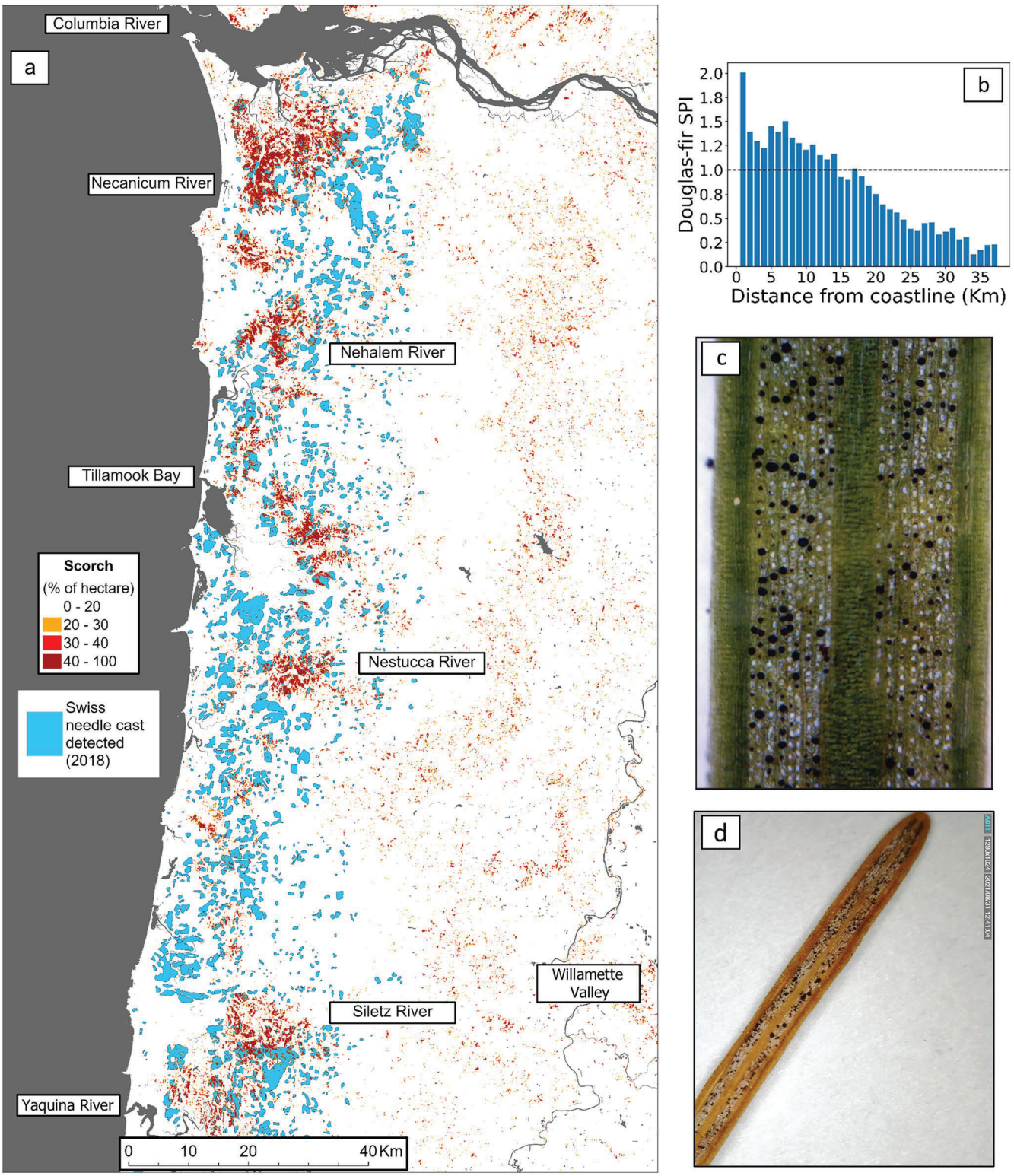

FIGURE 9 | (a) Map showing patterns of scorch in 2021 and polygons indicating where Swiss needle cast infection symptoms were observed in 2018, the time of the last Aerial Detection Survey campaign preheat wave. Visible symptoms of infection can vary in location from year to year and are displayed to illustrate the range of SNC as a function of distance from the coastline. (b) SPI of Douglas-fir as a function of distance from coastline. (c) Image of Douglas-fir needle with stoma plugged by SNC pseudothecia (photo credit: J. Schwandt). (d) Image of dead 1-year-old needle with SNC plugged stoma harvested shortly after the heat wave (credit: Gabriela Ritóková). Map lines delineate study areas and do not necessarily depict accepted national boundaries.

13652486, 2025, 11, Downloaded from https://onlinelibrary.wiley.com/doi/10.1111/gcb.70571 by National Forest Service Library, Wiley Online Library on [20/11/2025]. See the Terms and Conditions (https://onlinelibrary.wiley.com/terms-and-conditions) on Wiley Online Library for rules of use; OA articles are governed by the applicable Creative Commons License

had less leaf damage (Figure 3). Early flushing individuals may have had an enhanced ability to resist wilting and tissue damage during the heat wave, perhaps because they were able to transport water more effectively to the new shoots, regulate leaf osmotic potential, and dissipate excess solar energy. In contrast, late budburst dates tended to occur at high elevations, where maximum heatwave T_{air} and $T_{surface}$ were lower than at low elevations, likely leading to lower SPI in these trees.

In addition to the interaction of foliar phenology and heat wave temperatures, patterns of Swiss needle cast (SNC) infection corresponded closely with scorch hotspots. SNC is a common foliage disease of Douglas-fir near the coast in Oregon and Washington (Shaw et al. 2021). The fruiting bodies of the ascomycete microfungus, *Nothophaeocryptopus gaeumannii* block needle stomata (Figure 9c), causing chronic limitation of transpiration and carbon assimilation, which leads to poor foliage retention and reduced tree growth (Manter 2002). The near-coast zone, where SNC is most prevalent (Shaw et al. 2021), had the most foliage scorch, and scorch decreased with increasing distance from the coast (Figure 9b). Trees with a history of SNC infection may have been more susceptible to foliage death in the 2021 heat wave because of generally poor health compared to more inland trees (Saffell, Meinzer, Voelker, et al. 2014; Saffell, Meinzer, Woodruff, et al. 2014). SNC may have also reduced transpirational cooling (Manter 2002), driving foliage temperatures higher than in healthy needles, increasing the probability of foliar death. This is supported by observations in the Coast Range where scorch mostly occurred on the new foliage, but in the SNC areas, scorch was also pronounced on second-year needles (fig 9d, Still et al. 2023). It remains to be seen whether the 2021 heat wave will have measurable effects on long-term productivity or mortality of Coast Range Douglas-fir.

4.3 | Extreme Heat Poses a Multifaceted Challenge to Forests

Heat and drought events have been associated with increases in tree mortality in all of Earth's major forest ecosystems (Allen et al. 2015; Hammond et al. 2022). Our work highlights the complex interactions among biotic and abiotic factors that influence forest responses to extreme heat. These interactions resulted in the complex patterns of forest canopy scorch we observed after the 2021 heat wave in the PNW. Although this heat wave was remarkably unusual, similar heat waves were responsible for record-breaking temperatures across South America in the summer of 2022 (Rivera et al. 2023). In the winter of the following year (i.e., August and September 2023), the same region experienced another heat wave. Early reporting (Kew et al. 2023) indicated that this heat wave was also characterized by record-setting, out-of-season temperatures that caused substantial damage to vegetation.

The factors that affected leaf scorch from the 2021 heat wave included maximum temperatures, temperature anomalies, degree of sun exposure, species distributions, species-specific thermal tolerances, topographic position, timing of budburst, and perhaps the presence of foliar pathogens. Our findings revealed disproportionately greater damage to some late-successional, shade-tolerant tree species, such as western hemlock and western redcedar. If heat waves increase in frequency and severity, we may see major changes in the composition of old-growth forests and reduced productivity of Coast Range plantation forests.

The effects of rare extreme events are represented poorly in the models used to project forest change, resulting in overly optimistic projections of ecosystem resistance and resilience to climate change (Allen et al. 2015; Harmon and Bell 2020). Our remote sensing approach provides a valuable starting point for quantifying the effects of heat waves and other emerging forest disturbances (Kennedy et al. 2014; McDowell et al. 2015) and could be used to understand the effects of other heat waves on forest canopies in other regions. Our results also point to new laboratory, greenhouse, and field studies that would be valuable for increasing our understanding of how extreme heat leads to ecological consequences.

Author Contributions

Adam Sibley: conceptualization, data curation, formal analysis, funding acquisition, investigation, methodology, software, supervision, validation, visualization, writing – original draft, writing – review and editing. **Christopher Still:** conceptualization, formal analysis, funding acquisition, investigation, methodology, resources, writing – original draft, writing – review and editing. **Matthew Gregory:** conceptualization, data curation, formal analysis, investigation, methodology, resources, software, validation, visualization, writing – original draft. **Constance Harrington:** conceptualization, investigation, resources, validation, writing – original draft, writing – review and editing. **David Shaw:** conceptualization, investigation, resources, writing – original draft. **Nina Ferrari:** writing – original draft. **Alex Dye:** writing – original draft. **Mark Schulze:** conceptualization, formal analysis, investigation, methodology, resources, writing – review and editing. **Glenn Howe:** funding acquisition, resources, supervision, writing – review and editing. **David E. Rupp:** data curation, investigation, investigation, resources, resources, visualization, visualization, writing – review and editing, writing – review and editing. **Christopher Daly:** conceptualization, investigation, resources. **Daniel DePinte:** data curation, investigation, resources, validation, writing – review and editing. **Cameron E. Naficy:** investigation, methodology, writing – review and editing. **Chaney Hart:** conceptualization, writing – original draft, writing – review and editing. **David M. Bell:** conceptualization, formal analysis, funding acquisition, investigation, methodology, resources, supervision, validation, visualization, writing – original draft, writing – review and editing.

Acknowledgments

We thank Dr. Kevin Ford, USDA Forest Service, for sharing R code used to predict the date of spring budburst in 2021 for Douglas-fir; Caroline Walls for her field reports of foliar heat damage on the Olympic Peninsula; and Dr. Karla M. Jarecke for her helpful editorial reviews.

Conflicts of Interest

The authors declare no conflicts of interest.

Data Availability Statement

Data produced in this study is hosted on zenodo at https://doi.org/10.5281/zenodo.17268190, along with all figures at native resolution. Code can be accessed at https://doi.org/10.5281/zenodo.17329644. The Sentinel-2 MSI L2A SR data layers used in this study can be accessed at https://doi.org/10.5270/S2_-znk9xsj. Ecologically Relevant Geomorphology (ERGo) data can be accessed at https://www.sciencebase.gov/catalog/item/561819a8e4b0cdb063e3fd96. Forest attribute maps used in this study are permanently hosted at https://lemmadownload.forestry.oregonstate.edu/ and are freely

13652486, 2025, 11, Downloaded from https://onlinelibrary.wiley.com/doi/10.1111/gcb.70571 by National Forest Service Library, Wiley Online Library on [20/11/2025]. See the Terms and Conditions (https://onlinelibrary.wiley.com/terms-and-conditions) on Wiley Online Library for rules of use; OA articles are governed by the applicable Creative Commons License

available after filling out a data request form. PRISM climate data are available at https://doi.org/10.17616/R3S62R. MODIS Land surface temperature data can be accessed at http://doi.org/10.5067/MODIS/MOD11A1.061 and http://doi.org/10.5067/MODIS/MYD11A1.061. The 10-m resolution digital elevation model from USGS 3D elevation program can be accessed at https://doi.org/10.5069/G98K778D. Dynamic World landcover maps can be accessed at https://doi.org/10.1038/s41597-022-01307-4. Monitoring Trends in Burn Severity maps can be accessed at https://doi.org/10.5066/P9NETC0T. Swiss needle cast location data can be accessed at https://www.oregon.gov/ODF/ForestBenefits/Pages/ForestHealth.aspx.

References

Allen, C. D., D. D. Breshears, and N. G. McDowell. 2015. "On Underestimation of Global Vulnerability to Tree Mortality and Forest Die-Off From Hotter Drought in the Anthropocene." *Ecosphere* 6, no. 8: 1–55. https://doi.org/10.1890/ES15-00203.1.

Allen, C. D., A. K. Macalady, H. Chenchouni, et al. 2010. "A Global Overview of Drought and Heat-Induced Tree Mortality Reveals Emerging Climate Change Risks for Forests." *Forest Ecology and Management* 259, no. 4: 660–684. https://doi.org/10.1016/j.foreco.2009.09.001.

Anderegg, L. D. L., W. R. L. Anderegg, and J. A. Berry. 2013. "Not all Droughts Are Created Equal: Translating Meteorological Drought Into Woody Plant Mortality." *Tree Physiology* 33, no. 7: 672–683. https://doi.org/10.1093/treephys/tpt044.

Andrus, R. A., L. R. Peach, A. R. Cinquini, et al. 2024. "Canary in the Forest?—Tree Mortality and Canopy Dieback of Western Redcedar Linked to Drier and Warmer Summers." *Journal of Biogeography* 51, no. 1: 103–119. https://doi.org/10.1111/jbi.14732.

Bell, D. M., S. A. Acker, M. J. Gregory, R. J. Davis, and B. A. Garcia. 2021. "Quantifying Regional Trends in Large Live Tree and Snag Availability in Support of Forest Management." *Forest Ecology and Management* 479: 10. https://doi.org/10.1016/j.foreco.2020.118554.

Bell, D. M., M. J. Gregory, M. Palmer, and R. Davis. 2023. *Guidance for Forest Management and Landscape Ecology Applications of Recent Gradient Nearest Neighbor Imputation Maps in California, Oregon, and Washington* (No. PNW-GTR-1018; p. PNW-GTR-1018). U.S. Department of Agriculture, Forest Service, Pacific Northwest Research Station. https://doi.org/10.2737/PNW-GTR-1018.

Ben-Shachar, M., D. Lüdecke, and D. Makowski. 2020. "Effectsize: Estimation of Effect Size Indices and Standardized Parameters." *Journal of Open Source Software* 5, no. 56: 2815. https://doi.org/10.21105/joss.02815.

Berry, J., and O. Bjorkman. 1980. "Photosynthetic Response and Adaptation to Temperature in Higher Plants." *Annual Review of Plant Physiology* 31, no. 1: 491–543. https://doi.org/10.1146/annurev.pp.31.060180.002423.

Bongi, G., and S. P. Long. 1987. "Light-Dependent Damage to Photosynthesis in Olive Leaves During Chilling and High Temperature Stress." *Plant, Cell & Environment* 10, no. 3: 241–249. https://doi.org/10.1111/1365-3040.ep11602267.

Bose, A. K., J. Doležal, D. Scherrer, et al. 2024. "Revealing Legacy Effects of Extreme Droughts on Tree Growth of Oaks Across the Northern Hemisphere." *Science of the Total Environment* 926, no. 172: 49. https://doi.org/10.1016/j.scitotenv.2024.172049.

Brown, C. F., S. P. Brumby, B. Guzder-Williams, et al. 2022. "Dynamic World, Near Real-Time Global 10 m Land Use Land Cover Mapping." *Scientific Data* 9, no. 1: 251. https://doi.org/10.1038/s41597-022-01307-4.

Burrill, E., A. DiTommaso, J. Turner, et al. 2024. *The Forest Inventory and Analysis Database: FIADB User Guides Volume Database Description (VERSION 9.2), Nationwide Forest Inventory (NFI)*. U.S. Department of Agriculture, Forest Service. https://www.fs.usda.gov/research/products/dataandtools/datasets/fia-datamart.

Clemesha, R. E. S., K. Guirguis, A. Gershunov, I. J. Small, and A. Tardy. 2018. "California Heat Waves: Their Spatial Evolution, Variation, and Coastal Modulation by Low Clouds." *Climate Dynamics* 50, no. 11–12: 4285–4301. https://doi.org/10.1007/s00382-017-3875-7.

Colombo, S. J., and V. R. Timmer. 1992. "Limits of Tolerance to High Temperatures Causing Direct and Indirect Damage to Black Spruce." *Tree Physiology* 11, no. 1: 95–104. https://doi.org/10.1093/treephys/11.1.95.

Copernicus Sentinel-2 (processed by ESA). 2022. *MSI Level-2A BOA Reflectance Product. Collection 1. European Space Agency*. https://doi.org/10.5270/S2_-znk9xsj.

Davis, K. T., S. Z. Dobrowski, Z. A. Holden, P. E. Higuera, and J. T. Abatzoglou. 2019. "Microclimatic Buffering in Forests of the Future: The Role of Local Water Balance." *Ecography* 42, no. 1: 1–11. https://doi.org/10.1111/ecog.03836.

Davis, R. J., D. M. Bell, M. J. Gregory, et al. 2022. *Northwest Forest Plan—The First 25 Years (1994–2018): Status and Trends of Late-Successional and Old-Growth Forests*. Pacific Northwest Research Station, USDA Forest Service, PNW-GTR-1004.

De Frenne, P., J. Lenoir, M. Luoto, et al. 2021. "Forest Microclimates and Climate Change: Importance, Drivers and Future Research Agenda." *Global Change Biology* 27, no. 11: 2279–2297. https://doi.org/10.1111/gcb.15569.

De Frenne, P., F. Zellweger, F. Rodríguez-Sánchez, et al. 2019. "Global Buffering of Temperatures Under Forest Canopies." *Nature Ecology & Evolution* 3, no. 5: 744–749. https://doi.org/10.1038/s41559-019-0842-1.

Diaz, D., S. Loreno, G. Ettl, and B. Davies. 2018. "Tradeoffs in Timber, Carbon, and Cash Flow Under Alternative Management Systems for Douglas-Fir in the Pacific Northwest." *Forests* 9, no. 8: 447. https://doi.org/10.3390/f9080447.

Dobrowski, S. Z. 2011. "A Climatic Basis for Microrefugia: The Influence of Terrain on Climate." *Global Change Biology* 17, no. 2: 1022–1035. https://doi.org/10.1111/j.1365-2486.2010.02263.x.

Dye, A. W., B. Rastogi, R. E. S. Clemesha, et al. 2020. "Spatial Patterns and Trends of Summertime Low Cloudiness for the Pacific Northwest, 1996–2017." *Geophysical Research Letters* 47, no. 16: e2020GL088121. https://doi.org/10.1029/2020GL088121.

Eidenshink, J., B. Schwind, K. Brewer, Z.-L. Zhu, B. Quayle, and S. Howard. 2007. "A Project for Monitoring Trends in Burn Severity." *Fire Ecology* 3, no. 1: 3–21. https://doi.org/10.4996/fireecology.0301003.

Fauset, S., L. Oliveira, M. S. Buckeridge, et al. 2019. "Contrasting Responses of Stomatal Conductance and Photosynthetic Capacity to Warming and Elevated CO2 in the Tropical Tree Species Alchornea Glandulosa Under Heatwave Conditions." *Environmental and Experimental Botany* 158: 28–39. https://doi.org/10.1016/j.envexpbot.2018.10.030.

Fleishman, E., D. E. Rupp, P. C. Loikith, K. A. Bumbaco, and L. W. O'Neill. 2025. "Synthesis of Publications on the Anomalous June 2021 Heat Wave in the Pacific Northwest of the United States and Canada." *Bulletin of the American Meteorological Society* 106, no. 6: E1155–E1174. https://doi.org/10.1175/BAMS-D-24-0188.1.

Ford, K. R., C. A. Harrington, S. Bansal, P. J. Gould, and J. B. St. Clair. 2016. "Will Changes in Phenology Track Climate Change? A Study of Growth Initiation Timing in Coast Douglas-Fir." *Global Change Biology* 22, no. 11: 3712–3723. https://doi.org/10.1111/gcb.13328.

Förster, K., F. Hanzer, B. Winter, T. Marke, and U. Strasser. 2016. "An Open-Source MEteoroLOgical Observation Time Series DISaggregation Tool (MELODIST v0.1.1)." *Geoscientific Model Development* 9, no. 7: 2315–2333. https://doi.org/10.5194/gmd-9-2315-2016.

Franklin, J., and C. T. Dyrness. 1973. *Natural Vegetation of Oregon and Washington*. Gen. Tech. Rep. PNW-GTR-008. Department of Agriculture, Forest Service, Pacific Northwest Research Station.

13652486, 2025, 11, Downloaded from https://onlinelibrary.wiley.com/doi/10.1111/gcb.70571 by National Forest Service Library, Wiley Online Library on [20/11/2025]. See the Terms and Conditions (https://onlinelibrary.wiley.com/terms-and-conditions) on Wiley Online Library for rules of use; OA articles are governed by the applicable Creative Commons License

Franklin, J. F., H. H. Shugart, and M. E. Harmon. 1987. "Tree Death as an Ecological Process." *Bioscience* 37, no. 8: 550–556. https://doi.org/10.2307/1310665.

Frey, S. J. K., A. S. Hadley, S. L. Johnson, M. Schulze, J. A. Jones, and M. G. Betts. 2016. "Spatial Models Reveal the Microclimatic Buffering Capacity of Old-Growth Forests." *Science Advances* 2, no. 4: e1501392. https://doi.org/10.1126/sciadv.1501392.

Gavin, D. G., L. B. Brubaker, and K. P. Lertzman. 2003. "Holocene Fire History of a Coastal Temperate Rain Forest Based on Soil Charcoal Radiocarbon Dates." *Ecology* 84, no. 1: 186–201. https://doi.org/10.1890/0012-9658(2003)084%255B0186:HFHOAC%255D2.0.CO;2.

Gilson, L. W., and D. A. Maguire. 2021. "Drivers of Productivity Differences Between Douglas-Fir Planted Within Its Native Range in Oregon and on Exotic Sites in New Zealand." *Forest Ecology and Management* 498, no. 119: 525. https://doi.org/10.1016/j.foreco.2021.119525.

Gorelick, N., M. Hancher, M. Dixon, S. Ilyushchenko, D. Thau, and R. Moore. 2017. "Google Earth Engine: Planetary-Scale Geospatial Analysis for Everyone." *Remote Sensing of Environment* 202: 18–27. https://doi.org/10.1016/j.rse.2017.06.031.

Gray, A. N., and T. R. Whittier. 2014. "Carbon Stocks and Changes on Pacific Northwest National Forests and the Role of Disturbance, Management, and Growth." *Forest Ecology and Management* 328: 167–178. https://doi.org/10.1016/j.foreco.2014.05.015.

Grossiord, C., T. N. Buckley, L. A. Cernusak, et al. 2020. "Plant responses to rising vapor pressure deficit." *New Phytologist* 226, no. 6: 1550–1566. https://doi.org/10.1111/nph.16485.

Hammond, W. M., A. P. Williams, J. T. Abatzoglou, et al. 2022. "Global Field Observations of Tree Die-Off Reveal Hotter-Drought Fingerprint for Earth's Forests." *Nature Communications* 13, no. 1: 1761. https://doi.org/10.1038/s41467-022-29289-2.

Harmon, M. E., and D. M. Bell. 2020. "Mortality in Forested Ecosystems: Suggested Conceptual Advances." *Forests* 11, no. 5: 572. https://doi.org/10.3390/f11050572.

Harrington, C. A., P. J. Gould, and R. Cronn. 2023. "Site and Provenance Interact to Influence Seasonal Diameter Growth of *Pseudotsuga menziesii*." *Frontiers in Forests and Global Change* 6, no. 1: 173707. https://doi.org/10.3389/ffgc.2023.1173707.

Huete, A., K. Didan, T. Miura, E. P. Rodriguez, X. Gao, and L. G. Ferreira. 2002. "Overview of the Radiometric and Biophysical Performance of the MODIS Vegetation Indices." *Remote Sensing of Environment* 83, no. 1–2: 195–213. https://doi.org/10.1016/S0034-4257(02)00096-2.

Huff, M. H. 1995. "Forest Age Structure and Development Following Wildfires in the Western Olympic Mountains, Washington." *Ecological Applications* 5, no. 2: 471–483. https://doi.org/10.2307/1942037.

Hulley, G., and S. Hook. 2021. *MODIS/Terra Land Surface Temperature/3-Band Emissivity Daily L3 Global 1km SIN Grid Day V061*. NASA EOSDIS Land Processes DAAC. https://doi.org/10.5067/MODIS/MOD21A1D.061.

Hüve, K., I. Bichele, B. Rasulov, and Ü. Niinemets. 2011. "When It Is Too Hot for Photosynthesis: Heat-Induced Instability of Photosynthesis in Relation to Respiratory Burst, Cell Permeability Changes and H_2O_2 Formation." *Plant, Cell & Environment* 34, no. 1: 113–126. https://doi.org/10.1111/j.1365-3040.2010.02229.x.

Javad, A., V. Premugh, R. Tiwari, et al. 2025. "Leaf Temperatures in an Indian Tropical Forest Exceed Physiological Limits but Durations of Exposures Are Currently Not Sufficient to Cause Lasting Damage." *Global Change Biology* 31, no. 2: e70069. https://doi.org/10.1111/gcb.70069.

Jiang, Y., J. B. Kim, A. T. Trugman, Y. Kim, and C. J. Still. 2019. "Linking Tree Physiological Constraints With Predictions of Carbon and Water Fluxes at an Old-Growth Coniferous Forest." *Ecosphere* 10, no. 4: e02692. https://doi.org/10.1002/ecs2.2692.

Kala, J., M. G. De Kauwe, A. J. Pitman, et al. 2016. "Impact of the Representation of Stomatal Conductance on Model Projections of Heatwave Intensity." *Scientific Reports* 6, no. 1: 23,418. https://doi.org/10.1038/srep23418.

Kennedy, R. E., S. Andréfouët, W. B. Cohen, et al. 2014. "Bringing an Ecological View of Change to Landsat-Based Remote Sensing." *Frontiers in Ecology and the Environment* 12, no. 6: 339–346. https://doi.org/10.1890/130066.

Kew, S., I. Pinto, L. Alves, et al. 2023. *Strong Influence of Climate Change in Uncharacteristic Early Spring Heat in South America*. Grantham Research Institute, Imperial College. https://doi.org/10.25561/106753.

Kim, H., B. C. McComb, S. J. K. Frey, D. M. Bell, and M. G. Betts. 2022. "Forest Microclimate and Composition Mediate Long-Term Trends of Breeding Bird Populations." *Global Change Biology* 28, no. 21: 6180–6193. https://doi.org/10.1111/gcb.16353.

Krause, G. H., K. Winter, B. Krause, et al. 2010. "High-Temperature Tolerance of a Tropical Tree, Ficus Insipida: Methodological Reassessment and Climate Change Considerations." *Functional Plant Biology* 37, no. 9: 890. https://doi.org/10.1071/FP10034.

Lancaster, L. T., and A. M. Humphreys. 2020. "Global Variation in the Thermal Tolerances of Plants." *Proceedings of the National Academy of Sciences* 117, no. 24: 13,580–13,587. https://doi.org/10.1073/pnas.1918162117.

Lavender, D. P., and R. K. Hermann. 2014. *Douglas-fir: The genus Pseudotsuga*. Oregon Forest Research Laboratory, Oregon State University. hdl.handle.net/1957/47168.

Loikith, P. C., and D. A. Kalashnikov. 2023. "Meteorological Analysis of the Pacific Northwest June 2021 Heatwave." *Monthly Weather Review* 151, no. 5: 1303–1319. https://doi.org/10.1175/MWR-D-22-0284.1.

Ma, H., Q. Qin, and X. Shen. 2008. "Shadow Segmentation and Compensation in High Resolution Satellite Images." *IGARSS 2008–2008 IEEE International Geoscience and Remote Sensing Symposium*, II-1036-II-1039. https://doi.org/10.1109/IGARSS.2008.4779175.

Manter, D. K. 2002. "Energy Dissipation and Photoinhibition in Douglas-Fir Needles With a Fungal-Mediated Reduction in Photosynthetic Rates." *Journal of Phytopathology* 150, no. 11–12: 674–679. https://doi.org/10.1046/j.1439-0434.2002.00801.x.

Marchin, R. M., M. Esperon-Rodriguez, M. G. Tjoelker, and D. S. Ellsworth. 2022. "Crown Dieback and Mortality of Urban Trees Linked to Heatwaves During Extreme Drought." *Science of the Total Environment* 850, no. 157: 915. https://doi.org/10.1016/j.scitotenv.2022.157915.

Marias, D. E., F. C. Meinzer, D. R. Woodruff, and K. A. McCulloh. 2016. "Thermotolerance and Heat Stress Responses of Douglas-Fir and Ponderosa Pine Seedling Populations From Contrasting Climates." *Tree Physiology, Treephys* 37: tpw117v1. https://doi.org/10.1093/treephys/tpw117.

Mass, C., D. Ovens, J. Christy, and R. Conrick. 2024. "The Pacific Northwest Heat Wave of 25–30 June 2021: Synoptic/Mesoscale Conditions and Climate Perspective." *Weather and Forecasting* 39, no. 2: 275–291. https://doi.org/10.1175/WAF-D-23-0154.1.

McCune, B., and D. Keon. 2002. "Equations for Potential Annual Direct Incident Radiation and Heat Load." *Journal of Vegetation Science* 13, no. 4: 603–606. https://doi.org/10.1111/j.1654-1103.2002.tb02087.x.

McDowell, N. G., N. C. Coops, P. S. A. Beck, et al. 2015. "Global Satellite Monitoring of Climate-Induced Vegetation Disturbances." *Trends in Plant Science* 20, no. 2: 114–123. https://doi.org/10.1016/j.tplants.2014.10.008.

Münchinger, I. K., P. Hajek, B. Akdogan, A. T. Caicoya, and N. Kunert. 2023. "Leaf Thermal Tolerance and Sensitivity of Temperate Tree Species Are Correlated With Leaf Physiological and Functional Drought Resistance Traits." *Journal of Forestry Research* 34, no. 1: 63–76. https://doi.org/10.1007/s11676-022-01594-y.

13652486, 2025, 11, Downloaded from https://onlinelibrary.wiley.com/doi/10.1111/gcb.70571 by National Forest Service Library, Wiley Online Library on [20/11/2025]. See the Terms and Conditions (https://onlinelibrary.wiley.com/terms-and-conditions) on Wiley Online Library for rules of use; OA articles are governed by the applicable Creative Commons License

Neuner, G., and O. Buchner. 2023. "The Dose Makes the Poison: The Longer the Heat Lasts, the Lower the Temperature for Functional Impairment and Damage." *Environmental and Experimental Botany* 212: 105,395. https://doi.org/10.1016/j.envexpbot.2023.105395.

Ohmann, J. L. 2012. "Mapping Change of Older Forest With Nearest-Neighbor Imputation and Landsat Time-Series." *Forest Ecology and Management* 272: 13–25.

Ohmann, J. L., and M. J. Gregory. 2002. "Predictive Mapping of Forest Composition and Structure With Direct Gradient Analysis and Nearest- Neighbor Imputation in Coastal Oregon, U.S.A." *Canadian Journal of Forest Research* 32, no. 4: 725–741. https://doi.org/10.1139/x02-011.

Olofsson, P., G. M. Foody, S. V. Stehman, and C. E. Woodcock. 2013. "Making Better Use of Accuracy Data in Land Change Studies: Estimating Accuracy and Area and Quantifying Uncertainty Using Stratified Estimation." *Remote Sensing of Environment* 129: 122–131. https://doi.org/10.1016/j.rse.2012.10.031.

O'Sullivan, O. S., M. A. Heskel, P. B. Reich, et al. 2016. "Thermal Limits of Leaf Metabolism Across Biomes." *Global Change Biology* 23, no. 1: 209–223. https://doi.org/10.1111/gcb.13477.

Picotte, J. J., K. Bhattarai, D. Howard, et al. 2020. "Changes to the Monitoring Trends in Burn Severity Program Mapping Production Procedures and Data Products." *Fire Ecology* 16, no. 1: 16. https://doi.org/10.1186/s42408-020-00076-y.

Potapov, P., X. Li, A. Hernandez-Serna, et al. 2021. "Mapping Global Forest Canopy Height Through Integration of GEDI and Landsat Data." *Remote Sensing of Environment* 253: 112,165. https://doi.org/10.1016/j.rse.2020.112165.

PRISM Climate Group. 2023. *PRISM Weather Data*. Oregon State University. https://prism.oregonstate.edu.

R Core Team. 2024. "_R: A Language and Environment for Statistical Computing_." R Foundation for Statistical Computing, Vienna, Austria. https://www.R-project.org/.

Rivera, J. A., P. A. Arias, A. A. Sörensson, et al. 2023. "2022 Early-Summer Heatwave in Southern South America: 60 Times More Likely due to Climate Change." *Climatic Change* 176, no. 8: 102. https://doi.org/10.1007/s10584-023-03576-3.

Saffell, B. J., F. C. Meinzer, S. L. Voelker, et al. 2014. "Tree-Ring Stable Isotopes Record the Impact of a Foliar Fungal Pathogen on CO_2 Assimilation and Growth in Douglas-Fir." *Plant, Cell & Environment* 37, no. 7: 1536–1547. https://doi.org/10.1111/pce.12256.

Saffell, B. J., F. C. Meinzer, D. R. Woodruff, et al. 2014. "Seasonal Carbohydrate Dynamics and Growth in Douglas-Fir Trees Experiencing Chronic, Fungal-Mediated Reduction in Functional Leaf Area." *Tree Physiology* 34, no. 3: 218–228. https://doi.org/10.1093/treephys/tpu002.

Salomón, R. L., R. L. Peters, R. Zweifel, et al. 2022. "The 2018 European Heatwave Led to Stem Dehydration but Not to Consistent Growth Reductions in Forests." *Nature Communications* 13, no. 1: 28. https://doi.org/10.1038/s41467-021-27579-9.

Scafaro, A. P., B. C. Posch, J. R. Evans, G. D. Farquhar, and O. K. Atkin. 2023. "Rubisco Deactivation and Chloroplast Electron Transport Rates Co-Limit Photosynthesis Above Optimal Leaf Temperature in Terrestrial Plants." *Nature Communications* 14, no. 1: 2820. https://doi.org/10.1038/s41467-023-38496-4.

Schowalter, T. 2017. "Arthropod Diversity and Functional Importance in Old-Growth Forests of North America." *Forests* 8, no. 4: 97. https://doi.org/10.3390/f8040097.

Sharkey, T. D. 2005. "Effects of Moderate Heat Stress on Photosynthesis: Importance of Thylakoid Reactions, Rubisco Deactivation, Reactive Oxygen Species, and Thermotolerance Provided by Isoprene." *Plant, Cell & Environment* 28, no. 3: 269–277. https://doi.org/10.1111/j.1365-3040.2005.01324.x.

Shaw, D. C., G. Ritóková, Y.-H. Lan, et al. 2021. "Persistence of the Swiss Needle Cast Outbreak in Oregon Coastal Douglas-Fir and New Insights From Research and Monitoring." *Journal of Forestry* 119, no. 4: 407–421. https://doi.org/10.1093/jofore/fvab011.

Slot, M., and K. Winter. 2017. "Photosynthetic Acclimation to Warming in Tropical Forest Tree Seedlings." *Journal of Experimental Botany* 68, no. 9: 2275–2284. https://doi.org/10.1093/jxb/erx071.

Spies, T. A., P. A. Stine, R. A. Gravenmier, J. W. Long, and M. J. Reilly. 2018. *Synthesis of Science to Inform Land Management Within the Northwest Forest Plan area* (No. PNW-GTR-966; p. PNW-GTR-966). U.S. Department of Agriculture, Forest Service, Pacific Northwest Research Station. https://doi.org/10.2737/PNW-GTR-966.

Stangler, D. F., A. Hamann, H.-P. Kahle, and H. Spiecker. 2016. "A Heat Wave During Leaf Expansion Severely Reduces Productivity and Modifies Seasonal Growth Patterns in a Northern Hardwood Forest." *Tree Physiology, Treephys* 37, no. 1: tpw094v1. https://doi.org/10.1093/treephys/tpw094.

Still, C., A. Sibley, M. Schulze, et al. 2021. *Mini-Symposium on June 2021 Heat Dome Foliage Scorch*. Oregon State University.

Still, C. J., A. Sibley, D. DePinte, et al. 2023. "Causes of Widespread Foliar Damage From the June 2021 Pacific Northwest Heat Dome: More Heat Than Drought." *Tree Physiology* 43: 203–209. https://doi.org/10.1093/treephys/tpac143.

Teskey, R., T. Wertin, I. Bauweraerts, M. Ameye, M. A. Mcguire, and K. Steppe. 2015. "Responses of Tree Species to Heat Waves and Extreme Heat Events." *Plant, Cell & Environment* 38, no. 9: 1699–1712. https://doi.org/10.1111/pce.12417.

Theobald, D. M., D. Harrison-Atlas, W. B. Monahan, and C. M. Albano. 2015. "Ecologically-Relevant Maps of Landforms and Physiographic Diversity for Climate Adaptation Planning." *PLoS One* 10, no. 12: e0143619. https://doi.org/10.1371/journal.pone.0143619.

Thompson, V., A. Kennedy-Asser, E. Vosper, et al. 2022. "The 2021 Western North America Heat Wave Among the Most Extreme Events Ever Recorded Globally." *Science Advances* 8: eabm6860. https://doi.org/10.1126/sciadv.abm6860.

U.S. Forest Service-PNW Forest Health Protection. 2023. "Aerial Detection Surveys (ADS)." https://www.fs.usda.gov/detail/r6/forest-grasslandhealth/insects-diseases/?cid=stelprdb5286951.

White, R. H., S. Anderson, J. F. Booth, et al. 2023. "The Unprecedented Pacific Northwest Heatwave of June 2021." *Nature Communications* 14, no. 1: 727. https://doi.org/10.1038/s41467-023-36289-3.

Wolf, C., D. M. Bell, H. Kim, M. P. Nelson, M. Schulze, and M. G. Betts. 2021. "Temporal Consistency of Undercanopy Thermal Refugia in Old-Growth Forest." *Agricultural and Forest Meteorology* 307: 108520. https://doi.org/10.1016/j.agrformet.2021.108520.

Zhu, L., A. P. Scafaro, E. Vierling, et al. 2024. "Heat Tolerance of a Tropical–Subtropical Rainforest Tree Species *Polyscias Elegans*: Time-Dependent Dynamic Responses of Physiological Thermostability and Biochemistry." *New Phytologist* 241, no. 2: 715–731. https://doi.org/10.1111/nph.19356.

Supporting Information

Additional supporting information can be found online in the Supporting Information section. **Data S1:** gcb70571-sup-0001-Supinfo.pdf.

13652486, 2025, 11, Downloaded from https://onlinelibrary.wiley.com/doi/10.1111/gcb.70571 by National Forest Service Library, Wiley Online Library on [20/11/2025]. See the Terms and Conditions (https://onlinelibrary.wiley.com/terms-and-conditions) on Wiley Online Library for rules of use; OA articles are governed by the applicable Creative Commons License

List of Refereed Publications

Disease Distribution, Severity and Epidemiology

Agne, MC, Beedlow PA, Shaw DC, Woodruff DR, Lee EH, Cline S, Comeleo RL. 2018. Interactions of predominant insects and diseases with climate change in Douglas-fir forests of western Oregon and Washington, U.S.A.. Forest Ecology and Management. 409:317-332.

Hansen, E. M., Stone, J. K., Capitano, B. R., Rosso, P., Sutton, W., Winton, L., Kanaskie, A. and M. G. McWilliams. 2000. Incidence and impact of Swiss needle cast in forest plantations of Douglas-fir in coastal Oregon. Plant Disease. 84: 773-779.

Hennon, P.E., Frankel, S.J., Woods, A.J., Worrall, J.J., Ramsfield, T.D., Zambino, P.J., Shaw, D.C., Ritóková, G., Warwell, M.V., Norlander, D. and Mulvey, R.L., 2021. Applications of a conceptual framework to assess climate controls of forest tree diseases. Forest Pathology, 51(6), p.e12719.

Lan Y-H, Shaw D.C., Beedlow P.A., Lee E.H., Waschmann R.S.. 2019. Severity of Swiss needle cast in young and mature Douglas-fir forests in western Oregon, USA. Forest Ecology and Management. 442:79-95.

Manter, D. K., Reeser, P. W., and J. K. Stone. 2005. A climate-based model for predicting geographic variation in Swiss needle cast severity in the Oregon coast range. Phytopathology. 95: 1256-1265.

Ritóková, G, Shaw DC, Filip GM, Kanaskie A, Browning J, Norlander D. 2016. Swiss Needle Cast in Western Oregon Douglas-Fir Plantations: 20-Year Monitoring Results. Forests. 7(155)

Ritóková, G, Mainwaring, D.B., Shaw D.C., Lan, Y-H. 2020. Douglas-fir foliage retention dynamics across a gradient of Swiss needle cast in coastal Oregon and Washington. Canadian Journal of Forest Research. https://doi.org/10.1139/cjfr-2020-0318

Rosso, P. H. and E. M. Hansen. 2003. Predicting Swiss needle cast disease distribution and severity in young Douglas-fir plantations in coastal Oregon. Phytopathology. 93: 790-798.

Shaw D.C., Ritóková, G, Lan, Y-H, Mainwaring, D.B., Russo, A., Comeleo, R., Navaro, S., Norlander, D., Smith, B. 2021. Persistence of the Swiss Needle Cast Outbreak in Oregon Coastal Douglas-fir, and New Insights from Research and Monitoring. Journal of Forestry.

Stone, J. K., Hood, I. A., Watt, M. S. and J. L. Kerrigan. 2007. Distribution of Swiss needle cast in New Zealand in relation to winter temperature. Australasian Plant Pathology. 36: 445-454.

Stone, J. K., Capitano, B. R. and J. L. Kerrigan. 2008. The histopathology of *Phaeocryptopus gaeumannii* on Douglas-fir needles. Mycologia. 100: 431-444.

Stone, J. K., Coop, L. B. and D. K. Manter. 2008. Predicting the effects of climate change on Swiss needle cast disease severity in Pacific Northwest forests. Canadian Journal of Plant Pathology. 30: 169-176.

Watt, M. S., Stone, J. K., Hood, I. A. and D. J. Palmer. 2010. Predicting the severity of Swiss needle cast on Douglas-fir under current and future climate in New Zealand. Forest Ecology and Management (*in press*).

Forest Protection Issues

Kelsey, R. G. and D. K. Manter. 2004. Effect of Swiss needle cast on Douglas-fir stem ethanol and monoterpene concentrations, oleoresin flow, and host selection by the Douglas-fir beetle. Forest Ecology and Management. 190: 241-253.

Shaw, D. C., Filip, G. M., Kanaskie, A., Maguire, D. A. and W. Littke. 2011. Managing an epidemic of Swiss needle cast in the Douglas-fir region of Oregon: The Swiss Needle Cast Cooperative. Journal of Forestry (*in press*).

Shaw, David C. 2025. Forum Article: Why a Network of Old-Growth and Mature Forests Across the Douglas-Fir Region is Good for the Timber Industry. Journal of Forestry. 1-18.

Sibley, A., Still, C., Gregory, M., Harrington, C., Shaw, D., Ferrari, N., ... & Bell, D. M. 2025. Extreme Heatwave Causes Immediate, Widespread Mortality of Forest Canopy Foliage, Highlighting Modes of Forest Sensitivity to Extreme Heat. Global Change Biology, 31(11), e70571.

Genetic Resistance/Tolerance in Douglas-fir

Jayawickrama, K.J.S., D. Shaw, and T.Z. Ye. 2012. Genetic Selection in Coastal Douglas-fir for tolerance to Swiss Needle Cast Disease. Proceedings of the fourth international workshop on the genetics of host-parasite interactions in forestry: Disease and insect resistance in forest trees. Gen. Tech. Rep. PSW-GTR-240. Albany, CA: Pacific Southwest Research Station, Forest Service, U.S. Department of Agriculture. 372 p.

Johnson, G. R. 2002. Genetic variation in tolerance of Douglas-fir to Swiss needle cast as assessed by symptom expression. Silvae Genetica. 51: 80-86.

Kastner, W., Dutton, S. and D. Roche. 2001. Effects of Swiss needle cast on three Douglas-fir seed sources on a low-elevation site in the northern Oregon Coast Range: Results after five growing seasons. Western Journal of Applied Forestry. 16 (1): 31-34.

Temel, F., Johnson, G. R. and J. K. Stone. 2004. The relationship between Swiss needle cast symptom severity and level of *Phaeocryptopus gaeumannii* colonization in coastal Douglas-fir (*Pseudotsuga menziesii var. menziesii*). Forest Pathology. 34: 383-394.

Temel, F., Johnson, G. R. and W. T. Adams. 2005. Early genetic testing of coastal Douglas-fir for Swiss needle cast tolerance. Canadian Journal of Forest Research. 35: 521-529.

Wilhelmi, N.P., Shaw D.C., Harrington C.A., St. Clair J.B., Ganio L.M. 2017. Climate of seed source affects susceptibility of coastal Douglas-fir to foliage diseases. Ecosphere. 8(12):e02011.

Genetics of Nothophaeocryptopus gaeumannii

Bennett P, Hood P.I, Stone J.K.. 2018. The genetic structure of populations of the Douglas-fir Swiss needle cast fungus *Nothophaeocryptopus gaeumannii* in New Zealand. Phytopathology. 109:446-455.

Bennett P, Stone J.K.. 2019. Environmental variables associated with *Nothophaeocryptopus gaeumannii* population structure and Swiss needle cast severity in Western Oregon and Washington. Ecology and Evolution. 9(19):11379-11394.

Herpin-Saunier, N.Y., Sambaraju, K.R., Yin, X., Feau, N., Zeglen, S., Ritokova, G., Omdal, D., Côté, C. and Hamelin, R.C.. 2022. Genetic lineage distribution modeling to predict epidemics of a conifer disease. Frontiers in Forests and Global Change. 4:229-243.

Winton, L. M., Hansen, E. M. and J. K. Stone. 2006. Population structure suggests reproductively isolated lineages of *Phaeocryptopus gaeumannii*. Mycologia. 98 (5): 781-791.

Winton. L. M., Stone, J. K. and E. M. Hansen. 2007. The systematic position of *Phaeocryptopus gaeumannii*. Mycologia. 99: 240-252.

Hydrology

Bladon KD, Bywater-Reyes S, LeBoldus JM, Keriö S, Segura C, Ritóková G, Shaw D.C.. 2019. Increased streamflow in catchments affected by a forest disease epidemic. Science of The Total Environment. 691:112-123.

Mensuration and growth effects

Lee, E.H., Beedlow P.A., Waschmann R.S., Tingey D.T., Cline S., Bollman M., Wickham C., Carlile C. 2017. Regional patterns of increasing Swiss needle cast impacts on Douglas-fir growth with warming temperatures. Ecology and Evolution. 7(24):11167–11196.

Maguire D. A., Kanaskie, A., Voelker, W., Johnson, R. and G. Johnson. 2002. Growth of young Douglas-fir plantations across a gradient in Swiss needle cast severity. Western Journal of Applied Forestry. 17: 86-95.

Maguire, D. A. and A. Kanaskie. 2002. The ratio of live crown length to sapwood area as a measure of crown sparseness. Forest Science. 48: 93-100.

Maguire, D. A., Mainwaring, D. B. and Kanaskie A. 2011. Ten-year growth and mortality in young Douglas-fir stands experiencing a range in Swiss needle cast severity. Can. J. For. Res. 41: 2064-2076.

Mainwaring, D. B., Ritóková, G., Shaw, D. C., Brooks, R. K., and Omdal, D. W. 2023. Site-level estimates of Douglas-fir foliage retention from climate, soil, and topographic variables. Forest Ecology and Management. 537:120930.

Susaeta A., Okolo C., and Shaw D. 2024. Effects of swiss needle cast on the profitability and optimal management of douglas-fir plantations in western Oregon. Forest Science. 70(5-6): 335-339.

Weiskittel, A. R., Garber, S. M., Johnson, G. P., Maguire, D. A. and R.A. Monserud. 2007. Annualized diameter and height growth equations for Pacific Northwest plantation-grown Douglas-fir, western hemlock, and red alder. Forest Ecology and Management. 250: 266-278.

Weiskittel, A. R., Maguire, D. A., Garber, S. M. and A. Kanaskie. 2006. Influence of Swiss needle cast on foliage age class structure and vertical distribution in Douglas-fir plantations of north coastal Oregon. Canadian Journal of Forest Research. 36: 1497-1508.

Weiskittel, A. R., Maguire, D. A. and R. A. Monserud. 2007. Modeling crown structural responses to competing vegetation control, thinning, fertilization, and Swiss needle cast in coastal Douglas-fir of the Pacific Northwest, USA. Forest Ecology and Management. 245: 96-109.

Weiskittel, A. R., Maguire, D. A. and R. A. Monserud. 2007. Response of branch growth and mortality to silvicultural treatments in coastal Douglas-fir plantations: Implications for predicting tree growth. Forest Ecology and Management. 251: 182-194.

Weiskittel, A. R. and D. A. Maguire. 2007. Response of Douglas-fir leaf area index and litterfall dynamics to Swiss needle cast in north coastal Oregon, USA. Annals of Forest Science. 64: 121-132.

Weiskittel, A. R. and D. A. Maguire. 2006. Branch surface area and its vertical distribution in coastal Douglas-fir. Trees. 20: 657-667.

Weiskittel, A. R., Temesgen, H., Wilson, D. S. and D. A. Maguire. 2008. Sources of within and between-stand variability in specific leaf area of three ecologically distinct conifer species. Annals of Forest Science. 65: 103-112.

Zhao, J., Maguire, D. A., Mainwaring, D. B., Kanaskie, A. 2012. Climatic influences on needle cohort survival mediated by Swiss needle cast in coastal Douglas-fir. Trees 26: 1361-1371

Zhao, J., Mainwaring, D. B., Maguire, D. A., Kanaskie, A. 2011. Regional and annual trends in Douglas-fir foliage retention: Correlations with climatic variables. For. Ecol. And Management 262: 1872-1886

Zhao, J, Maguire DA, Mainwaring DB, Kanaskie A. 2015. The effect of within-stand variation in Swiss needle cast intensity on Douglas-fir stand dynamics. Forest Ecology and Management. 347:75-82.

Zhao, J., Maguire, D. A., Mainwaring, D. B., Wehage, J., Kanaskie, A. 2013. Thinning Mixed Species Stands of Douglas-Fir and Western Hemlcok in the Presence of Swiss Needle Cast: Guidelines Based on Relative Basal Area Growth of Individual Trees. For. Sci. 60 (1): 191-199.

Nutrition and soil interactions

El-Hajj, Z., Kavanagh, K., Rose, C., and Z. Kanaan-Atallah. 2004. Nitrogen and carbon dynamics of a foliar biotrophic fungal parasite in fertilized Douglas-fir. New Phytologist. 163: 139-147.

Lan Y-H, Shaw D.C., Ritóková G, Hatten J. 2019. Associations between Swiss Needle Cast Severity and Foliar Nutrients in Young-Growth Douglas-Fir in Coastal Western Oregon and Southwest Washington, USA. For. Sci. 65(5):537-542.

Mulvey, R.L., Shaw, D.C., Maguire, D.A. 2013. Fertilization impacts on Swiss needle cast disease severity in Western Oregon. Forest Ecology and Management 287: 147-158.

Perakis, S. S., Maguire, D. A., Bullen, T. D., Cromack, K., Waring, R. H. and J. R. Boyle. 2005. Coupled nitrogen and calcium cycles in forests of the Oregon Coast Range. Ecosystems. 8: 1-12.

Waring, R. H., Boyle, J., Cromack, K. Jr., Maguire, D. and A. Kanaskie. 2000. Researchers offer new insights into Swiss needle cast. Western Forester. 45 (6): 10-11.

Pathology and physiological host effects

Bennett, P., Stone, J. 2016. Assessments of Population Structure, Diversity, and Phylogeography of the Swiss Needle Cast Fungus (*Phaeocryptopus gaeumannii*) in the U.S. Pacific Northwest. Forests: 7, 14.

Black, B. A., Shaw, D. C. and J. K. Stone. 2010. Impacts of Swiss needle cast on overstory Douglas-fir forests of western Oregon Coast Range. Forest Ecology and Management. 259: 1673-1680.

Gervers, K. A., Thomas, D. C., Roy, B. A., Spatafora, J. W. and Busby, P. E. 2022. Crown closure affects endophytic leaf mycobiome compositional dynamics over time in *Pseudotsuga menziesii* var. *menziesii*. Fungal Ecology. 57–58:101155.

Lee, E.H., Beedlow, P.A., Waschmann, R.S., Cline, S., Bollman, M., Wickham, C. and Testa, N., 2021. Tree-ring history of Swiss needle cast impact on Douglas-fir growth in Western Oregon: correlations with climatic variables. J Plant Sci Phytopathol. 5:076-087.

Lee, E.H., Beedlow, P.A., Brooks, J.R., Tingey, D.T., Wickham, C. and Rugh, W., 2022. Physiological responses of Douglas-fir to climate and forest disturbances as detected by cellulosic carbon and oxygen isotope ratios. Tree Physiology, 42(1):5-25.

Lee, H.E., Beedlow, P.A., Waschamnn, R.S., Burdick, C.A., Shaw, D.C. 2013. Tree-ring analysis of the fungal disease Swiss needle cast in western Oregon coastal forests. Can Journal of For. 43(8):677-690.

Manter, D. K., Bond, B. J., Kavanagh, K. L., Rosso, P. H. and G. M. Filip. 2000. Pseudothecia of Swiss needle cast fungus, *Phaeocryptopus gaeumannii,* physically block stomata of Douglas-fir, reducing CO_2 assimilation. New Phytologist. 148 (3): 481-491.

Manter, D. K. 2002. Energy dissipation and photoinhibition in Douglas-fir needles with a fungal-mediated reduction in photosynthetic rates. Phytopathology. 150: 674-679.

Manter, D. K., Bond, B. J., Kavanagh, K. L., Stone, J. K. and G. M. Filip. 2003. Modeling the impacts of the foliar pathogen, *Phaeocryptopus gaeumannii*, on Douglas-fir physiology: net canopy carbon assimilation, needle abscission and growth. Ecological Modeling. 164: 211-226.

Manter, D. K. and Kavanagh, K. L. 2003. Stomatal regulation in Douglas-fir following a fungal-mediated chronic reduction in leaf area. Trees. 17: 485-491.

Manter, D. K., Kelsey, R. G., and J. K. Stone. 2001. Quantification of *Phaeocryptopus gaeumannii* colonization in Douglas-fir needles by ergosterol analysis. Forest Pathology. 31: 229-240.

Manter, D. K., Winton, L. M., Filip, G. M. and J. K. Stone. 2003. Assessment of Swiss needle cast disease: temporal and spatial investigations of fungal colonization and symptom severity. Phytopathology. 151: 344-351.

Saffell, B.J., Meinzer, R.C., Voelker, S.L., Shaw, D.C., Brooks, R.J., Lachenbruch, B, McKay, J. 2014. Tree-ring stable isotopes record the impact of a foliar fungal pathogen on CO_2 assimilation and growth in Douglas-fir. Plant, Cell & Environment. doi: 10.1111/pce.12256

Winton, L. M., Manter, D. K., Stone, J. K. and E. M. Hansen. 2003. Comparison of biochemical, molecular and visual methods to quantify *Phaeocryptopus gaeumannii* in Douglas-fir foliage. Phytopathology. 93: 121-126.

Winton, L. M., Stone, J. K., Watrud, L. S. and E. M. Hansen. 2002. Simultaneous one-tube quantification of host and pathogen DNA with real-time polymerase chain reaction. Phytopathology. 92: 112-116.

Winton, L. M., Stone, J. K. and E. M. Hansen. 2007. Polymorphic microsatellite markers for the Douglas-fir pathogen *Phaeocryptopus gaeumannii*, causal agent of Swiss needle cast disease. Molecular Ecology. 7: 1125-1128.

Silviculture and Control

Filip, G., Kanaskie, A., Kavanagh, K., Johnson, G., Johnson, R. and D. Maguire. 2000. Research Contribution 30, Forest Research Laboratory, College of Forestry, Oregon State University, Corvallis, Oregon.

Mainwaring, D. B., Maguire, D. A., Kanaskie, A. and J. Brandt. 2005. Growth responses to commercial thinning in Douglas-fir stands with varying intensity of Swiss needle cast. Canadian Journal of Forest Research. 35: 2394-2402.

Stone, J. K., Reeser, P. W. and A. Kanaskie. 2007. Fungicidal suppression of Swiss needle cast and pathogen reinvasion in a 20-year-old Douglas-fir stand. Western Journal of Applied Forestry. 22: 248-252.

Wood Quality

Grotta, A. T., Leichti, R. J., Gartner, B. L. and G. R. Johnson. 2004. Effect of growth ring orientation and placement of earlywood and latewood on MOE and MOR of very-small clear Douglas-fir beams. Wood and Fiber Science. 37: 207-212.

Johnson, G. R., Gartner, B. L., Maguire, D. and A. Kanaskie. 2003. Influence of Bravo fungicide applications on wood density and moisture content of Swiss needle cast affected Douglas-fir trees. Forest Ecology and Management. 186: 339-348.

Johnson, G. R., Grotta, A. T., Gartner, B. L. and G. Downes. 2005. Impact of the foliar pathogen Swiss needle cast on wood quality of Douglas-fir. Canadian Journal of Forest Research. 35: 331-339.

Lachenbruch, B., Johnson, G.R. 2020. Different radial growth rate effects on outerwood properties of coastal Douglas-fir in healthy trees vs. trees impacted by Swiss Needle Cast. Canadian Journal of Forest Research. https://doi.org/10.1139/cjfr-2020-0199